Clock Synchronisation for UWB and DECT Communication Networks

by

Margaret Uzunma Anyaegbu

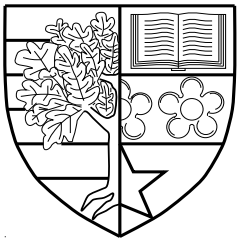

A thesis submitted in partial fulfilment for the degree of Engineering Doctorate

at

Heriot-Watt University

School of Engineering and Physical Sciences

July 2013

Abstract

Synchronisation deals with the distribution of time and/or frequency across a network of nodes dispersed in an area, in order to align their clocks with respect to time and/or frequency. It remains an important requirement in telecommunication networks, especially in Time Division Duplexing (TDD) systems such as Ultra Wideband (UWB) and Digital Enhanced Cordless Telecommunications (DECT) systems. This thesis explores three different research areas related to clock synchronisation in communication networks; namely algorithm development and implementation, managing Packet Delay Variation (PDV), and coping with the failure of a master node.

The first area proposes a higher-layer synchronisation algorithm in order to meet the specific requirements of a UWB network that is based on the European Computer Manufacturers Association (ECMA) standard. At up to 480 Mbps data rate, UWB is an attractive technology for multimedia streaming. Higher-layer synchronisation is needed in order to facilitate synchronised playback at the receivers and prevent distortion, but no algorithm is defined in the ECMA-368 standard. In this research area, a higher-layer synchronisation algorithm is developed for an ECMA-368 UWB network. Network simulations and FPGA implementation are used to show that the new algorithm satisfies the requirements of the network.

The next research area looks at how PDV can be managed when Precision Time Protocol (PTP) is implemented in an existing Ethernet network. Existing literature indicates that the performance of a PDV filtering algorithm usually depends on the delay profile of the network in which it is applied. In this research area, a new sample-mode PDV filter is proposed which is independent of the shape of the delay profile. Numerical simulations show that the sample-mode filtering algorithm is able to match or out-perform the existing sample minimum, mean, and maximum filters, at different levels of network load.

Finally, the thesis considers the problem of dealing with master failures in a PTP network for a DECT audio application. It describes the existing master redundancy techniques and shows why they are unsuitable for the specific application. Then a new alternate master cluster technique is proposed along with an alternative BMCA to suit the application under consideration. Network simulations are used to show how this technique leads to a reduction in the total time to recover from a master failure.

To my parents

Acknowledgments

This goes out to the poeple who got me started on this never-ending (it seemed) EngD journey; those who supported me along the way; and those who helped me finish.

First of all, a huge thanks to all those who supervised me at one time or the other. Sandy and Dr Wang, thank you for giving me this opportunity. Your encouragement and guidance helped a lot, especially in the early years. Stephen, thank you for mentoring and supporting me when I worked on the FPGA platform. I learnt a lot from you. Special thanks to William for always giving feedback and keeping me on my toes. I didn't utilise you nearly enough, but thank you for being *the one who stayed*.

In the past four years, I've also had the pleasure of working with many great people. My friends and colleagues in the AWiTec Research Group at Heriot Watt University, both past and present: Xuemin Hong, Xiang Cheng, Omar Saeed Salih, Zengmao Chen, Raul Jose Hernandez Fernandez, Chui Choon Ivan Ku, Fu Yu, Ammar Ghazal, Yi Yuan, and Fourat Haider - you made research seeem like fun!

For all the folks at TES Electronic Solutions Ltd, I really enjoy working with you. Thank you for the encouragement, support, feedback, and pastries. I'm sorry for making you sit through so many lunchtime seminars.

The financial support from the Engineering and Physical Sciences Research Council, TES Electronic Solutions Ltd, EUWB Research project, and EngD centre for Optics and Photonics is gratefully acknowledged.

To all the friends who stood by me and encouraged me when I felt like giving up - Truth, Cheta, Nneoma, Tokoni, Brookey, Hannah, Richard, David, Chioma and Janine. Good friends are like gold.

Lastly, thanks to my very wonderful family for always believing in me, praying for me, supporting me unreservedly, and consistently reminding me that I "can do all things through Christ who strengthens me". You guys rock! I really couldn't have done it without you.

Contents

List of Figures

List of Tables

Abbreviations

(V)HDR	(Very) High Data Rate
ANSI	American National Standards Institute
AP	Access Point
BMCA	Best Master Clock Algorithm
BP	Beacon Period
BPST	Beacon Period Start Time
CoS	Class of Service
CSMA/CA	Carrier Sense Multiple Access with Collision Avoidance
DECT	Digital Enhanced Cordless Telecommunications
DME	Device Management Entity
DRP	Distributed Reservation Protocol
DTP	Data Transfer Period
ECMA	European Computer Manufacturers Association
EUWB	European Ultra Wideband
FIFO	First In First Out

FSM	Finite State Machine
GPS	Global Positioning System
GSM	Global System for Mobile Communications
HDR	High Data Rate
HMAC	Hardware MAC
IE	Information Element
IP	Internet Protocol
IPoUWB	IP over UWB
ITU-T	International Telecommunication Union standardization sector
LMAC	Lower MAC
LTE	Long Term Evolution
lwIP	light-weight IP
MAC	Medium Access Control
MAS	Medium Access Slot
MIFS	Minimum Inter-Frame Spacing
MLME	MAC Layer Management Entity
NTP	Network Time Protocol
OCXO	Oven Controlled Crystal Oscillator
OFDM	Orthogonal Frequency Division Multiplexing
OSI	Open Systems Interconnection
OTT	one-way transit time
PAL	Protocol Abstraction Layer

PCA	Prioritized Contention Access
PDF	Probability Distribution Function
PDH	Plesiochronous Digital Hierarchy
PDV	Packet Delay Variation
PHY	Physical Layer
PLCP	Physical Layer Convergence Protocol
PLME	Physical Layer Management Entity
PMD	Physical Medium Dependent
ppb	parts per billion
ppm	parts per million
PRC	Primary Reference Clock
PSU	Passenger Service Unit
PTP	Precision Time Protocol
PTSF	Packet Timing Signal Fail
QoE	Quality of Experience
QoS	Quality of Service
RCF	Rate Compensation Factor
RF	Radio Frequency
RTP	Real Time Protocol
SAP	Service Access Point
SDH	Synchronous Digital Hierarchy
SIFS	Short Inter-frame Spacing
SONET	Synchronous Optical Networking
SOOC	slave-only-ordinary-clock
TAI	International Atomic Time
TCP	Transmission Control Protocol
TDD	Time Division Duplexing

TDMA	Time Division Multiple Access
UDP	User Datagram Protocol
UMAC	Upper MAC
UMTS	Universal Mobile Telecommunications System
UTC	Coordinated Universal Time
UWB	Ultra Wideband
VLAN	Virtual Local Area Network
W-USB	Wireless Universal Serial Bus
WLAN	Wireless Local Area Network

Symbols

θ	clock offset
μ	clock frequency
σ	clock skew
ρ	clock drift rate
f	synchronisation interval
RTE	timing difference between expected and actual beacon reception time
RTE_{ppm}	relative timing error in ppm
RTE_{sf}	relative timing over a superframe
BT_{act}	actual beacon reception time
BT_{exp}	expected beacon reception time
d_i	one-way transit time of the ith packet
d_{trans}	transmission delay of packet
d_{prop}	propagation delay of packet
d_{queue_i}	queuing delay of the ith packet
d_{ms}	one-way transit time from master to slave
d_{sm}	one-way transit time from slave to master
M_i	master origin timestamp of the ith $SYNC$ packet
L_i	slave timestamp corresponding to the master's origin timestamp for the ith $SYNC$
S_i	slave reception timestamp of the ith $SYNC$ packet
E_{best}	set of clock attributes for the best clock in a PTP domain
D_0	set of clock attributes for a PTP node

δ_i	packet delay delta value for the ith $SYNC$ packet
W	window size for PDV filtering
α	threshold value for PDV filtering
$\lceil \cdot \rceil$	ceiling operator
$\lfloor \cdot \rfloor$	floor operator
N_{bins}	total number of bins
η	synchronisation accuracy
RCF	rate compensation factor
R_i	rank value of the ith node
R_{ij}	*iRankYou* value of j as computed by i or *YouRankMe* value of j received from i
SLR_i	scaled log rank value corresponding to R_i
SLR_{ij}	scaled log rank value corresponding to R_ij

Chapter 1

Introduction

1.1 Problem Statement

Clock synchronisation is one of the most fundamental problems in distributed systems. Broadly speaking, the goal of clock synchronisation is to ensure that physically distributed processors have a common notion of time and/or frequency. In telecommunications, network-wide synchronisation in both time and frequency is a crucial requirement. Frequency synchronisation is necessary for facilitating seamless handover and preserving connection integrity in cellular wireless systems, while time synchronisation is required for reducing interference or improving capacity in systems that employ Time Division Duplexing (TDD) or Time Division Multiple Access (TDMA) techniques.

Traditionally, network-wide synchronisation has been provided via physical layer timing references in circuit-switched links such as Plesiochronous Digital Hierarchy (PDH), Synchronous Optical Networking (SONET) and Synchronous Digital Hierarchy (SDH). However with the recent migration of network operators towards packet-switched Ethernet-based Next-Generation Networks, there are new requirements to provide accurate and reliable Primary Reference Clocks (PRCs) at the network nodes [2]–[4]. This is typically achieved in either of two ways. A PRC such as Global Positioning

System (GPS) can be deployed at each individual node that requires a timing reference. This is recommended for base stations in large cellular networks such as Global System for Mobile Communications (GSM) where the base stations have a view of the sky and any additional cost of GPS deployment can be borne by many users. For smaller networks such as Digital Enhanced Cordless Telecommunications (DECT), a more appropriate solution uses a single PRC at a central *master* node. The master node derives its time from the PRC and distributes this time to other *slave* nodes via the traffic network or a dedicated network. Such a solution could use a master-slave packet synchronisation protocol such as Precision Time Protocol (PTP) [5] or Network Time Protocol (NTP) [6] to distribute timing and frequency to other nodes on the network. However, unlike the physical layer timing references or GPS receivers, packet synchronisation protocols are susceptible to Packet Delay Variation (PDV). Additionally, the performance of such protocols depends on the availability of the master, which represents a single point of failure in the system.

Aside from network-wide synchronisation which occurs at the lower layers of the Open Systems Interconnection (OSI) model, higher-layer synchronisation can be performed above the Medium Access Control (MAC) layer for the purpose of synchronising real-time applications such as multimedia streaming that are transported over the communication network. In general, a multimedia stream contains multiple audio and/or video streams, that could be transported to different locations such as multiple audio tracks from a single source transported to different loudspeakers. For such applications, the presentation times must be synchronised within acceptable thresholds in order to deliver satisfactory levels of Quality of Service (QoS) [7].

This thesis explores three different areas in synchronisation, namely: how to achieve higher-layer synchronisation in an Ultra Wideband (UWB) network, how to deal with the effects of PDV when PTP is used to synchronise base stations in an Ethernet network, and how to reduce the downtime caused by failure in the master node when PTP is used to synchronise DECT base stations.

1.2 Motivation

When multimedia streaming applications are run on wireless networks such as UWB, the presentation or play-back times must be synchronised in order to deliver an acceptable level of QoS from the perspective of the application provider, as well as a satisfactory Quality of Experience (QoE) for the end user. In the ECMA-368 UWB standard [8], an optional higher-layer synchronisation feature is highlighted in the standard, however no algorithm has been defined. The standard also includes a MAC layer synchronisation algorithm; however it cannot be adapted for higher-layer synchronisation since the algorithm does not actually provide clock correction. Hence in the first research area, we propose a higher-layer synchronisation algorithm for an ECMA-368 UWB network.

In the second research area, we consider how a desired level of synchronisation accuracy can be maintained when PTP is deployed in an Ethernet network that also carries non-synchronisation or background traffic. A typical scenario for this is a DECT audio network comprising of multiple base stations connected over Ethernet and in which PTP is deployed for network-wide synchronisation of the base stations. Contention of the PTP synchronisation traffic with the background audio traffic gives rise to PDV and filtering is one of the techniques for dealing with PDV. The existing literature on PDV filtering algorithms indicates that the suitability of any algorithm depends on the delay distribution of the underlying network, which in turn depends on the network topology and background network utilisation [9]–[12]. For instance, the authors of [10] showed that a sample-minimum PDV filtering algorithm was suitable for a given network at a background network utilisation of less than 40% because most of the packets experienced the minimum delay. However at higher levels of background utilisation levels, they observed that sample-mean or sample-maximum algorithms performed better. Hence, they proposed an adaptive filtering algorithm that switches between sample-minimum, sample-maximum, and sample-mean filters, depending on the delay distribution. However, this approach fails to cater for the case in which the amount of delay experienced by most packets is not the minimum, mean, or maximum delay. Therefore, we theorised that a better approach might be

obtained if the mode delay was used as the criteria for selecting "good" packets for synchronisation.

Lastly, we look at how to maintain a desired level of synchronisation accuracy in the event of a master node failure when using PTP. The application scenario is also the DECT audio network in which base stations are synchronised using PTP. Additionally, the network is deployed in an indoor environment where the base stations do not have access to a PRC. Existing master redundancy techniques in the literature generally fall into two categories. One category assumes that more than one node with PRC capability exists, such that if one fails, the remaining slave nodes can quickly switch over to another PRC-capable node, without loss of synchronisation. The other category involves a group of master nodes that use a democratic algorithm to obtain a *group time* which is then broadcast to the remaining nodes via a fault-tolerant *group speaker*. This essentially transfers the single point of failure from the master node to the *group speaker*. As neither of these approaches fit well with the application scenario under consideration, a new technique was necessary.

1.3 Contributions

The key contributions of the thesis are summarised as follows:

- **A higher-layer synchronisation algorithm for UWB Networks:** We develop a new higher-layer drift-correcting synchronisation algorithm for an ECMA-368 UWB network and propose new primitives for implementing the algorithm.
- **A sample-mode PDV filtering algorithm for PTP synchronisation:** We propose a new sample-mode PDV filter for PTP synchronisation. The algorithm incorporates a new skew-estimating algorithm based on linear programming and "de-noised" samples, and selects synchronisation packets from within a mode bin for estimating the offset.

- **An alternate master cluster with alternative Best Master Clock Algorithm (BMCA) for PTP synchronisation:** We design an alternate master cluster technique with alternative BMCA, as a means of dealing with master failures in PTP synchronisation networks. The technique enhances the optional grandmaster cluster and alternate master features described in the standard and uses a new ranking algorithm to reduce the downtime and accumulated offset caused by a master failure.

The work presented in this thesis has led to the following publications:

Journals

1. **M. Anyaegbu**, C. -X. Wang, and W. Berrie, "Dealing with Packet Delay Variation in IEEE 1588 Synchronization Using a Sample-Mode Filter," *IEEE Intelligent Transportation Systems Magazine*, accepted for publication, 2013.

Conferences

1. **M. Anyaegbu**, C. -X. Wang, and W. Berrie, "A Sample-Mode Packet Delay Variation Filter for IEEE 1588 Synchronization," in *Proc. IEEE ITST'12*, Taipei, Taiwan, Nov. 2012, pp. 1–6.

2. **M. Anyaegbu**, A. Weir, and C. -X. Wang, "Higher layer synchronization in an ECMA-368 Ultra Wideband network," in *Proc. IEEE ICUWB'10*, Nanjing, China, Sep. 2010, vol. 2, pp. 1–4.

Patents

1. **M. Anyaegbu**, C. -X. Wang, and W. Berrie, "An Alternate Master Cluster with an Alternate Best Master Clock Algorithm for PTP Synchronisation," in draft form, 2013.

Technical Reports

1. **M. Anyaegbu**, "High precision synchronisation for large mesh networks," EUWB Deliverable D8a.3.6, Jun. 2011.

2. **M. Anyaegbu** and A. Weir, "High precision synchronization for large mesh networks : Application Requirements for Clock Synchronisation Accuracy," EUWB Deliverable D8a.3.6.1, Aug. 2009.

1.4 Thesis Organisation

The remainder of this thesis is organised as follows:

Chapter 2 begins by providing some background for the three research areas that comprise this thesis. Some important terms related to clocks and synchronisation that will be used throughout the thesis are then defined. Finally, an overview of each research area is provided, together with a review of existing work in the areas.

Chapter 3 provides an in-depth description of the work done in proposing the new higher layer synchronisation algorithm for UWB Networks, evaluating it via simulations, and validating it on an existing UWB FPGA development platform.

Chapter 4 proposes a new sample-mode filtering algorithm for combatting the effects of PDV. A small cross-traffic network and a larger inline traffic network are used as case studies. The delay distributions of the networks are characterised and the performance of the sample-mode algorithm is evaluated on the networks, using network simulation. The sample-mode filter is shown to match or outperform popular filters in the literature.

Chapter 5 provides an in-depth description of a new alternate master cluster with alternative BMCA for PTP synchronisation that can reduce the downtime and accumulated offset caused by a master failure, with minimal implementation effort.

Finally, Chapter 6 concludes the thesis and gives some suggestions for future research topics.

Chapter 2

Background

This chapter provides some background for the three research areas that comprise this thesis. In Section 2.1, some important terms related to clocks and synchronisation that will be used throughout the thesis are defined. Section 2.2 gives a brief overview of ECMA-368 UWB, before describing the two forms of synchronisation in the UWB network. In Section 2.3, an overview of the IEEE 1588 synchronisation protocol is given and the origin of PDV is explored. Some existing PDV algorithms in the literature are also described in this section. Section 2.4 delves deeper into the master selection algorithm, the default BMCA, in the IEEE 1588 standard. Other techniques for coping with master failures in the literature are also explored in this section. Finally, a summary of the chapter is provided in Section 2.5.

2.1 Overview of clocks and synchronisation

This section provides formal definitions for some clock terminologies, as well as a classification of synchronisation algorithms.

2.1.1 Clock Definitions

A physical or hardware clock is a device that periodically counts the oscillations of a crystal or quartz, in order to measure time [13]. At each oscillation, the internal counter is decremented. When the counter value gets to 0, a "tick" is generated and the counter is reset from a holding register. For each "tick" of the physical clock, the corresponding software clock, is incremented by 1.

Mathematically, a clock *C(t)* is modelled as a piecewise continuous function of t that is twice differentiable except on a finite set of isolated jump points where the clock is reset [14], [15]. A perfect clock or "true" clock runs at a constant rate of unity and reports the "true" time at any time. The closest examples of this are Coordinated Universal Time (UTC), which is based on the earth's rotation, and International Atomic Time (TAI), which is a weighted average of the time kept by over 200 atomic clocks operating in various national establishments [16]. For a "true" clock C_t,

$$C_t(t) = t.$$

Real clocks do not report "true" time. Given two real clocks C_a and C_b, the following terms can be defined [17]:

1) *Offset:* The instantaneous difference between the clock's reading and "true" time. The offset of C_a is $(C_a(t) - t)$, while the relative offset of clock C_b with respect to C_a at time $t \geq 0$ is $C_b(t) - C_a(t)$. In this thesis, θ is used to denote a clock's offset.

2) *Frequency:* The rate at which the clock progresses. The frequency of C_a at time t is $C'_a(t)$. If $C'_a(t) > 1$, then C_a runs faster than the "true" clock C_t; else if $C'_a(t) < 1$, then C_a runs slower than C_t. A "true" clock has a frequency of unity. In this thesis, μ is used to denote a clock's frequency.

3) *Skew:* Also known as frequency offset, clock skew is the difference between the frequency of a real clock and the frequency of the "true" clock. The skew of C_a is $(C'_a(t) - 1)$, while the relative skew of clock C_b with respect to C_a is

$(C'_b(t) - C'_a(t))$. A fast clock has a positive skew, a slow clock has a negative skew, while a "true" clock has zero skew. In this thesis, σ is used to denote a clock's skew.

4) *Drift:* The rate at which the frequency of a clock changes, often due to temperature variation or oscillator aging. The drift of C_a is $C''_a(t)$, while the relative drift of clock C_b with respect to C_a at time $t \geq 0$ is $(C''_b(t) - C''_a(t))$. The performance of a hardware clock is usually specified in terms of its maximum drift rate in units of parts per million (ppm) or parts per billion (ppb). In this thesis, ρ is used to denote a clock's drift rate.

2.1.2 Overview of synchronisation algorithms

Broadly speaking, synchronisation is the process of instituting a common notion of time and/or frequency among two or more clocks [18]. Syntonisation refers to the notion that two clocks share the same rate or frequency; hence syntonisation is synonymous with frequency synchronisation [19]. Clocks are said to be synchronised in time when their relative offset is zero and synchronised in frequency when their relative skew is zero. Due to the drift that is inherent in practical clocks, it is necessary to periodically re-synchronise clocks even though they may have been initially synchronised. The period between two consecutive synchronisation rounds is the synchronisation interval *f*. Given a maximum specified drift rate ρ_{max} of a clock, the maximum allowed synchronisation interval that can guarantee a maximum allowed clock offset θ_{max} in between synchronisation rounds can be computed using

$$f = \frac{\theta_{max}}{2\rho_{max}}. \tag{2.1}$$

The American National Standards Institute (ANSI) standard [20] classifies clocks into different stratum levels, depending on their drift rates. The lowest strata corresponds to the highest accuracy, as shown in Table 2.1. Additionally, a clock at a given stratum level should not synchronise to any clock at a higher stratum level.

TABLE 2.1: Clock stratum levels.

Stratum	Accuracy (ppm)
1	1 x 10^{-11}
2	1.6 x 10^{-8}
3	4.6 x 10^{-6}
4	32 x 10^{-6}

A stratum 1 clock refers to a completely autonomous source of timing which is either derived from an atomic standard such as Cesium Beam, or directly controlled by a perfect clock such as UTC. Stratum 2 clocks can track input signals from stratum 1 clocks, and maintain an estimate of the reference frequency even when operating conditions are impaired. Typical examples are Rubidium standards and Double Oven Controlled Crystal Oscillators (OCXOs). In the same vein, stratum 3 clocks track stratum 2 clocks and are tracked by stratum 4 clocks. Simple OCXOs exist in stratum 3 while generic quartz clocks can be found at the highest strata. Perfect or true clocks are assumed to be at stratum 0.

Some key parameters that describe the performance of a synchronisation algorithm are accuracy, precision, and convergence. Accuracy describes the ability of a clock to remain synchronised with respect to a global time source while precision refers to the ability of the a clock to remain synchronised to other clocks on the system while the system runs, i.e. between two consecutive synchronisation rounds [6], [21]. Thus, while accuracy is a measure of the maximum clock offset in the network, precision measures the maximum *relative* clock offset in the network. Convergence describes the ability of the algorithm to synchronise the clocks by measuring how close the clocks are after synchronisation and how many rounds are needed to achieve synchronisation.

Clock synchronisation algorithms can be classified in various ways, including master-slave versus peer-to-peer; clock correction versus untethered clocks; sender-to-receiver versus receiver-to-receiver; internal versus external synchronisation; and probabilistic versus deterministic algorithms [13].

1) *Master-Slave versus Peer-to-Peer:* In master-slave algorithms, one node (usually the one with the most accurate clock, the most powerful processor, or the lowest

load) is designated as master while the others are slaves; the slaves consider the master's local time as the reference time and attempt to synchronise with the master. By contrast, each node in a peer-to-peer algorithm can synchronise to any other node in the network.

2) *Clock Correction versus Untethered Clocks:* Clock correction algorithms achieve synchronisation by adjusting the local clock in each network node to run at par with a global time source or reference clock, and maintain synchronisation by continually reducing the offset between the clocks. For untethered clock algorithms, however, each clock maintains its own version of time together with a table that relates its local clock to every other clock on the network. Local timestamps are compared and translated appropriately by means of this table, while the different clocks remain uncorrected.

3) *Sender-to-receiver versus Receiver-to-receiver:* Sender-to-receiver synchronisation is the conventional method in which a receiver achieves synchronisation with a sender based on the timing information it receives from it, while receiver-to-receiver algorithms perform synchronisation between receivers by comparing the time at which they receive the same message from the same sender.

4) *Internal versus External:* External synchronisation algorithms synchronise the local clocks to a standard reference time source such as UTC or TAI, while internal algorithms do not have access to a standard source and so aim to minimise the maximum clock offset in the network. It is important to note that while internal synchronisation can be achieved in a master-slave or peer-to-peer fashion, external synchronisation can only be achieved in a master-slave manner because it requires a master node that can synchronise itself first, and then other nodes, to an external time source.

5) *Probabilistic versus Deterministic:* Probabilistic algorithms provide a probabilistic guarantee on the maximum clock offset permitted in the network, together with a failure probability while deterministic techniques guarantee an upper bound on the clock offset with certainty.

2.2 Higher Layer Synchronisation in ECMA-368 Ultra Wideband

In recent years, commercial sectors such as personal computing, consumer electronics and mobile communications have turned their attention towards short-range, high-speed wireless connectivity for the delivery of real-time multimedia applications such as video streaming. With its high data rates, advanced QoS, low complexity and low system costs [22], UWB technology has the potential for delivering such applications [23]. As a result, various collaborative research projects such as [24] and [25] were commissioned to explore the economic and commercial opportunities for UWB technology. The higher layer synchronisation project described in this chapter was derived from one of such collaborative projects, European Ultra Wideband (EUWB) [24], [26], which was commissioned by the European Commission under the 7th Framework Programme.

2.2.1 Overview of ECMA-368 UWB

The High Data Rate (HDR) UWB standard [1], [8], developed by the now-defunct WiMedia industrial consortium and standardised by European Computer Manufacturers Association (ECMA), is based on a Multi-Band Orthogonal Frequency Division Multiplexing (OFDM) Physical Layer (PHY) and is capable of supporting data rates up to 480 Mbps for expected distances of up to 3 m. The maximum transmission range is 10 m, but this is only typically achievable at the lowest data rate of 53.3 Mbps and usually in an ideal operating environment. The 7.5 GHz UWB frequency spectrum is split into 14 separate bands and the 528 MHz band spacing guarantees that each OFDM symbol fits perfectly within a band. There are three mandatory data rates (53.3, 106.7, and 200 Mbps) and five optional data rates between 80 and 480 Mbps specified in the standard. Spreading techniques together with convolutional coding are used to vary the data rates and provide a robust signal at the low transmitter power levels specified by the regulators.

ECMA-368 UWB was designed as a platform for the convergence of multiple technologies such as Wireless Universal Serial Bus (W-USB), Bluetooth alternative MAC, and Internet Protocol (IP). All the technologies converge at the MAC sublayer and this provides a guaranteed QoS across the common wireless channel. The convergence is accomplished by means of Protocol Abstraction Layers (PALs); such that from the perspective of the MAC sublayer, each technology and its PAL form a MAC client. Thus, in a sense, the MAC acts as a server for the different technologies, coordinating the activities of the different MAC clients so that they can coexist peacefully and access the shared channel efficiently, but without direct communication between the clients [1]. Fig. 2.1 provides a detailed view of the ECMA-368 UWB platform, showing the different layers and the data exchanged between the layers.

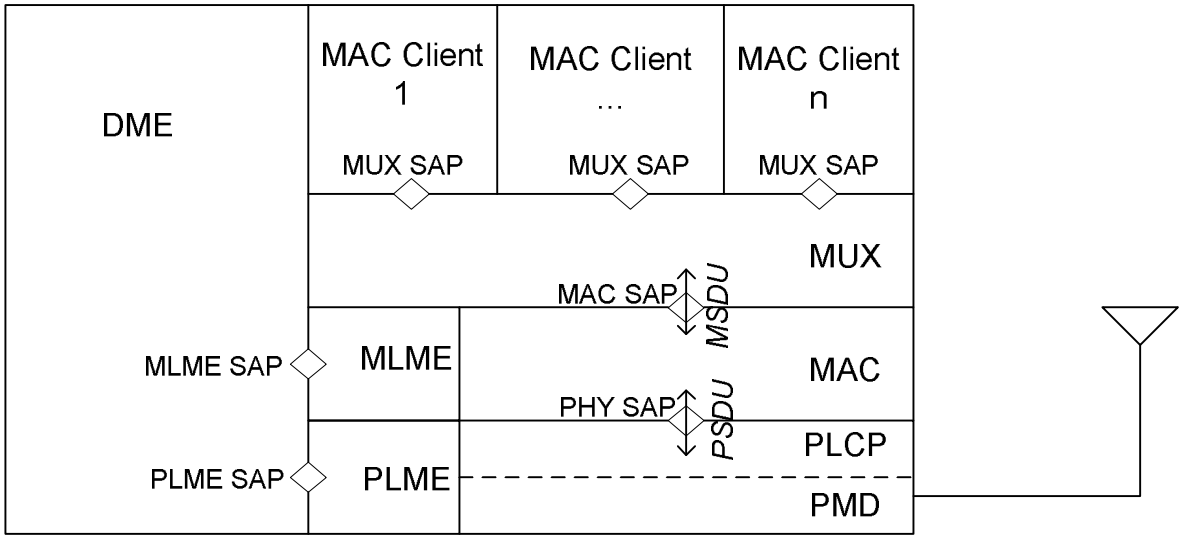

FIGURE 2.1: ECMA-368 PHY and MAC platform [1].

The PHY is split into an upper Physical Layer Convergence Protocol (PLCP) sublayer and a lower Physical Medium Dependent (PMD) sublayer. The PLCP sublayer is responsible for defining the interface between the MAC and the PHY while the PMD sublayer is responsible for the physical transmission and reception of data over the wireless channel. The Physical Layer Management Entity (PLME) and MAC Layer Management Entity (MLME) provide the management service interfaces for the PHY and MAC layer management functions respectively, through the Device Management Entity (DME). The DME is responsible for controlling the whole device, by gathering status of the layers for the layer management entities and also setting the value of

certain layer-specific parameters. The Service Access Points (SAPs) are logical interfaces used for data transfer and management of the PHY and MAC, e.g. the PHY SAP and MAC SAP are points of data communications while the PLME SAP and MLME SAP are points of management or control communications.

All the information in the PHY is transmitted in the form of packets, using standard mode or burst mode. In standard mode, consecutive packets are separated by means of a Short Inter-frame Spacing (SIFS) of duration 10μs, which allows a device to switch from transmit state to receive state or vice versa between packets. Burst mode, on the other hand, allows a sequence of packets to be sent from a single transmitter, such that consecutive packets are separated by the shorter Minimum Inter-Frame Spacing (MIFS) of duration 1.875μs.

The fully distributed architecture of the ECMA-368 MAC facilitates peer-to-peer, ad-hoc networking. The channel time is divided into Medium Access Slots (MASs), each of 256 μs duration. Each block of 256 consecutive MASs forms a superframe. Each superframe begins with a Beacon Period (BP) in which beacon frames are transmitted for the purpose of establishing and maintaining the network, followed by a Data Transfer Period (DTP) as illustrated in Fig. 2.2. The DTP provides the opportunity for devices to transmit their data, using either the Distributed Reservation Protocol (DRP) or the Prioritized Contention Access (PCA) mechanism. The Beacon Period Start Time (BPST) indicates the start of a superframe and any group of devices that have the same BPST and exchange beacon frames during the BP form a beacon group. Beacons frames carry most of the control information required for the existence and stability of the distributed UWB network, often in the form of Information Elements (IEs).

PCA is a contention-based Carrier Sense Multiple Access with Collision Avoidance (CSMA/CA) protocol which allows devices to contend for access to the medium based on the priority of their traffic, and is suitable for asynchronous traffic (with voice having the highest priority and acknowledgement packets having the lowest priority). As the name implies, DRP allows devices to reserve MASs for the transmission of isochronous real-time traffic. A DRP reservation can either be specified implicitly

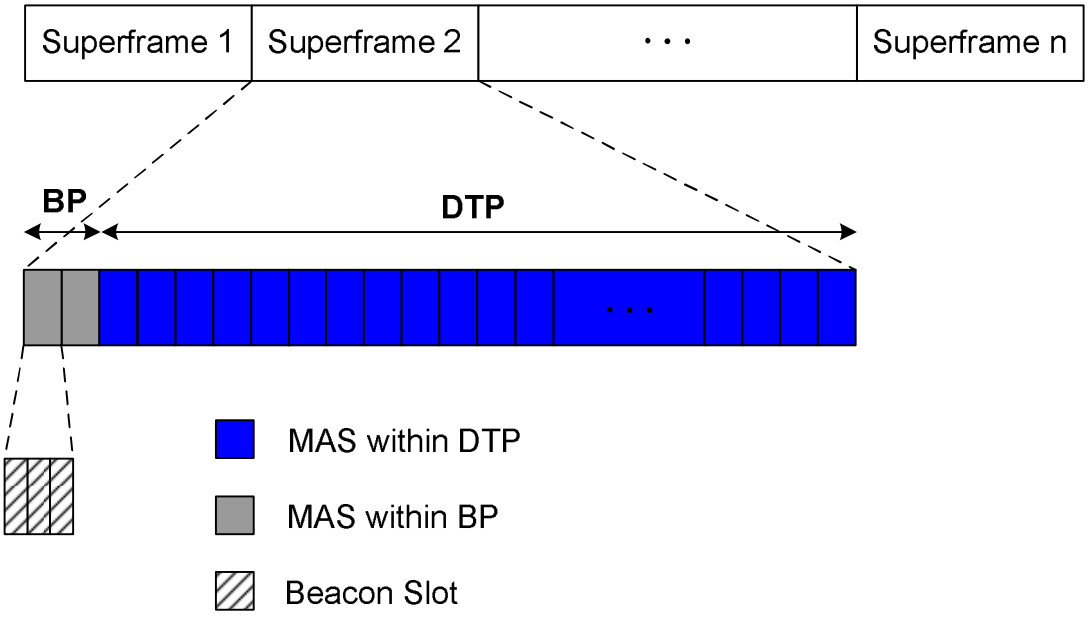

FIGURE 2.2: ECMA-368 UWB superframe structure.

using a DRP IE within a beacon frame, or explicitly by means of DRP reservation request/ response command frames. A reservation includes information about the number of MASs to be reserved and can be hard, soft or private. A hard reservation gives exclusive transmission rights to the owner of the reservation, while private reservations are used for high-layer MAC clients. A soft reservation, on the other hand, gives highest-priority transmission rights to the owner so that unused MASs can be used by other devices. Reservations can also be classed as either safe or unsafe. Unlike unsafe reservations, safe reservations are not preemptible, i.e. they cannot be taken over by other devices. A device can have a maximum of 112 safe MAS reservations. In order to prevent collisions, all devices within a beacon group must respect the reservations made by their neighbours.

The superframe is often viewed in the form of a two-dimensional matrix of MASs known as a MAS map. The MAS map view, illustrated in Fig. 2.3, is useful because it minimises the number of bits required to identify the reserved MASs in a DRP IE. A 2-byte field known as the Zone Bitmap identifies the zone(s) in the superframe while another 2-byte field known as the MAS Bitmap specifies the reserved MAS(s) within the identified zone(s).

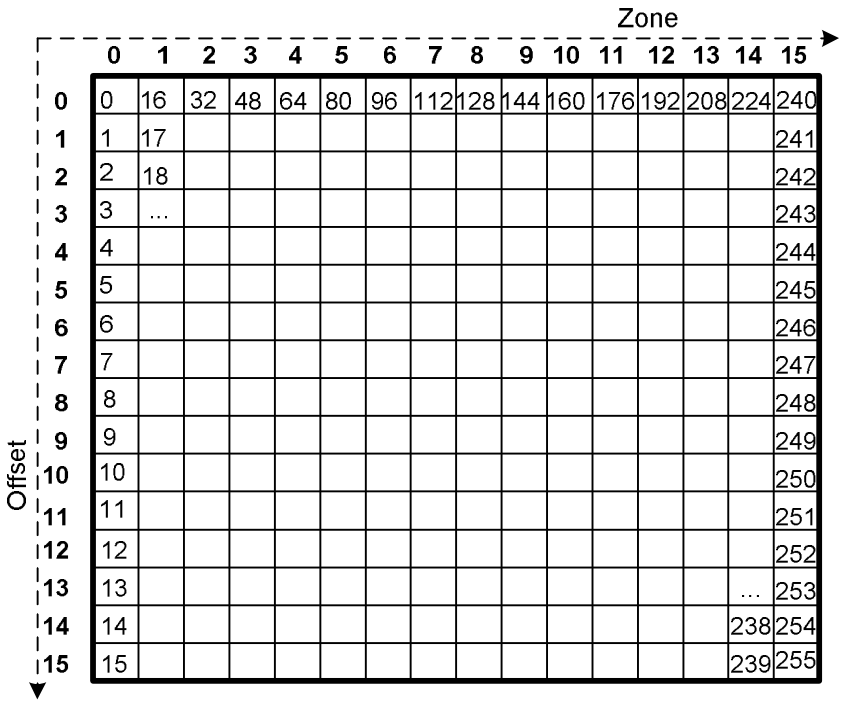

FIGURE 2.3: ECMA-368 UWB superframe MAS map.

2.2.2 Synchronisation in an ECMA-368 UWB Network

Two types of synchronisation are mentioned in the ECMA-368 standard; namely synchronisation in the MAC layer, and higher layer synchronisation. MAC layer synchronisation ensures that each device has a common notion of the superframe so that beacons can be transmitted at the correct time in the BP and data transmission or reception can be coordinated during the DTP. The idea behind higher layer synchronisation is that applications residing in layers above the MAC layer can transmit timestamps and achieve synchronisation by using some of the services provided by the MAC layer. This section provides an overview of these two types of synchronisation.

2.2.2.1 MAC-Layer Synchronisation

As ECMA-368 compliant UWB devices are designed for distributed ad-hoc networking, each device has its own internal PHY clock with a maximum allowed clock drift of ± 20 ppm specified in the standard. From this specification, the worst case clock drift between two devices would be 40 ppm (i.e. when one device's clock is slower by 20

ppm and the other is faster by the same amount). Thus for every 1 s of elapsed time, a maximum of 40 μs clock drift is permitted. Hence for the 65.536 ms superframe, the maximum allowed drift is calculated as

$$40 * 10^{-6} * 65.536 * 10^{-3} = 2.62\mu\text{s}.$$

Without synchronisation, the clock drift will accumulate indefinitely, leading to significant errors over time and making the superframe and MAS timing structure useless. In addition to clock drift, the internal clock resolution and propagation delay are additional sources of timing error. Since the clock accuracy resolution at the MAC layer is 1 μs, any timing information in the MAC can have up to ± 1 μs of error. The propagation delay is in the nanoseconds range, due to the short duration of UWB signals [1].

The goal of synchronisation in the MAC layer is to preserve the timing and structure of the superframe. This is achieved by means of BPST alignment, i.e. each device aligns its BPST with that of its slowest neighbour [27]. The slowest member of a beacon group is the last device to finish its superframe so other devices delay the start of the next superframe in order to align with the slowest device. To enable the alignment each device maintains a table of relative time errors RTE. Each entry in the table represents the timing difference between the actual arrival time BT_{act} and the expected arrival time BT_{exp} of a unique neighbour's beacon, i.e.

$$RTE = BT_{act} - BT_{exp} \tag{2.2}$$

The table of timing differences may contain positive or negative values for each neighbour. A positive value indicates that the neighbour's clock is slower while a negative value indicates a faster clock [28]. Thus the highest positive value corresponds to the slowest member of a devices beacon group and using this value, the device can compute the relative time error in ppm as

$$RTE_{ppm} = \frac{RTE}{BT_{exp} - BPST}. \tag{2.3}$$

This ppm error is mapped to the error over a superframe interval using (2.4).

$$RTE_{sf} = RTE_{ppm} * 65536\mu s. \tag{2.4}$$

RTE_{sf} is the actual clock offset, in unit of seconds, within a superframe between a device and its slowest neighbour. A device achieves synchronisation by delaying the start of its next superframe by the value of this clock offset. The synchronisation is done every superframe in order to prevent the accumulation of clock drift.

The MAC protocol allows missing beacons in a BP for up to three consecutive superframes. So if a device's beacon is missing from the BP, its neighbours may not assume that it has left the beacon group until at least four consecutive superframes have passed. Hence it is possible for clock drift to accumulate for up to four superframes, resulting in a possible maximum clock drift of 10.49 μs. For this reason, a 12 μs guard time *mGuardTime* is included after the SIFS at the end of every reservation block as protection against the maximum clock drift and to compensate for the 2 μs maximum resolution error inherent in the MAC.

To be considered as synchronised at the MAC layer, a device must receive a beacon within 2 * *mGuardTime* of its own beacon transmission, but the maximum synchronisation adjustment that a device can make is 4 μs. Theoretically, this implies that beacons would eventually converge and maintain synchronisation to within 4 μs, but practical experience shows that the synchronisation is not maintained for more than a few superframes due to the amount of clock drift between devices. As a result, it is very difficult to maintain an ECMA-368 UWB system with beacon reception within 2.62 μs of transmission of the slowest device in the beacon group.

2.2.2.2 Higher-Layer Synchronisation

From the description in Section 2.2.2.1, it is clear that the MAC sublayer synchronisation algorithm uses a peer-to-peer, deterministic, receiver-to-receiver, internal synchronisation approach with untethered clocks. Since the local clocks in each device

are not corrected during synchronisation, reliable timestamps (required for real-time applications such as multimedia streaming and online transactions) cannot be generated by the network. For instance when a single source of multimedia content is streamed to multiple end devices, the audio and video contents require synchronous play in order to meet QoS targets and achieve a satisfactory QoE for the end user. Synchronisation is also required in collaborative video conferencing applications such as [29], where each participant is required to view the same content at exactly the same time. Hence, a more precise timing and synchronisation mechanism is needed for generating accurate timestamps and coordinating media playback in ECMA-368 networks.

The ECMA-368 standard [8] defines an optional mechanism that enables higher layers to accurately synchronise timers located in different devices, using the MLME. This facility can be used concurrently by different applications. The MLME alerts the MAC whenever a transmitted or received data frame contains a specific multicast address in its *DestAddr* field. The synchronisation process is described as follows. When a higher layer protocol initiates the synchronisation process, an *MLME-HL-SYNC.request* primitive is generated. This contains the multicast address of all the devices in a group that are to receive synchronisation frames. On receipt, the MLME issues an *MLME-HL-SYNC.confirm* primitive that indicates the result of the request: *SUCCESS* (if the synchronisation mechanism has been activated) or *NOT_SUPPORTED* (if the device does not support the higher layer synchronisation mechanism or if the address provided by the *MLME-HL-SYNC.request* is not a multicast address). Subsequently, whenever a higher layer synchronisation frame is successfully transmitted or received by the MAC, an *MLME-HL-SYNC.indication* primitive is generated and the DME is notified. Although the synchronisation process is described, the actual mechanism for achieving higher layer synchronisation is beyond the scope of the standard.

Higher-layer synchronisation is especially important for UWB because the MAC layer synchronisation algorithm does not correct the clocks. This is in contrast to the MAC layer synchronisation mechanism in Wireless Local Area Networks (WLANs) which

corrects the cloks based on timestamps transmitted in beacon frames. As a result, a higher-layer application in WLAN can use the existing MAC-layer algorithm but this is not possible with UWB. To the best of our knowledge, no higher layer synchronisation algorithm has been proposed for an ECMA-368 UWB network. Hence in Chapter 3, we propose a higher layer synchronisation algorithm for an ECMA-368 network. Three candidate algorithms were evaluated using network simulation and the best algorithm was implemented on an FPGA demonstration platform, as part of the EUWB project.

2.3 Packet Delay Variation Filtering for IEEE 1588 Synchronisation

IEEE 1588 [5], also known as PTP, is a standard for clock synchronisation in packet-based networks. It is a master-slave, deterministic, sender-to-receiver, clock-correction synchronisation algorithm. The protocol was originally designed for achieving sub-microsecond synchronisation accuracy in testing and automation industries, but has now gained popularity in the telecommunications industry. For instance, the International Telecommunication Union standardization sector (ITU-T) has released a Telecom Profile describing how PTP can be deployed for the syntonisation of base stations in cellular networks such as GSM, Universal Mobile Telecommunications System (UMTS), and Long Term Evolution (LTE) [30], [31]. Some DECT system providers have also started using PTP for synchronising base stations connected over an Ethernet backbone [32], [33]. According to [34] and [35], PDV is the main issue that affects the accuracy of slave clocks when using packet synchronisation protocols such as PTP. This is typically because the synchronisation traffic has to compete with the non-synchronisation traffic for network resources. Hence, the existing PTP-based DECT Ethernet systems in the market tend to be deployed on separate Ethernet segments and without layer-3 switches in order to prevent PDV.

In this section, we formally explain the concept of PDV in Section 2.3.1 and give an overview of PTP in Section 2.3.2. The effect of PDV on PTP synchronisation is shown

in Section 2.3.3, while Section 2.3.4 surveys the existing techniques for dealing with PDV.

2.3.1 The concept of PDV

PDV refers to the variation in one-way transit times (OTTs) between consecutive packets from a source node to a particular destination node. This end-to-end OTT d_i of a packet typically comprises of the propagation delay d_{prop}, transmission delay d_{trans}, and the queuing delay d_{queue_i}, i.e.

$$d_i = d_{trans} + d_{prop} + d_{queue_i} \tag{2.5}$$

Since the packet size is usually fixed for all synchronisation packets, d_{trans} is constant; and if the packets follow the same route from the source to the destination, d_{prop} will also be constant. It is thus the variable queuing delay d_{queue_i} that is the main cause of PDV.

2.3.2 Overview of PTP Synchronisation

The basic principle of PTP is that the most precise clock on the network (termed the grandmaster) is used to synchronise all other clocks on the network. The grandmaster clock is selected from all the clocks in the network based on the source of time it is connected to, using a BMCA. Apart from the grandmaster, a PTP network also includes several masters serving groups of local clocks as shown in Fig. 2.4. A logical grouping of clocks that communicate with each other using the IEEE 1588 protocol in known as a PTP domain and each domain is served by a single master.

In PTP, synchronisation is carried out in two phases using four types of messages. During the Offset Measurement phase the master sends multicast *SYNC* messages to its slaves in a periodic manner. Each *SYNC* message contains a time estimate of when

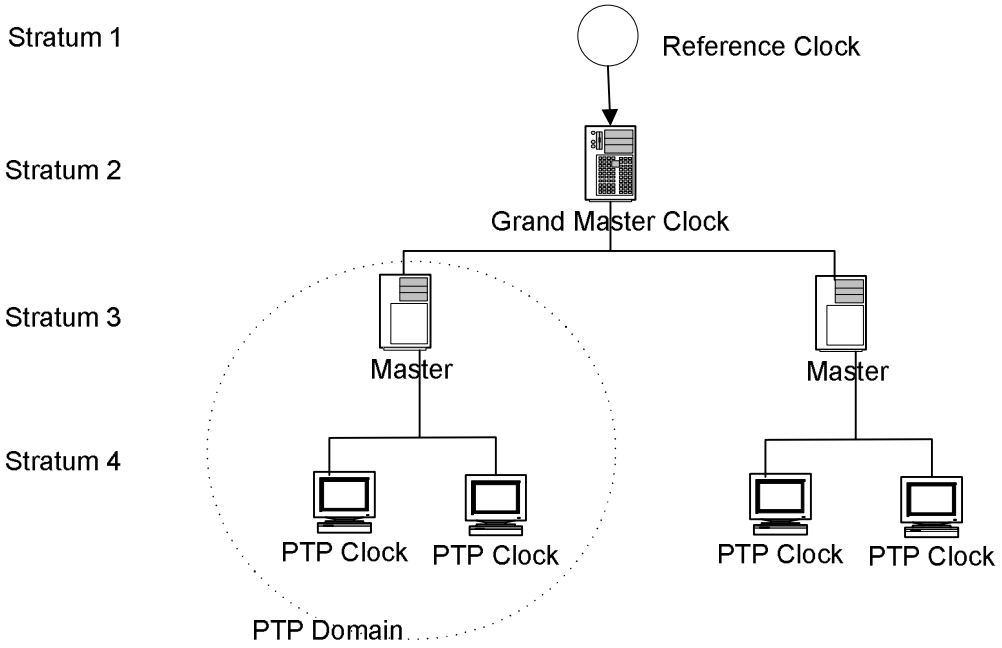

FIGURE 2.4: Generic network topology for PTP.

the message will leave the master. The slaves measure the exact time of reception of the *SYNC* message. If a two-step clock is used then the master also sends a *FOLLOW_UP* message containing the exact time at which the *SYNC* message was transmitted. During the Delay Measurement phase the slave sends a *DELAY_REQUEST* message to the master. In response, the master sends a *DELAY_RESPONSE* message containing the exact time at which it received the *DELAY_REQUEST message*. The sequence of messages transmitted is shown in Fig. 2.5.

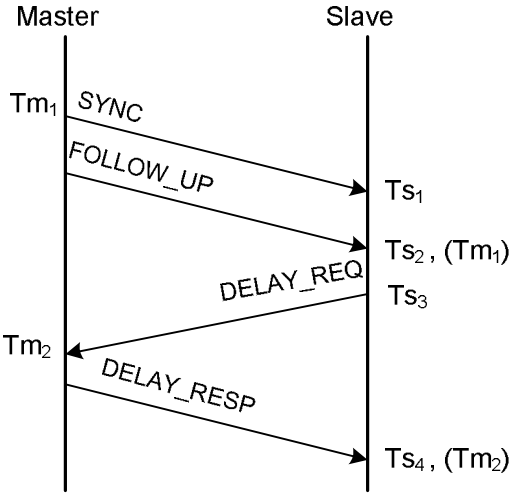

FIGURE 2.5: Message sequence for PTP synchronisation.

From Fig. 2.5, the following relations hold:

$$T_{s_1} = T_{m_1} + d_{ms} - O_{sm} \tag{2.6}$$

$$T_{m_2} = T_{s_2} + d_{sm} - O_{sm}, \tag{2.7}$$

where d_{ms} and d_{sm} are the OTTs from master to slave and from slave to master, respectively, and O_{sm} is the clock offset of the slave with respect to the master.

If the delay is symmetric, $d_{ms} = d_{sm} = d$. Hence, O_{sm} and d can be calculated from (2.6) and (2.7) as:

$$O_{sm} = 0.5 * ((T_{s_1} - T_{m_1}) - (T_{m_2} - T_{s_2})) \tag{2.8}$$

$$d = 0.5 * ((T_{s_1} - T_{m_1}) + (T_{m_2} - T_{s_2})). \tag{2.9}$$

PTP can also correct for the clock rate mismatch or relative clock skew between the master and slaves, using a series of *SYNC* messages. If the master origin timestamps for the ith and jth *SYNC* messages are denoted by M_i and M_j, the corresponding reception timestamps at a slave are S_i and S_j, and $j > i$, then the Rate Compensation Factor (RCF) is computed as:

$$RCF = \frac{S_j - S_i}{M_j - M_i}. \tag{2.10}$$

This RCF is an estimate of the relative clock skew of the slave with respect to the master. As long as the OTTs d_i and d_j are equal, the estimation will be accurate.

2.3.3 Effect of PDV on the synchronisation performance of PTP

When PTP is deployed in an existing network, the synchronisation traffic must contend for the network path and share existing network elements with background traffic in the network. This contention causes variable packet queuing delays at the output queue buffers of network switches, thus giving rise to PDV. If left unchecked, this PDV will adversely affect the synchronisation accuracy of the protocol. The specific effect of PDV on synchronisation accuracy is twofold.

Firstly, the variable queuing delay masks the one-way delays such that it becomes impossible to distinguish between the one-way transit delay, clock offset and queuing delay within a timestamp delta value $\delta_i = S_i - M_i$. Secondly, variable queuing delay means that $d_i \neq d_j$, and results in an inaccurate computation of RCF. Thus, the variation in queuing delay from packet to packet in the network essentially introduces noise in the slave's estimation of the master's clock. If the delay was constant, it would produce a fixed offset that could be easily removed; however the variable delay produces a varying estimate of the offset that degrades the performance of the slave clock.

To illustrate this, we consider a simple PTP network comprising of a master and node connected via intermediate switches. In one scenario there is no background traffic, while the other scenario considers the case where the network is statically loaded with the ITU-T data-centric background traffic [36] at 30% utilisation. Fig. 2.6 shows the variable delay caused by the background traffic and queuing elements, while Fig. 2.7 shows the effect on the synchronisation performance.

2.3.4 Techniques for dealing with PDV

The PTP standard recognizes the problem caused by PDV and offers some techniques for dealing with it, such as deploying specialised PTP switches at intermediate nodes in the network, traffic design, priority tagging of synchronisation traffic, and PDV

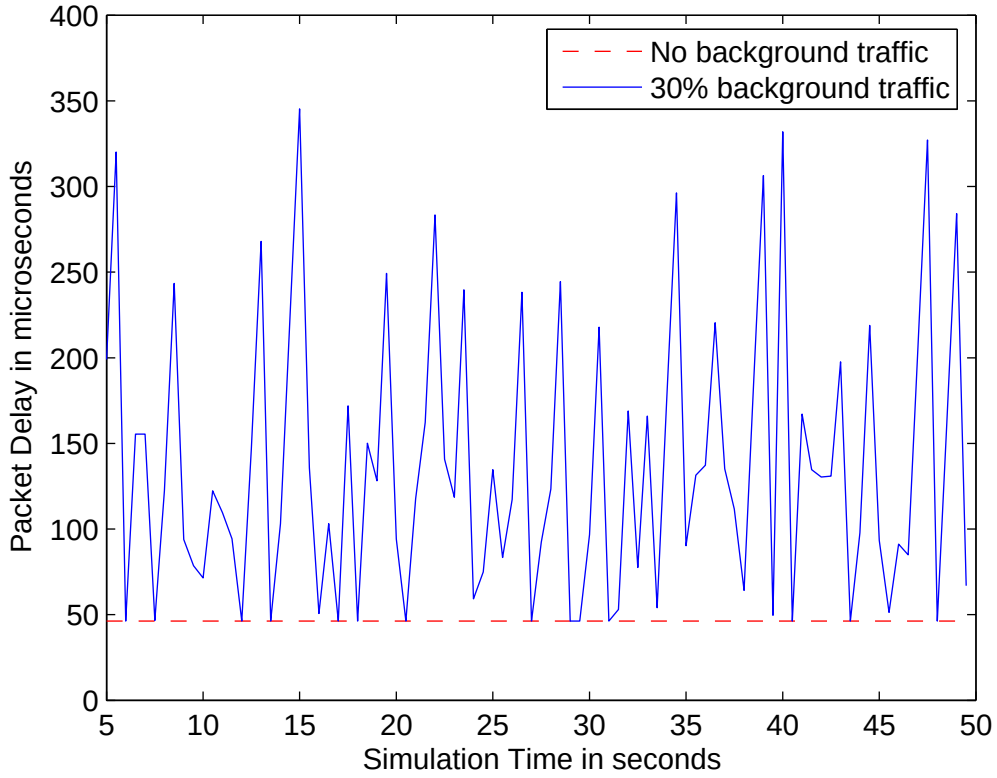

FIGURE 2.6: Illustration of PDV in packet delay measurements.

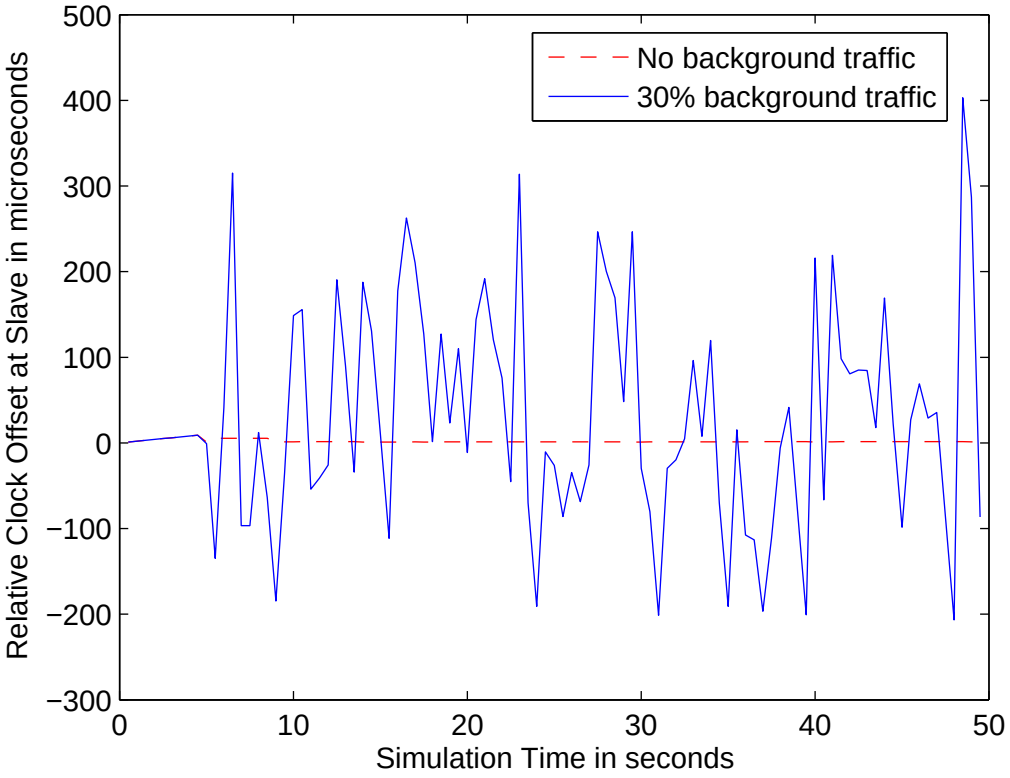

FIGURE 2.7: Illustration of PTP synchronisation with PDV.

filtering. Other techniques in the literature deal with PDV by coordinating the background traffic packet departures with the synchronisation packet generation so as to completely eliminate PDV [37], or by applying Kalman filtering to the received synchronisation packets in order to estimate the master time [38], [39]. In most cases, more than one technique may be required.

Use of Specialised Switches

PTP transparent clocks or boundary clocks can be deployed in place of standard switches at intermediate nodes in the network, in order to prevent PDV. A boundary clock is a multiple-port PTP device, with each port providing access to a separate PTP communication path. It acts as an interface between separate PTP domains, intercepting and processing all PTP messages while passing all other network traffic. One port is the slave port while all other ports are master ports, as determined by the BMCA. The slave port synchronises to the master port of the domain it is connected to, and then provides this synchronised time to all other master ports on the device. Each master port then provides this synchronised time to the domain connected to it. In this way, cascades of queuing elements are avoided during synchronisation and PDV is prevented. A transparent clock, on the other hand, is a single-port PTP device which measures the amount of time a packet spends in the queue buffers of output ports and stores this *residence time* in the *correction field* of the PTP packet [40]. This residence time is subtracted from the timestamp delta value δ_i in order to accurately determine d_{ms} and d_{sm}, and then added on to the computed offset, for accurate synchronisation.

Specialised switches are likely to be the preferred solution for new network installations, as the switches can be factored into the design and costing of the network. For existing installations however, it is often cumbersome and costly to replace the existing network devices.

Traffic Design

Where possible, the traffic patterns in a network can be designed in such a way as to minimise the amount of background traffic as well as the variation in the traffic load, so as to reduce PDV. Assuming that each intermediate network switch is an M/M/1 queue, the entire network will behave like a system of cascaded queues and in steady state, each queue will have a backlog of packets that are yet to be processed. The mean backlog B of unprocessed packets can be expressed in terms of the network utilisation as [41]

$$B = \frac{\rho}{1-\rho}. \tag{2.11}$$

For a network utilisation level of 80%, the mean backlog is 4 packets. A synchronisation packet arriving at the queue will have to wait until the backlog is cleared, thus incurring additional latency. If the amount of background traffic is reduced, the utilisation decreases, with a corresponding decrease in latency and PDV. Traffic design can also be implemented by coordinating the background traffic packet departures with the synchronisation packet generation so as to completely eliminate PDV [37]. However, this can only be utilised in a network that strictly carries non-real time traffic such as data.

Priority Tagging of Synchronisation Traffic

The PTP standard also recommends that PTP event messages are sent with a higher priority, compared with other traffic on the network. In contrast to general messages, PTP event messages are timed messages that require the generation of accurate timestamps when transmitted and received. Such messages include *SYNC* messages and *DELAY_REQ* messages.

Prioritisation of synchronisation traffic is useful for managing delay fluctuations at the ingress ports of switches, but it cannot completely eliminate PDV at the egress ports. This is because of the way modern switches are designed. In general, a modern Ethernet switch has the basic internal architecture illustrated in Fig. 2.8. If QoS is implemented, the traffic manager classifies the incoming traffic based on a traffic

policy such as Class of Service (CoS) while the buffer manager places the traffic in queues according to the classification. At egress, the buffer manager schedules the packets for transmission while the traffic manager implements any egress traffic policies. Regardless of whatever traffic policies or prioritisations are applied, the MAC unit represents a common First In First Out (FIFO) queue into which all packets eventually enter [42], [43]. Thus even if PTP event packets are prioritised over background traffic, the PTP packets would still experience queuing as long as there is a backlog of packets in the MAC unit. Hence prioritisation of synchronisation traffic cannot completely eliminate PDV.

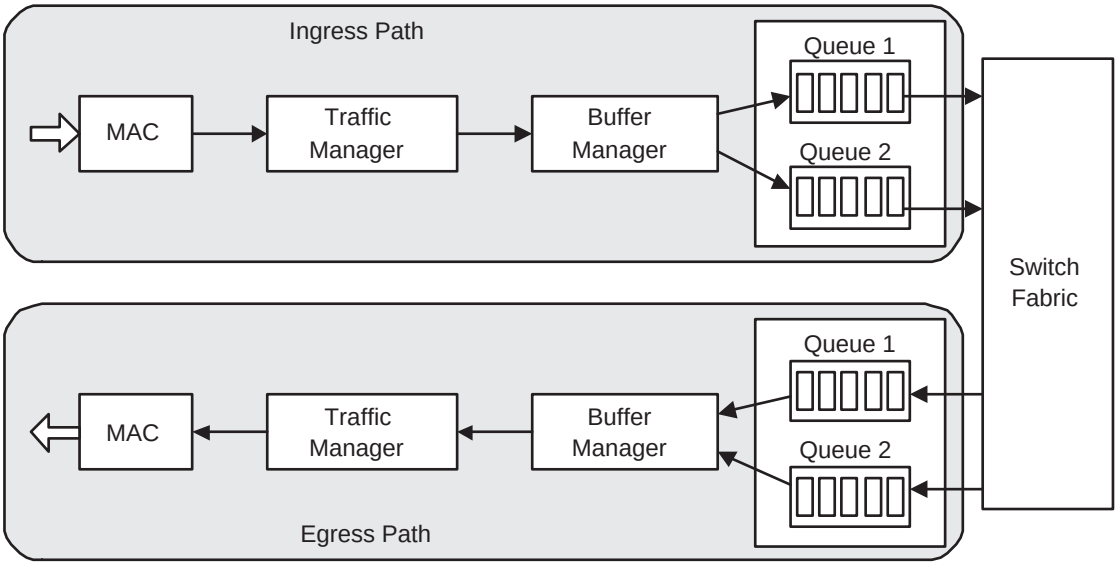

FIGURE 2.8: Internal architecture of a generic Ethernet switch.

PDV Filtering

Two categories of PDV filtering can be observed in the literature. One category takes a set of noisy or PDV-impacted synchronisation packets and tries to generate an estimate of the master's time by filtering off the PDV. This is the approach adopted by [38], [39], [44] in which Kalman filtering is applied to the received synchronisation packets in order to estimate the master time. However, it has been observed that Kalman filtering as a means of combatting PDV in synchronisation networks is only optimal when the network delays follow a Gaussian distribution [44], and this is not

usually the case in real Ethenet networks [45]. The other category of PDV filtering tries to filter off those packets that were heavily impacted by PDV so that the remaining "good" packets can be used to estimate the master time. It is this second category that is the focus of our second research area.

In general, the goal is to select at least one "good" packet out of several packets within the received synchronisation traffic and then use the good packet or packets to achieve synchronisation. However, the definition of "good" can be very subjective. For most of the PDV filtering algorithms in the literature [11], [12], [46], a "good" packet is defined as one with the shortest transit time through the network. Hence these algorithms tend to group the received synchronisation packets into non-overlapping windows, select the ones that were least impacted by queuing delay, and discard the remaining packets. The PDV filters which employ such algorithms are referred to as sample-minimum or earliest arrival packet filters.

Sample-minimum filters can work effectively, as long as packets with minimal queuing delay are delivered at appropriate intervals. In [9], [10], the authors showed that this depends on the packet delay distribution of the network, which in turn depends on the network topology as well as on the network utilisation. The authors also observed that in some scenarios such as heavily-loaded cross-traffic networks and moderately-loaded high-hop in-line traffic networks where the probability of finding a minimum-delay packet was significantly reduced, a sample-mean or sample-maximum filter could outperform the popular sample-minimum filter.

Since the performance of a PDV filter depends on the probability of finding "good" packets to use for synchronisation and "good" packets are packets that experienced the same amount of delay, it seems intuitive that the best place to find such packets is around the mode packet delay value. Hence in Chapter 4, we propose a new sample-mode PDV filtering algorithm for a PTP network and use numerical simulations to compare the performance of the sample-mode filter with the performance of the existing sample-minimum, sample-maximum, and sample-mean filters.

2.4 Dealing with Master Failures in IEEE 1588 Synchronisation

As mentioned in Section 2.3.2, PTP is a type of master-slave synchronisation algorithm in which slave clocks synchronise to a single master clock in a domain. Thus, the master node represents a single point of failure in the system. However, the master node is not usually hard-wired into the system; rather each node can be in any one of 9 different states at any time, including *MASTER* and *SLAVE* states. The master node is the node in the PTP domain that is currently operating in the *MASTER* state and at any given time, only one node can be in this state. A node transitions to the *MASTER* state if it is elected as the best clock based on a standard BMCA which compares the attributes of the different clocks. A failure of the master clock results in the election of a new master using the same BMCA, but the downtime caused by the failure can lead to an accumulation of offset and loss of synchronisation which may be unacceptable for certain applications.

In this section, we summarise the state of the art, as described in [5]. Then we highlight the different existing approaches to dealing with master failures, comment on the advantages and drawbacks of the existing methods and consider the suitability of the existing methods for our target application.

2.4.1 Description of State-of-the-art

2.4.1.1 PTP Node States

9 possible PTP states exist as shown in Table 2.2 and a node can be in either one of the states at any particular time.

Table 2.2: PTP node states.

State	Description
INITIALIZING	Used for initialising data sets, hardware, and communication facilities.
LISTENING	In order to ensure the orderly addition of new PTP nodes, an initialised node waits in this state for the *ANNOUNCE_RECEIPT_TIMEOUT* to expire or to receive an *ANNOUNCE* message from a master.
MASTER	The node behaves like a master clock.
SLAVE	The node synchronises to the selected master clock.
UNCALIBRATED	A transient state to update data sets when a new master is detected and a node is preparing to synchronise with it.
PREMASTER	A transient state to allow a new master to take over from an existing master.
PASSIVE	Used for grandmaster clocks that derive their time from an external reference time, but which are not elected as the master of the domain.
FAULTY	The faulty state of the protocol.
DISABLED	The disabled state of the protocol.

2.4.1.2 PTP Clock Categories

Based on the number of PTP ports, clocks can be categorised as either boundary clocks or ordinary clocks. An ordinary clock has a single PTP port in a domain, while a boundary clock has more than one PTP ports in the domain. The BMCA is run on each port in a PTP domain, so all the ports on a boundary clock do not necessarily operate in the same state. This allows a boundary clock to receive synchronisation in one domain using a port in the *SLAVE* and then transfer the synchronisation to another domain using a port in the *MASTER* state.

In addition, clocks are classified as either one-step or two-step clocks. In a one-step clock, each *SYNC* message prepared by the master contains an estimate of when the message would be sent. Two-step clocks, on the other hand, also transmit a *FOLLOW_UP* message containing the exact time at which the previous *SYNC* message was sent. All the models and simulations in this thesis are based on one-step ordinary clocks.

2.4.1.3 PTP Clock Attributes

Clock attributes are configured at initialisation and stored locally at each node in a *default data set*. They define the characteristics of a clock, are transmitted in *ANNOUNCE* messages, and are used during a like-for-like comparison of other clocks in the BMCA. Table 2.3 describes the attributes that are used in the BMCA.

TABLE 2.3: PTP clock attributes.

Attribute	Description
priority1	Orders the set of clocks in the PTP domain
clockClass	Defines a clock's traceability to TAI
clockAccuracy	Defines a clock's accuracy
offsetScaledLogVariance	Defines a clock's stability
priority2	Provides a finer-grained ordering among equivalent clocks
clockIdentity	Unique clock identity used as a tie-breaker in the BMCA

In addition to its *default data set*, each clock also stores the attributes of its current master clock in a *parent data set*. Each attribute in the *parent data set* has a corresponding attribute in the *default data set*. For example, *GM priority1* is the *priority1* attribute of a slave's master clock. The *parent data set* is updated each time an *ANNOUNCE* message is received from the current master. For the grandmaster clock at the highest PTP stratum, the *parent data set* is identical to the *default data set*.

2.4.1.4 The Default BMCA

Once every announce interval, each clock runs the BMCA to determine if the best clock in its PTP domain has changed. This could happen if the previous best clock becomes faulty or disabled, or if a new clock with better attributes is added to the network. There are two stages in the BMCA. First of all, a clock compares the attributes of all the other clocks from which it received qualified *ANNOUNCE* messages in order to determine the best received clock E_{best}. Clock comparison is done each time an *ANNOUNCE* message is received and qualified. Fig. 2.9 illustrates the process of clock comparison in the BMCA.

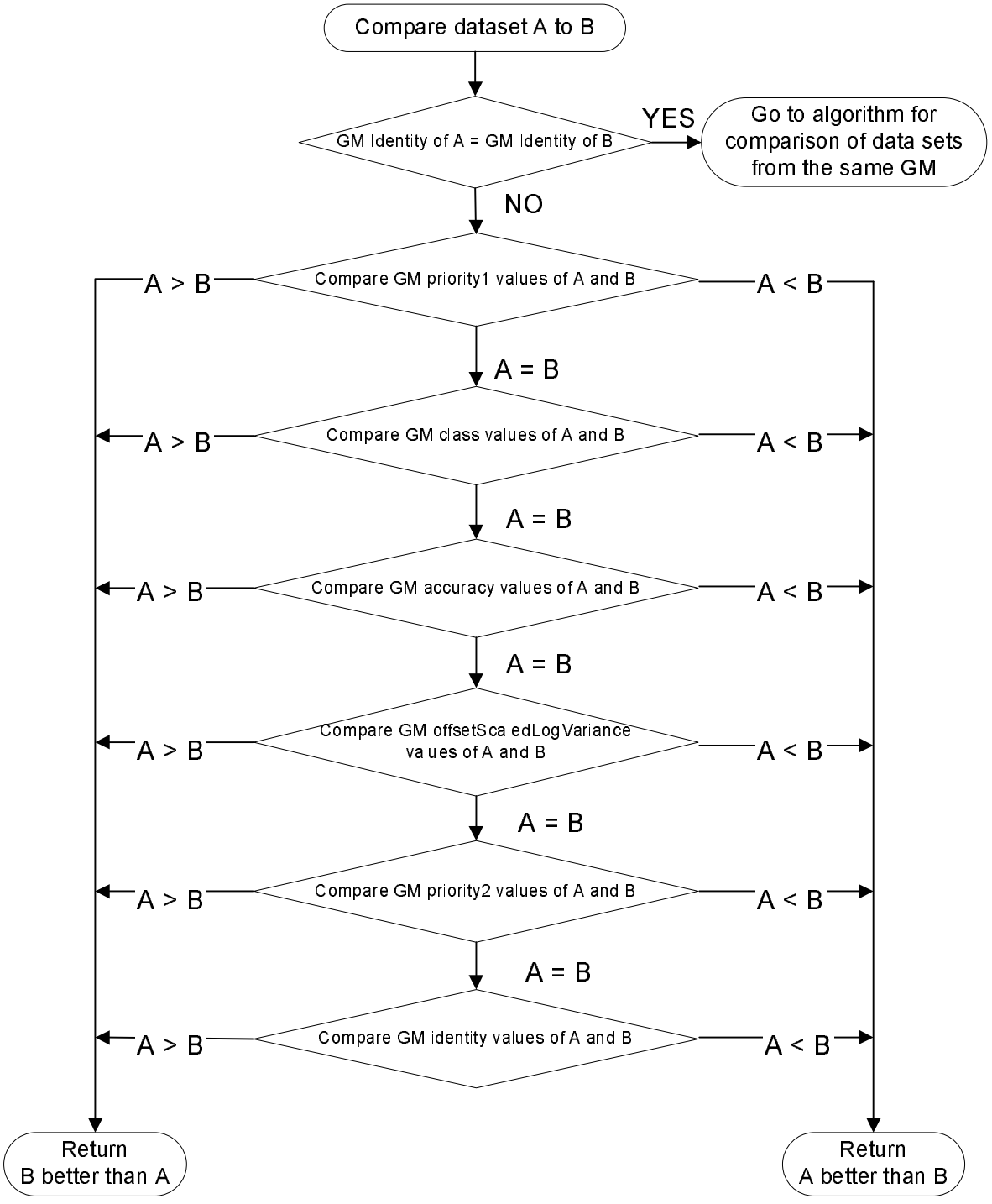

FIGURE 2.9: Clock comparison algorithm for the default BMCA.

The second stage is the state decision algorithm which recommends a state for the clock, by comparing its own attributes from the *default data set* D_0 with the attributes of E_{best}. The state decision algorithm is run once every announce interval. The state decision algoithm is described in Fig. 2.10.

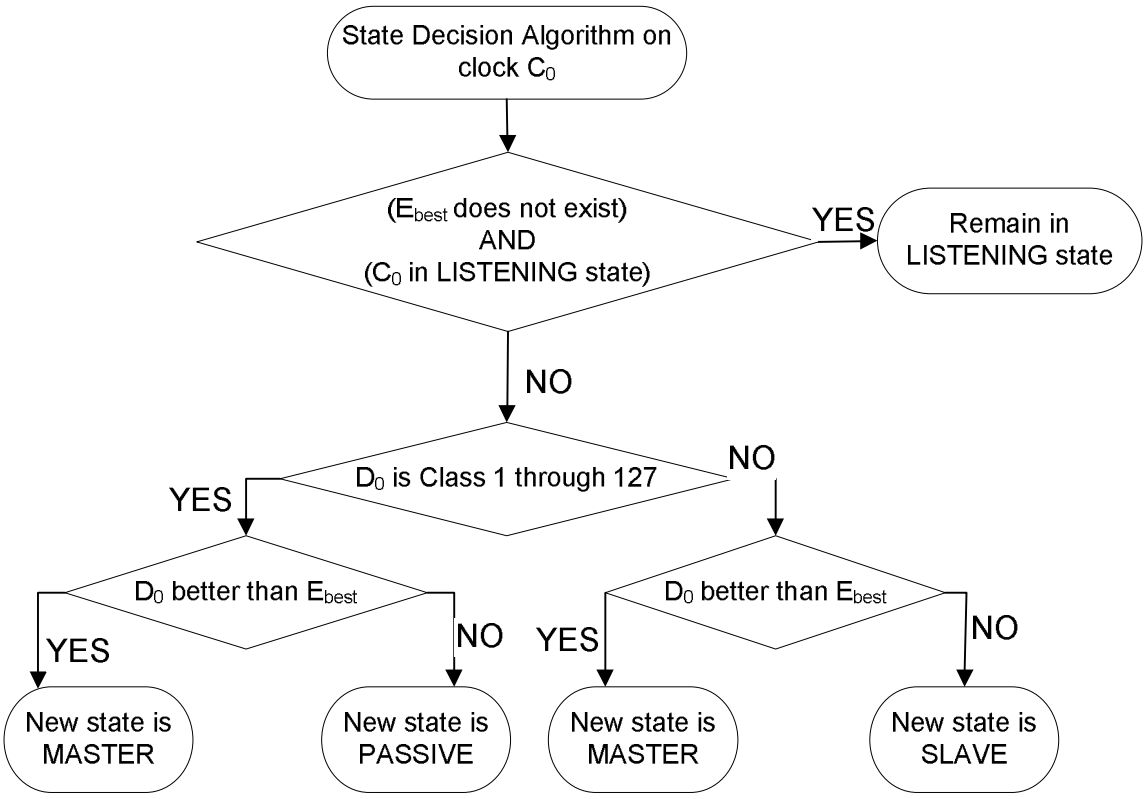

FIGURE 2.10: State decision algorithm for the default BMCA.

A clock class value of 1 through to 127 indicates that the clock will not synchronise to another clock on the network. Hence if such a clock is not elected as the master, it must be in the *PASSIVE* state. This is typically the case when there is more than one clock in the PTP domain that is connected to a trusted external standard reference such as UTC.

2.4.1.5 Master Failure and Recovery

If the existing master clock fails, the second best clock is elected as the new master, using the BMCA described in Section 2.4.1.4. In the period between the current master clock failure and the first instance of synchronisation with a newly-elected master, all the slave clocks within the PTP domain run freely, and the amount of accumulated offset may be unacceptable for certain applications. This period can be broken down into a number of distinct phases, namely:

1. Detection Phase

2. Election Phase

3. Re-synchronisation Phase

A master node sends *ANNOUNCE* messages to all slaves once every announce interval. At each slave, an *ANNOUNCE_RECEIPT_TIMEOUT* timer is used to track the amount of time elapsed since the receipt of the most recent *ANNOUNCE* message from the master. Thus, the timer is restarted every time an *ANNOUNCE* message is received from the current master. The timer expires when it reaches the *ANNOUNCE_RECEIPT_TIMEOUT* value. If this happens, the slaves conclude that the master has failed and proceed to elect a new master. Hence, the duration of the detection phase is equivalent to the *ANNOUNCE_RECEIPT_TIMEOUT* value. According to [5], the *ANNOUNCE_RECEIPT_TIMEOUT* value should be x times the announce interval, where $x = \{3, 4, 5, ..., 10\}$ and the announce interval = {1, 2, 4, 8, 16} seconds. Typical values of x and announce interval are 10 and 2 seconds, respectively.

At the expiry of its *ANNOUNCE_RECEIPT_TIMEOUT* timer, a slave transitions to the *MASTER* state and starts transmitting *ANNOUNCE* messages. In the election phase, each slave (now operating in a *MASTER* state) implements the BMCA using all the received *ANNOUNCE* messages. If its own clock is better than all the other clocks as specified in the received messages, it becomes the new master and remains in the *MASTER* state; otherwise it transitions to the *SLAVE* state and prepares to synchronise to the best master. This election phase can take up to 2 times the announce interval.

After the election phase, the slaves re-synchronize to the new master. At least 2 times the synchronisation interval is required to correct for the clock offset and skew, assuming that a *DELAY_REQ* message can be sent immediately. The default value of the synchronisation interval is 1 second.

From the above descriptions, the total period between a master failure and resynchronisation to a newly-elected master can be reduced by decreasing the values of the announce interval and synchronisation interval. However, these measures result

in an increase in the amount of multicast traffic on the network when there are no failures in the system. Therefore the anticipated benefit of such measures must be weighed against the cost of increased traffic, with consideration for the probability of node failure. This is especially true in the case of the announce interval because the clock attributes contained in *ANNOUNCE* messages do not change frequently and the BMCA must be run each announce interval. Thus in a fully functional non-faulty system, decreasing the announce interval results in the same clock attributes transmitted more frequently with more iterations of the BMCA which all yield the same outcome. Furthermore, reducing the announce interval, synchronisation interval, or both will not completely remove the accumulated offset because the nodes still run freely until a new master is elected.

2.4.2 Survey of Existing Techniques for dealing with PTP Master Failure

A number of techniques have been considered for dealing with the effects of a master failure. As mentioned in Section 1.2, the existing techniques tend to be based on either one of two approaches: deploying multiple nodes with PRC capability or utilising a democratic master group. From an implementation perspective, we can also categorise them into pure master-based approaches, pure slave-based approaches, or hybrid approaches; depending on the how they differ from the state of the art.

2.4.2.1 Master-based Approaches

We define master-based approaches as those techniques in which additional functionality is only required at the master nodes. For example, the PTP standard [5] defines an optional grandmaster cluster feature, in which two to five ordinary or boundary clocks are designated as members of a grandmaster cluster. Each cluster member maintains a table with the addresses of other cluster members so that it can periodically exchange unicast query *ANNOUNCE* messages with all the other cluster members in the domain. The received *ANNOUNCE* messages are then used as inputs

to the BMCA, in order to determine the state of each node. All the cluster members are potential master clocks, with higher priorities than all the other clocks in the domain. Failure of the current master is detected in the cluster within 1 announce interval and a new master is elected within another announce interval. Hence, both the failed master detection time and new master election time are reduced. The drawback of this technique is that, like the name implies, the feature is only described for grandmasters. This means that within the grandmaster cluster, the other nodes that are not operating in the MASTER state must be in PASSIVE mode, and therefore do not synchronize to each other. In practice, this would necessitate the provision of independent synchronisation to a trusted external timing source such as GPS at each grandmaster clock within the cluster.

Another master-based approach is the democratic master group proposed by the authors of [47]–[50] as a means of providing fault-tolerance in IEEE 1588 synchronisation. The IEEE 1588 master is replaced with a group of masters that synchronise to each other using a fault-tolerant peer-to-peer algorithm. In this way, a faulty or malfunctioning master clock can be sorted out, without affecting the accuracy of the slaves. The speaker for the master group is a specially-designed fault-tolerant switch which is responsible for keeping track of the democratically agreed time and transmitting it to the slaves via *SYNC* packets. In order to maintain some compatibility with the PTP standard, the democratic stack is derived from the IEEE 1588 protocol and the messages exchanged between master group members are similar to PTP *SYNC* packets. This is useful because the slaves do not require any special functionality; however the master group speaker is a new device with special functionality. Also, some modification is required at the master nodes, in order to support the democratic algorithm.

2.4.2.2 Slave-based Approaches

We define slave-based approaches as those techniques that only require changes to the slave nodes. For example, the ITU-T has defined a new telecoms profile for applications that require only frequency synchronisation [30]. It uses unicast transmissions

to separate PTP domains. Unicast messaging ensures that master clocks are isolated from each other. Moreover, masters do not communicate with each other. Each slave device consists of multiple instances of independent PTP slave-only-ordinary-clocks (SOOCs); each SOOC participates in a single PTP domain and is associated with a single master. Each slave also maintains a list of all the masters it is allowed to communicate with, together with their priorities. This list is used to instantiate the SOOC instances. Since the profile is geared towards frequency synchronisation, it is not mandatory for a slave to support the delay request-response mechanism; however the master clock must support it. An alternate BMCA is used that produces a value of M1 (grandmaster clock) for all the master clocks and S1 (slave clock) for all the SOOC instances. The slave device uses three attributes in order to select a specific master: the Packet Timing Signal Fail (PTSF) which specifies the failure condition of a master, the clock class attribute, and the master priority. It selects the master with the lowest clock class attribute that is not in a failure condition. If the clock class values are identical, then the master with the highest priority value is selected [51]. The timestamps corresponding to the selected master are used for achieving frequency synchronisation.

Another slave-based approach is the architecture proposed by [52] in which grandmaster clocks are isolated from each other using separate IEEE802.1Q VLANs. The grandmaster clocks use the same free-running oscillator so there is no time error between them at any point and the slave is a VLAN-aware device, so it is able to receive messages from all the grandmaster clocks. The slave maintains a separate feedback loop for each grandmaster and synchronises to the grandmaster that announces the lowest priority1 value. Thus if the current grandmaster clock fails, the failure does not propagate to the other grandmaster clocks. The slave detects the failure when it does not receive an *ANNOUNCE* message, and can immediately switch to the next functioning grandmaster with the lowest priority1 value. This method requires that the same oscillator is used for all grandmaster clocks so that the slave can quickly switch over to a new grandmaster without any transient error at the time of switching.

2.4.2.3 Hybrid Approaches

We define hybrid approaches as those techniques that require changes to both master and slave nodes. An example of this is the optional alternate master feature defined in the PTP standard [5]. This feature allows nodes that are not currently operating in the MASTER state to send *SYNC*, *ANNOUNCE* and *DELAY_RESPONSE* messages to slave nodes. It also allows slave nodes to send *DELAY_REQUEST* messages to nodes that are not currently operating in the MASTER state. In this way, if the slaves have to switch over to an alternate master when the current master fails, the amount of offset during the re-synchronisation phase would be reduced. However, the lengths of the detection and election phases remain unchanged.

2.4.3 Drawbacks of Existing PTP Master Redundancy Techniques

In the period between a master clock failure and the first instance of synchronisation with a newly-elected master, all the slave clocks in the PTP domain run freely, and the amount of accumulated offset during the period may be unacceptable for certain applications. The existing techniques described in Section 2.4.2 have some disadvantages. The grandmaster cluster technique [5] reduces both the failed master detection time and the new master election time; however all the nodes within the cluster must be synchronised to an external reference time source, such as GPS. The democratic master group technique [47], [48] uses an averaging algorithm to obtain a common time for the master group, which is then communicated to the slaves via a fault-tolerant master group speaker. This master group speaker is a new expensive device that must be factored into the cost of the system, and essentially represents a single point of failure in the system. The multi-SOOC slave nodes proposed by [30] do not offer time synchronisation, and the isolated grandmaster clock architecture described in [52] requires co-located grandmaster nodes. Lastly, the alternate master technique [5] has limited effect as it only shortens the re-synchronisation phase.

Our target application is a network of DECT base stations at separate physical locations that are connected over an Ethernet backbone. The base stations, which do not have access to an external reference time source, require time synchronisation and reduced downtime in the event of a master failure. The drawbacks of the technique make them unsuitable for the target application. In Chapter 5, we describe the target application in more detail and propose a new alternate master cluster technique for meeting the requirements of the application.

2.5 Summary

This chapter has provided an overview of the three different research areas that comprise this thesis. Section 2.1 has defined some of the important terms related to clocks and synchronisation and described the existing classes of synchronisation algorithms.

An overview of ECMA-368 UWB has been presented and the two forms of synchronisation have been described in Section 2.2. We have shown that the existing MAC layer synchronisation is unsuitable for providing synchronisation to higher-layer MAC clients because the clocks are not corrected and hence the accumulation of clock drift leads to frequent loss of synchronisation. We have explained the usage of the higher layer synchronisation MLME primitives, but noted that no algorithms exist for implementing higher layer synchronisation. Therefore, in Chapter 3, we propose a new higher layer synchronisation algorithm for an ECMA-368 network.

Section 2.3 has provided an overview of the IEEE 1588 synchronisation protocol, explored the origin of PDV, and demonstrated the effect of PDV on PTP synchronisation. Some existing PDV algorithms in the literature have also been described. We have considered the category of PDV algorithms that filter off those packets that are heavily impacted by PDV and noted that the performance of the algorithms depends on the probability of finding "good" packets from among the received synchronisation traffic. Based on this observation, we have postulated that the probability of finding "good" packets can be maximised by selecting packets from around the mode delay

value. Hence, Chapter 4 proposes a new sample-mode PDV filtering algorithm for a PTP network.

Finally, Section 2.4 has described the default BMCA used for electing masters in the IEEE 1588 standard and explored some existing techniques for coping with master failures. We have noted that the drawbacks of the different techniques make them unsuitable for the target DECT Ethernet base station network. In Chapter 5, we will describe the target application in more detail and propose a new alternate master cluster technique for meeting the requirements of the application.

Chapter 3

Higher Layer Synchronisation in Ultra Wideband Networks

3.1 Introduction

In this chapter a synchronisation algorithm is developed for an ECMA-368 UWB network, in order to provide synchronisation for the higher layer applications or MAC clients that use the UWB network.

Section 3.2 describes the application requirements for the synchronisation algorithm, as detailed in the EUWB project documents [53]–[55]. Section 3.3 describes the process of selecting candidate algorithms for the higher layer synchronisation mechanism, before describing each algorithm in detail. Since the higher layer synchronisation algorithm is actually implemented in the MAC layer, Section 3.4 describes the design process in terms of how timestamps are transferred from the higher layer to the MAC layer before synchronisation, as well as how the computed offset and skew are transferred back to the higher layer after synchronisation. The UWB OPNET models we developed are presented in Section 3.5. Simulation results obtained from implementing the three candidate algorithms are also presented and analysed. Based on the analysis, one candidate algorithm is selected and implemented on an FPGA UWB platform developed at TES Electronic Solutions Ltd. Section 3.6 gives an overview

of the FPGA platform, describes the modifications that were made in order to implement the algorithm, and presents some results obtained from implementation on the platform. A summary of the chapter is provided in Section 3.7.

3.2 Application Requirements

Real-time video streaming is an important application for the EUWB research project, in which two scenarios were considered: wireless aircraft cabin management systems [53], [54] and wireless home entertainment systems [55]. A typical use case for the former scenario involves the transmission of video, such as in-flight entertainment, from a cabin server to wireless passenger display units; while the latter might involve the transfer of video from portable media players to a central hub for subsequent streaming to television sets. A generic network topology suitable for either scenario consists of a video server streaming packets to multiple end devices over Ethernet and UWB links and via switches and access points, as illustrated in Fig. 3.1.

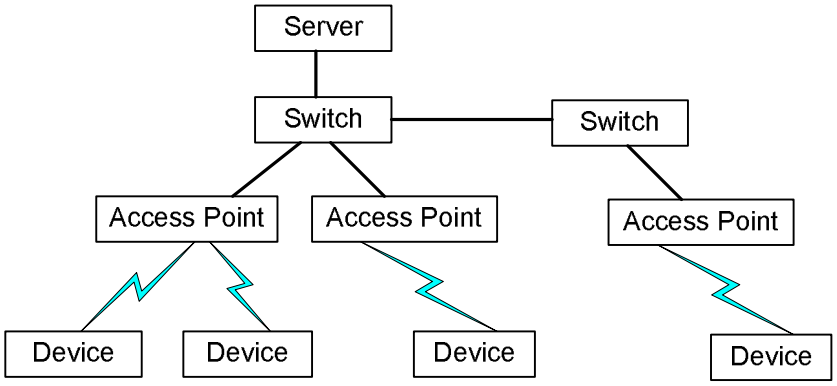

FIGURE 3.1: Generic network topology.

The generic network consists of a central server system from which data can be transferred to various wired and wireless end devices via switching units and wireless Access Points (APs). Multi-hops from a wireless AP to a device are not required. Two main types of traffic are transmitted over the network: multimedia and control traffic. Multimedia includes pure audio signals from loudspeakers, pure video signals from CCTV images, and a combination of audio and video signals (AV streaming) from in-flight

entertainment. Here, control traffic, refers to all other forms of data transmitted over the network, including data from sensors such as smoke detectors, lighting control data and data from cabin control terminals such as Passenger Service Units (PSUs) and exit signs. Traffic is transmitted from the server to the APs via switches. The AP forwards the traffic to the devices within its beacon group and apart from the mandatory exchange of beacons, there is no other communication between the end devices in the network.

There are two key QoS requirements for the network, namely: minimising packet jitter and minimising the timing difference between co-located devices. Packet jitter, also known as inter-packet delay variation, is the variation in end-to-end delays experienced by consecutive packets from the same stream. Factors such as lack of transmission opportunity, prioritisation of different streams, packet retransmission or the lack of guaranteed bandwidth in wireless networks generally give rise to packet jitter and a jitter buffer is commonly used to minimise the effects of jitter. Large delay variations, however, require a larger, more expensive buffer and ultimately results in the introduction of a larger amount of constant latency at the start of the application that is unsuitable for real-time streaming. Timing difference refers to the difference in the event start times of multiple end devices, e.g. audio playback in loudspeakers. When such end devices are in close proximity, minimising the timing difference becomes an important requirement in order to prevent distortion and achieve a satisfactory QoE for the end user. As well as minimising the timing difference between devices, synchronisation can reduce the size (and ultimately, cost) of the jitter buffer.

The requirements document for the EUWB project [53] specifies that the higher layer synchronisation mechanism must deliver a precision of 100μs or better across the entire network and must be scalable such that it can be extended from a simple beacon group of UWB devices to the larger scale hybrid wired/wireless network illustrated in Fig. 3.1.

3.3 Selection of Algorithms

Due to the sheer number of synchronisation algorithms available in the literature, it would have been onerous and impractical to sift through all of them to determine the most suitable one for the generic network. Hence a more realistic approach was adopted to first determine the most suitable class of algorithm for the network, and then analyse the algorithms within that class to see which one(s) could satisfy the application requirements. The specific class of algorithms was determined based on the classification described in Section 2.1.2.

Due to the hierarchical nature of the generic network and the fact that direct communication between devices is not required, a master-slave synchronization approach with clock correction is necessary in order to ensure that all devices on the network are synchronised. For the same reasons a sender-to-receiver algorithm is implied, although a receiver-to-receiver algorithm can be implemented provided that the time comparison occurs between the sender and receiver, as is the case of the Continuous Clock Synchronization algorithm described in [56]. Furthermore, the algorithm will support internal synchronisation since the nodes may not have access to a trusted external time source. Finally, a deterministic approach is necessary in order to guarantee the accuracy of the system.

Based on this classification, two candidate algorithms were selected, namely: Delay Measurement Time Synchronisation algorithm [57] and Continuous Clock Synchronisation algorithm [56], [58]. We also proposed a Linear Rate Synchronisation algorithm that fits with the desired class of algorithms. The following sub-sections describe these three algorithms.

3.3.1 Delay Measurement Time Synchronisation algorithm

The Delay Measurement Time Synchronisation algorithm combines a master's timestamp with delay measurements, in order to achieve synchronisation of the slaves. Each slave takes two timestamps: one when it receives the preamble of the synchronisation

message, and the other after the message has been processed. The difference between these timestamps is a measure of the data transfer time plus the processing delay. Each slave also estimates the time taken to transmit the message preamble. Finally, each slave sets its clock to the sum of the master's timestamp, the data transfer time plus processing delay, and the preamble transmission time.

3.3.2 Continuous Clock Synchronisation algorithm

The Continuous Clock Synchronisation algorithm uses an advanced rate-adjustment algorithm to spread clock correction over a finite interval in order to prevent the time discontinuity caused by instantaneous clock correction. In this way, the local clock time is corrected by gradually increasing or decreasing the clock rate. Each node in the network has both a physical and virtual clock. In this sense, a virtual clock is simply a transformation function that corrects the skew rate of a physical clock. For the sake of simplicity, a linear function is used and clock correction is achieved by changing the parameters of this function after every synchronisation round so that the slave's virtual clock matches the master's physical clock as closely as possible. The algorithm assumes that message reception is tight, such that a master node receives its own broadcast message at approximately the same time as the slave nodes [58]. Each synchronisation frame contains the time at which the master node received the last synchronisation message sent and by comparing this value with its own reception time for the same message, a slave is able to achieve synchronisation with the master.

The ECMA-368 PCA and DRP data transmission mechanisms do not permit any node to receive its own broadcast frame, hence adapting the Continuous Clock algorithm to a UWB network requires a calculation of the expected reception time at the master node. The processing delay between the synchronisation frame being scheduled by the MAC and the first symbol being received on-air by the remote device can be added to the master's transmission timestamp in order to obtain this value [59].

3.3.3 Linear Rate Synchronisation algorithm

Another possible implementation of synchronisation is based on a linear-rate function which relates a slave's clock to the master's clock. The master sends its timestamp to the slaves in the form of a command frame every synchronisation round and each slave records its local clock time when it receives the synchronisation frame, thus building a table of pair values in the form $[M_n S_n]$, where M_n is the local clock time at which the master sent the nth synchronisation frame and S_n is the local time at which the slave received the same frame. After two rounds the slave can calculate the relative skew σ and relative offset θ as follows:

$$\sigma = \frac{M_n - M_{n-1}}{S_n - S_{n-1}}. \tag{3.1}$$

$$\theta = M_n - \sigma S_n. \tag{3.2}$$

These values are then used to update the parameters of its virtual clock V which transforms the hardware clock H to mimic the behaviour of the master's clock as shown in (3.3).

$$V = \sigma H + \theta \tag{3.3}$$

3.4 Design of the Higher Layer Synchronisation Mechanism

As stated in Section 2.2.2.2, the ECMA-368 standard includes three MLME primitives to support the higher layer synchronisation function. The *MLME-HL-SYNC.request* primitive is sent from the higher layer to the MAC to initiate the synchronisation mechanism, the *MLME-HL-SYNC.confirm* returns the result of the request, while the *MLME-HL-SYNC.indication* primitive indicates the transmission or reception of a synchronisation frame.

Since the goal is to synchronise the clocks of higher layer protocols which may reside separately from the MAC, it makes sense for the MAC to be responsible for implementing the synchronisation algorithm. Before synchronisation, the higher layer clock value or timestamp on both master and slave devices must be transferred to the MAC layer. Furthermore, after synchronisation is complete, there is an additional requirement for transferring the calculated clock adjustment back to the higher layer on the slave device. The manner of fulfilling the first requirement depends on whether the MAC and higher layer protocol reside on the same entity or on separate entities, i.e. whether or not the MAC layer can directly access the higher layer clock. Both cases are considered in the following sub-sections. For the second requirement, a new service primitive has been defined: the *MLME-HL-CLOCK-UPDATE.indication* will transfer the calculated clock offset and skew back to the higher layer so that the parameters of the higher layer virtual clock can be updated.

3.4.1 Case 1: MAC Layer and Higher Layer Application on separate entities

In this case, the MAC layer has access to the PHY clock but not to the higher layer clock. Thus, there is a need for mapping higher layer clock values to PHY layer clock values, since it is the higher layer clock timestamps that are required as parameters of the synchronisation algorithm. This is the case in the OPNET UWB simulation model.

The higher layer clock values are transferred to the MAC layer using the timestamp field of an empty Real Time Protocol (RTP) packet. The generation of the RTP packet is triggered by the receipt of the *MLME-HL-SYNC.confirm* primitive at the higher layer. The MAC layer reads the PHY clock value immediately it obtains the higher layer clock and then calculates the relative offset between the higher layer and PHY layer clocks. The MAC subsequently uses this offset to transform a PHY layer clock reading to the corresponding higher layer value, as needed.

Furthermore, the receipt of an *MLME-HL-SYNC.indication* primitive also triggers the transfer of the higher layer clock to the MAC via an RTP packet. On receipt of this, the MAC again reads the PHY clock and subsequently updates the relative offset. This is particularly important when a synchronisation frame is received so that the slave device can transform its PHY reception timestamp value into the corresponding higher layer clock equivalent, before clock adjustment computations are done.

3.4.2 Case 2: MAC Layer and Higher Layer Application on the same entity

In this case, the MAC layer has direct access to both the PHY clock and the higher layer clock. Thus, the MAC can directly access the higher layer clock value, as needed, by simply reading the corresponding register. This is the case that exists on the (Very) High Data Rate ((V)HDR) FPGA UWB platform. For optimum performance of the synchronisation mechanism, the MAC layer updates the higher layer clock timestamp within the synchronisation frame just before transmission over the air.

3.5 Network Modelling and Simulation

Network modelling and simulation is a useful technique for designing and analysing protocols and applications for communication networks. OPNET Modeler [60] was selected because it is a powerful modelling tool for network design and analysis with in-built support for wireless network simulation. The huge library of ready-to-use network models includes an optional Wireless Suite with models for networks such as WLAN, UMTS, and Zigbee. Although there was no existing model for UWB, the huge amount of documentation provided as part of the built-in model libraries, together with the user-friendly nature of the software allowed us to develop a suitable UWB model for this project. The software was obtained free of charge under the University Program licence agreement.

3.5.1 Network Modelling

Each simulation project in OPNET has a hierarchical structure that is functionally split into three levels. The highest level is the network level which describes the physical layout of the network; individual devices like switches and servers are modelled at the node level, while the lowest process level is used for modelling individual protocols such as MAC and RTP. Editors are defined for specifying or modifying the features of each hierarchical level. The Network Editor is used to define the topology and characteristics of the network, the Node Editor describes the internal architecture of the nodes by illustrating the flow of data between the constituent modules in a node, while the Process Editor describes the behaviour and functionality of the programmable modules, using a Finite State Machine (FSM). Every state in the process editor includes C/C++ code with a functions library, which can be used for programming communication protocols.

3.5.1.1 OPNET Model for a UWB Beacon Group

Network Model

Our network model for a beacon group consists of at least two UWB nodes, one of which has AP functionality, as shown in Fig. 3.2. In this implementation, the AP is the initiator of all transmissions and serves as the master to which the other device(s) synchronise. Furthermore, the AP's DRP reservation MAS map is used for the entire beacon group such that a DRP Tx slot for the AP represents a DRP Rx slot for devices in its beacon group and vice versa.

FIGURE 3.2: OPNET network model for UWB beacon group.

Node Model

At the node level, each device consists of a source module, sink module, MAC interface module, MAC module and transceiver units, as illustrated in Fig. 3.3. The source is responsible for generating packets, the sink consumes packets, the MAC interface performs address resolution, while the MAC implements those functionalities of the ECMA-368 MAC layer described in Section 2.2.1, but using only the DRP data transfer mechanism. The source module is based on the standard OPNET *bursty_source* model with three states: an *INIT* state in which parameters are initialised, an *ON* state in which RTP packets are generated, and an *OFF* state in which no packets are generated.

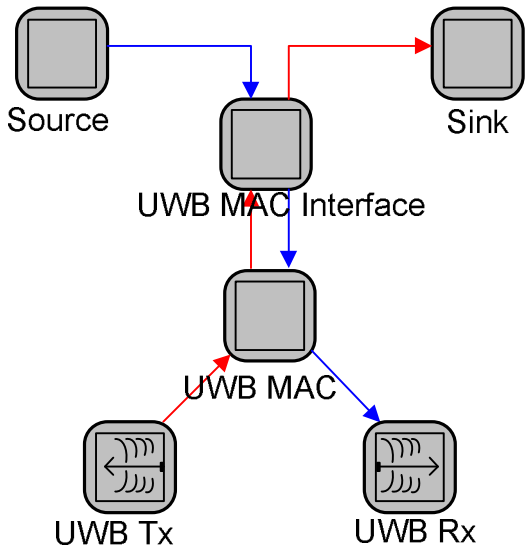

FIGURE 3.3: OPNET UWB node model.

The MAC interface module ensures that packets generated by a node are sent to valid MAC addresses. If the higher layer synchronisation mechanism is supported, then this module is also responsible for sending the *MLME-HL-SYNC.request* primitive at the start of the synchronisation process and for transferring the higher layer clock information to the MAC module using the header field of empty RTP packets. Each node also contains a higher layer clock and a PHY clock, both based on the drifting clock model presented in [61].

Process Model

The FSM for the UWB MAC module is illustrated in Fig. 3.4.

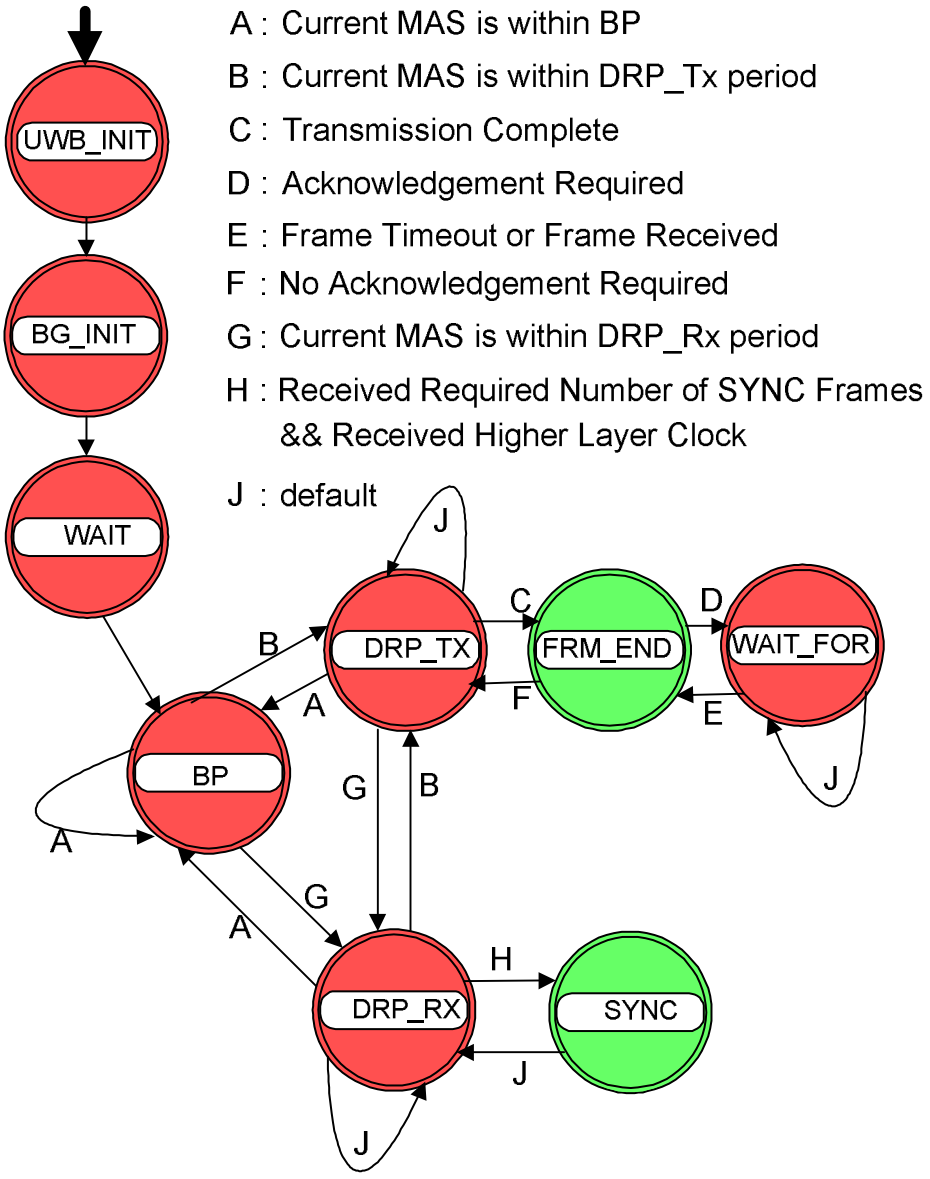

FIGURE 3.4: OPNET process model for UWB MAC.

Initialisation of variables and module registration take place during the *UWB_INIT* state. The *BG_INIT* state registers the node within a beacon group and gets information about other nodes within its beacon group. In the *WAIT* state, the MAS allocation map within a superframe is defined based on the DRP reservations for the node. The beacon period is not explicitly modelled so no beacon frames are actually transmitted; however the BP state observes the corresponding time interval to

ensure that no data frames are transmitted while in this state. At the end of the beacon period a node transitions to either the *DRP_Tx* or *DRP_Rx* state to begin transmitting or receiving data, respectively. The *DRP_Tx* state represents the hard DRP MAS reservation slots in which the reservation owner can transmit data or synchronisation frames while the *DRP_Rx* state represents the same hard DRP slots at the receiving device. The purpose of the *FRM_END* state is to determine the next state to transition to after the successful transmission of a frame. If the transmitted frame requires an acknowledgement, the node transitions to the *WAIT_FOR* state to wait for either the acknowledgement to be received or the timeout period to elapse, else it returns to the *DRP_Tx* state to resume frame transmission. A node transitions from the *DRP_Rx* state to the *SYNC* state when it has received the required number of synchronisation frames for the particular synchronisation algorithm and when the higher layer clock information has been received from the MAC Interface module.

3.5.1.2 OPNET Model for a Larger Scale Network

Network Model

Our network model for the larger scale network is similar to the generic network of Fig. 3.1 with at least one AP and at least two end devices, as shown in Fig. 3.5.

The key issue in extending the synchronisation protocol to a larger network is the task of transferring the server clock information to the AP. Once this is accomplished, the AP can use the same synchronisation approach proposed for the beacon group to synchronise the end devices. As previously mentioned, an empty RTP packet can be used to transfer the server clock information to the AP; however in order for this value to be accurate, the processing delay or latency on the path between the server and the AP must be estimated and added to the original clock information. The *Sync and Sense* method proposed by the authors of [62] is useful for estimating this delay as it uses regular RTP packets to sense the network and determine the delay.

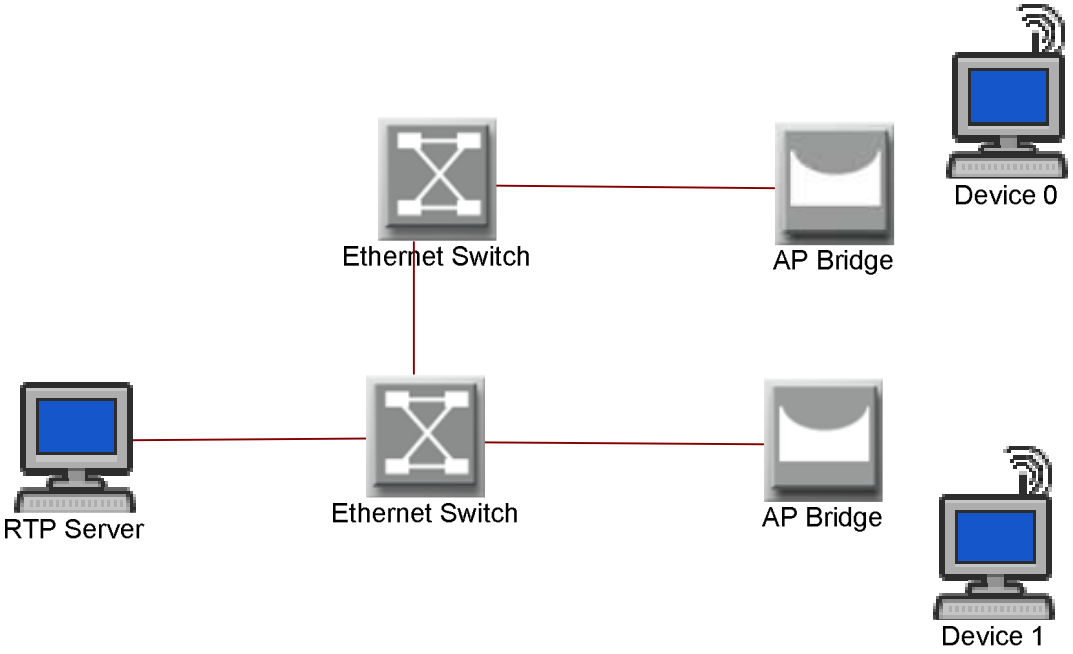

FIGURE 3.5: OPNET network model for larger scale network.

Node Models

The RTP server node model consists of source, sink, Ethernet MAC Interface and Ethernet MAC modules, together with transceiver units, as illustrated in Fig. 3.6.

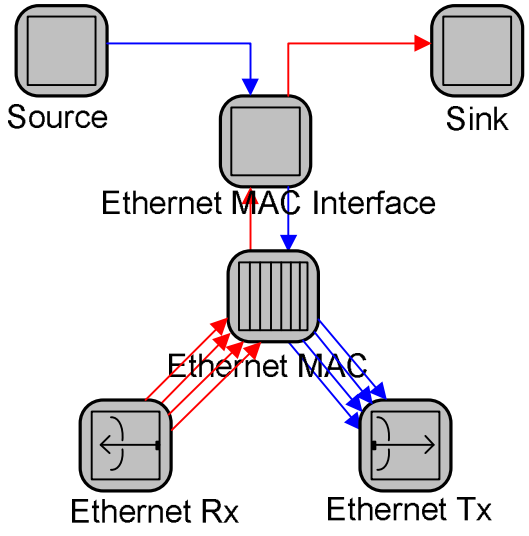

FIGURE 3.6: OPNET node model for RTP server.

The source module is responsible for generating RTP packets according to the user-specified traffic characteristics. It also periodically sends its clock information in the form of empty RTP packets every synchronisation interval. The sink, Ethernet MAC

Interface and Ethernet MAC modules are standard OPNET library models and hence they do not warrant further explanation. The multi-port Ethernet switch is also a standard OPNET library model that performs layer 2 switching functions.

The AP Bridge is responsible for connecting the wired Ethernet network to the wireless UWB network. Consequently, the implementation of this node in OPNET consists of both wired and wireless segments with two MAC modules, as illustrated in Fig. 3.7. The Ethernet MAC and Standard Bridge Functions modules are standard OPNET library process models while the UWB PAL serves as the interface between the UWB MAC and the higher layer MAC clients.

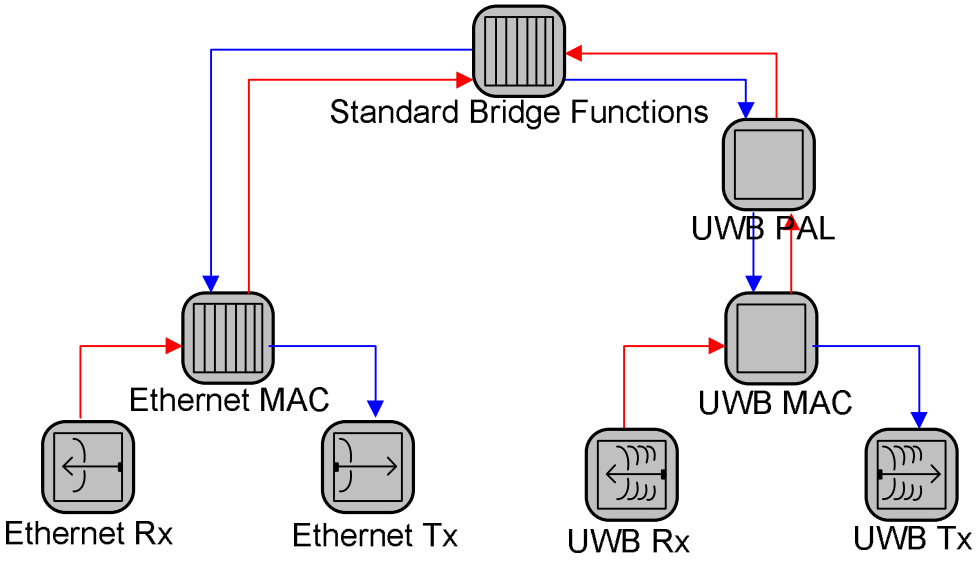

FIGURE 3.7: OPNET node model for AP bridge.

3.5.2 Results and Analysis

At the start of each simulation, the system is assumed to be operating in an active quiescent state, i.e. operating channels have been selected, the nodes are initially synchronized, and a beacon group has been formed. Furthermore, hard DRP reservations have already been negotiated and the nodes are ready to send and receive data over these reservations.

3.5.2.1 Simulations within a UWB Beacon Group

We simulated the simple two node beacon group illustrated in Fig. 3.2. The AP acted as the master while the device was the slave, with clock drift rates of 0ppm and -20ppm respectively. The synchronisation interval was 2.5 s and the target accuracy was 100 μs. The three candidate synchronisation algorithms were simulated in turn and each simulation was run for a period of 20 s. We also considered the scenario in which no synchronisation algorithm was applied. The results are presented in Fig. 3.8.

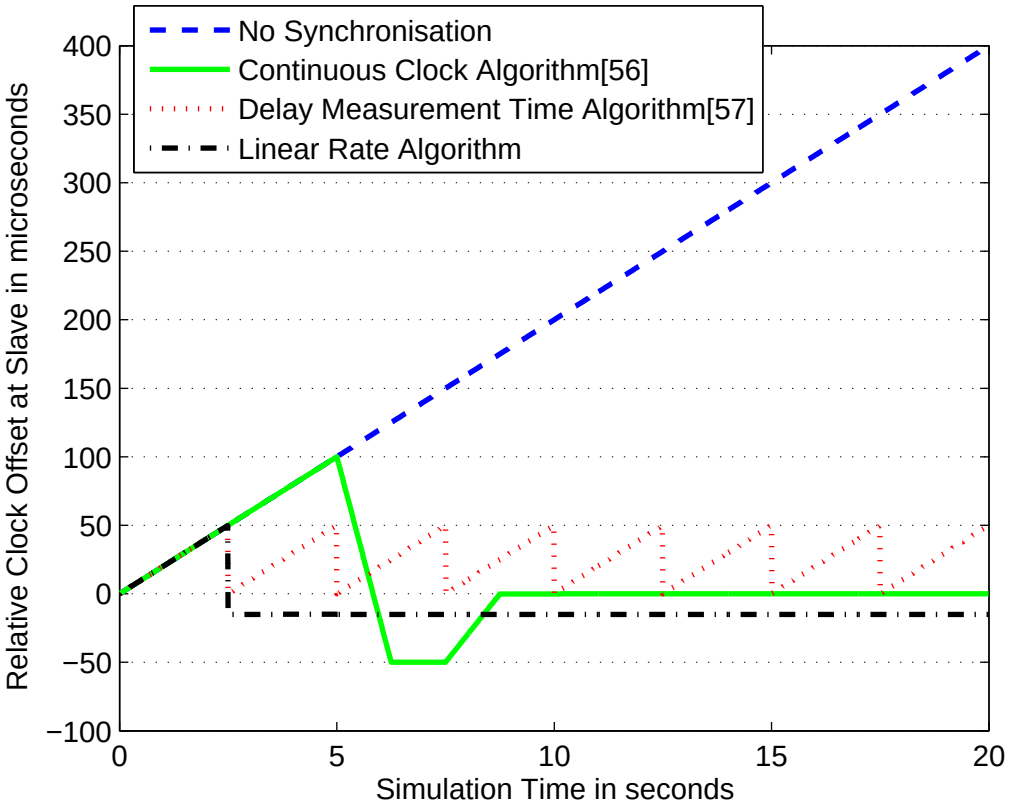

FIGURE 3.8: OPNET simulation results for a UWB beacon group.

As expected, without synchronisation the relative clock offset of the slave with respect to the master accumulates linearly, at a rate equal to the difference in their clock drifts. After each synchronisation round, the Delay Measurement Time algorithm reduces the clock offset to zero but between rounds the offset accumulation resumes. Since the Continuous Clock and Linear Rate algorithms correct for clock drift, they perform better than the Delay Measurement Time algorithm and are able to maintain synchronisation within the target accuracy of 100 μs for longer periods

between synchronisation rounds. Hence, we only consider the Continuous Clock and Linear Rate algorithms when simulating the larger hybrid network.

3.5.2.2 Simulations within a Larger Scale Network

We also simulated the larger scale UWB network illustrated in Fig. 3.5 in order to demonstrate the scalability of the higher layer synchronisation protocol. The clock drift rates were 0ppm for the RTP server, 20ppm for Device_0, and -10ppm for Device_1. The synchronisation interval was kept at 2.5 s and the simulation was also run for 20 seconds for the Continuous Clock and Linear Rate synchronisation algorithms. The results are provided in Fig. 3.8.

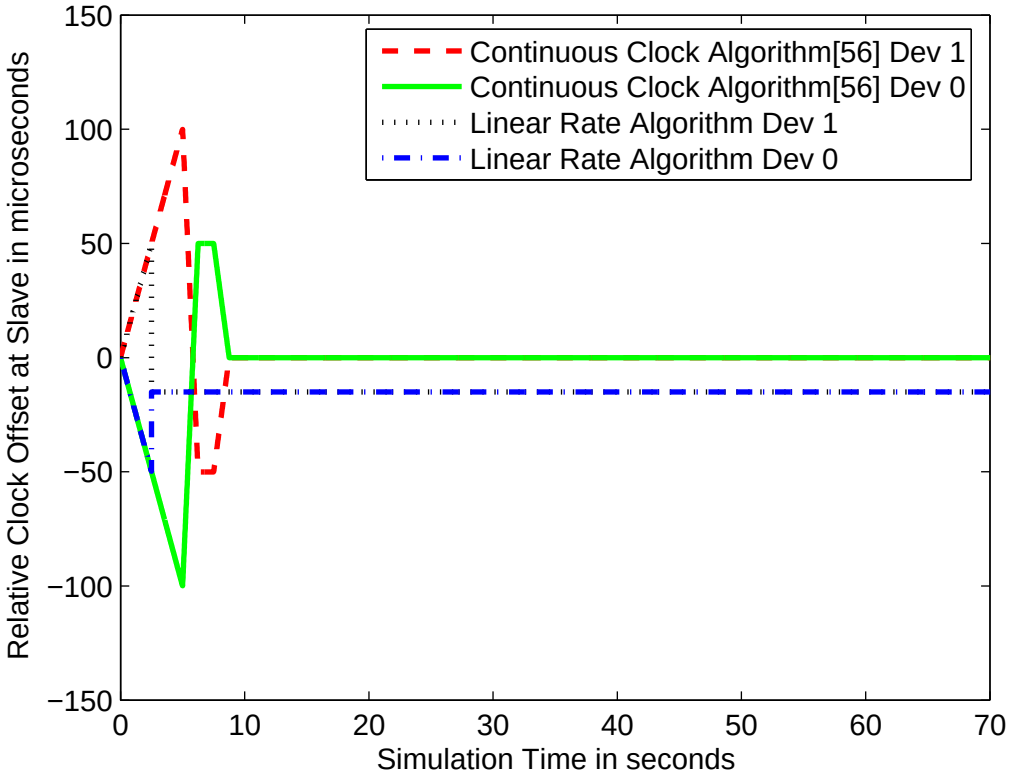

FIGURE 3.9: OPNET simulation results for larger scale network.

Again, the results show that the two drift-correcting algorithms are able to bring the end devices back to synchronisation with the server, within the target accuracy of 100 μs.

3.5.2.3 Analysis of Results

The simulation results shown in Fig. 3.8 and Fig. 3.9 indicate that the Continuous Clock and Linear Rate algorithms which correct for clock drift perform better than the Delay Measurement Time algorithm as they are able to maintain synchronisation within the target accuracy of 100 μs for longer periods between synchronisation rounds.

To identify the best algorithm for implementation, we consider the effects of packet loss and temperature variation. Packet loss results in missed synchronisation rounds while the latter may change the rate of clock drift. In algorithms, such as the Delay Measurement Time algorithm, that do not correct for clock drift, the effect of packet loss is similar to the case of no synchronisation as the clock offset will accumulate linearly beyond the target accuracy level. Such algorithms would also be least resistant to large changes in clock drift because they would no longer be able to achieve the target accuracy using the same synchronization interval.

Finally, although the Continuous Clock synchronisation algorithm yielded a better clock offset after convergence than the Linear Rate algorithm, the Linear Rate algorithm is more suitable for implementation on the UWB platform. This is because the Continuous Clock algorithm relies on the ability of the master node to receive its own broadcast frame, but the DRP and PCA mechanisms do not permit this. In the OPNET model, the processing delay between the synchronisation frame being scheduled by the MAC and the first symbol being received on-air by the remote device was added to the master's transmission timestamp in order to obtain an estimated reception time at the master node but this will not be possible on the platform. Therefore, from an implementation perspective, the Linear Rate algorithm is more suitable than the Continuous Clock algorithm. However, in order to improve its performance, the higher layer clock timestamp in each synchronisation should be updated prior to transmission. This will further reduce the residual clock offset in the linear rate algorithm.

3.6 Implementation on an FPGA Platform

Comparing the performance of the three potential synchronisation algorithms in Section 3.5.2 revealed that the linear rate algorithm was the most suitable for implementation. This section details the process and results of implementing this linear rate algorithm on the UWB Demonstration platform developed in-house at TES Electronic Solutions Ltd. Section 3.6.1 describes the TES UWB Demonstration Platform, Section 3.6.2 describes the modifications that were made in order to support the higher layer synchronisation mechanism, while Section 3.6.4 provides the results obtained from the platform.

3.6.1 Overview of the TES UWB Demonstration Platform

The TES UWB Demonstration platform consists of ECMA-368 MAC and PHY layers on which applications (e.g. video streaming or file transfer) are run. The MAC is implemented as a combination of digital hardware and software on an FPGA development platform while the PHY, which includes both the Radio Frequency (RF) and Baseband functionality, is provided on a daughter card. The platform also includes a MAC/ PHY interface that complies with the ECMA-369 specification [63]. The MAC module is implemented on a Virtex-5 FXT FPGA ML507 Evaluation board [64] while the PHY module is supplied by a third party as shown in Fig. 3.10. A Gigabit Ethernet host interface and thin client layer are provided on the firmware released with the development platform in order to facilitate direct implementation of IP-based application scenarios such as video streaming.

Fig. 3.11 illustrates the sub-system architecture of the platform. The functionality of the ECMA-368 MAC layer has been split into 3 sub-layers on the demonstration platform: the Upper MAC (UMAC), Lower MAC (LMAC), and Hardware MAC (HMAC). The UMAC is responsible for managing the exchange of protocols between peer MAC entities. It provides support for the MLME primitives via the MLME SAP and is responsible for managing the data flows on the medium. The data flows are managed in the form of links on the medium; each link identified by the pair of (Device

FIGURE 3.10: 3rd Party PHY daughtercard on TES Virtex-5 FPGA MAC.

Address, Stream Index) for the DRP channel access mechanism. The LMAC manages the transmission and reception of multiple streams of frames over the medium; each stream possessing a set of allocated MAS within a superframe. It is also responsible for the immediate control of the HMAC.

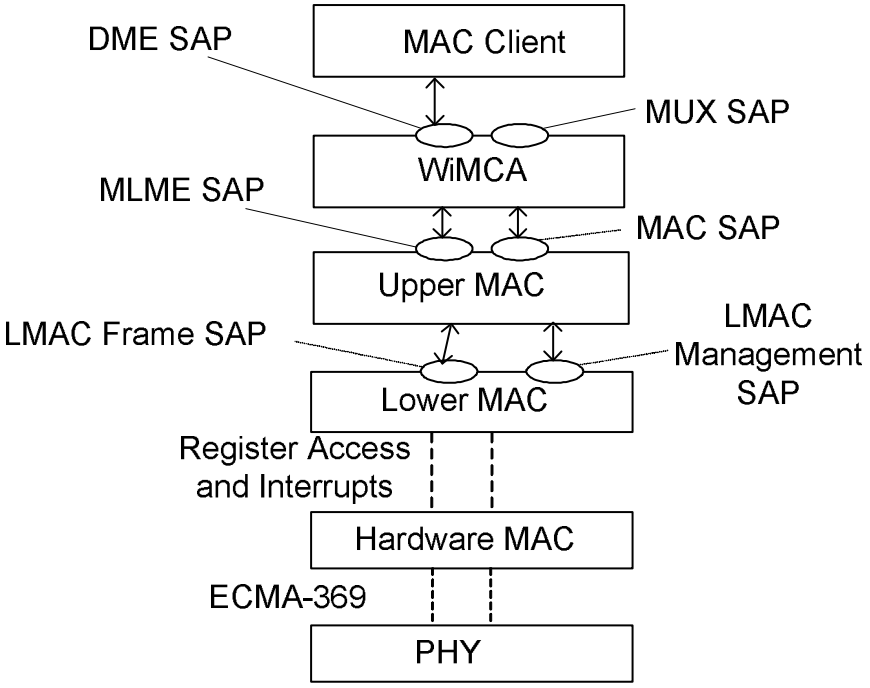

FIGURE 3.11: Sub-system architecture of TES demonstration platform.

The MAC client for the UWB platform is light-weight IP (lwIP). lwIP [65] is a low-resource open source TCP/IP stack developed for embedded systems. This makes it possible to run IP-based applications such as multimedia streaming and file sharing

over the UWB PHY. A host demonstration application provides an interface for initialising the platforms and making the hard DRP reservations required by the MAC client.

The host demonstration application supports two application types: MAC Performance Evaluation in which test frames are transmitted for the purpose of testing and evaluating the performance of the MAC sublayer, and IP over UWB (IPoUWB) for transmitting real IP packets over the UWB link. For each application type, a UWB node can either be the initiator (i.e. a local "server" device), or the target (i.e. a local "client" device) of the application. Furthermore, the IPoUWB application type supports both streaming and non-streaming modes for User Datagram Protocol (UDP) and Transmission Control Protocol (TCP) applications, respectively.

The type of reservation required depends on the type of application. Streaming applications, such as video transfer, use most of the MASs in the superframe for transmission of data, as illustrated in Fig. 3.12.

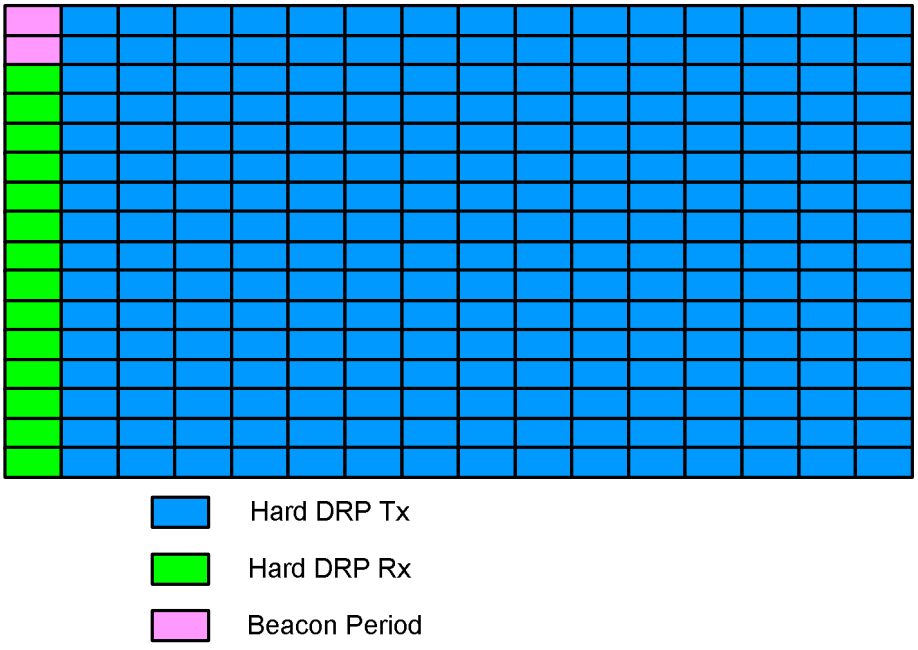

FIGURE 3.12: IPoUWB MAS reservation map at initiator for streaming mode.

For the TCP-based non-streaming mode, the split between Tx and Rx slots is approximately 50/50 as shown in Fig. 3.13, since TCP requires acknowledgments from the receiver. Fig. 3.12 and Fig. 3.13 show the MAS reservation map for each superframe,

from the perspective of the application initiator or server. At the target device, the Tx slots are Rx slots, and vice versa, but the beacon period is identical.

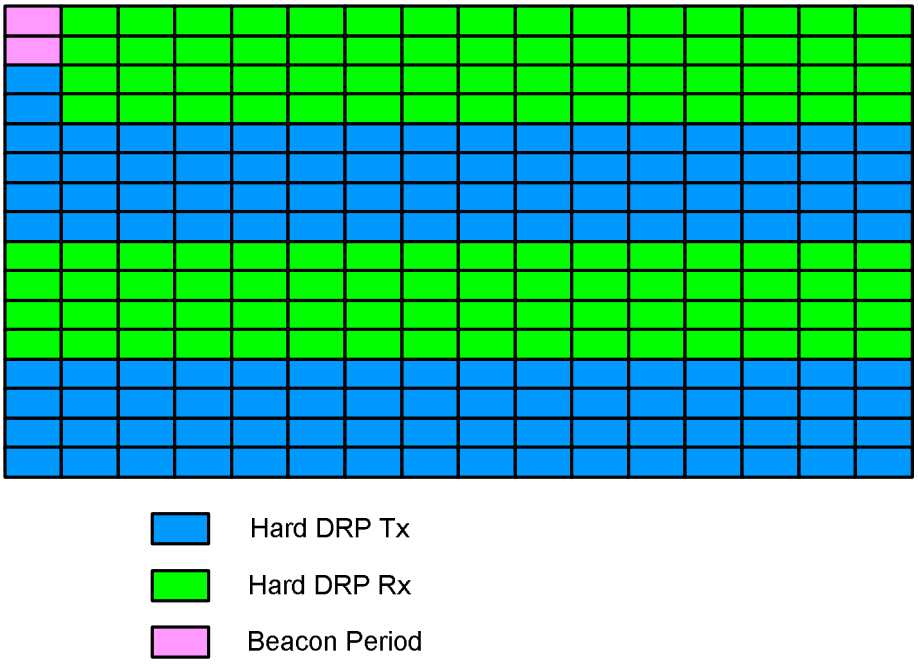

FIGURE 3.13: IPoUWB MAS reservation map at initiator for non-streaming mode.

3.6.2 Modifications to the TES UWB Demonstration Platform

In this section, we detail the modifications and extensions that were done on the platform in order to support the higher layer synchronisation mechanism.

3.6.2.1 Updating the Host Demonstration Application

Since the MAC Performance Evaluation application is purely for test purposes, it does not support the higher layer synchronisation mechanism. However, the synchronisation mechanism is supported for both streaming and non-streaming modes of the IPoUWB application. The IPoUWB application initiator also serves as the Sync Master, while the IPoUWB target serves as the Sync Slave. Thus, the target device synchronises to the initiator using the timestamps it provides.

Additional features have been added to the C# host demonstrator application, in order to facilitate the higher layer synchronisation mechanism. These features allow a user to select a particular synchronisation interval between 2.5 and 30 seconds, select a multicast EUI address for transmitting the synchronisation frames, and click a button for enabling the higher layer synchronisation mechanism, as illustrated in Fig. 3.14.

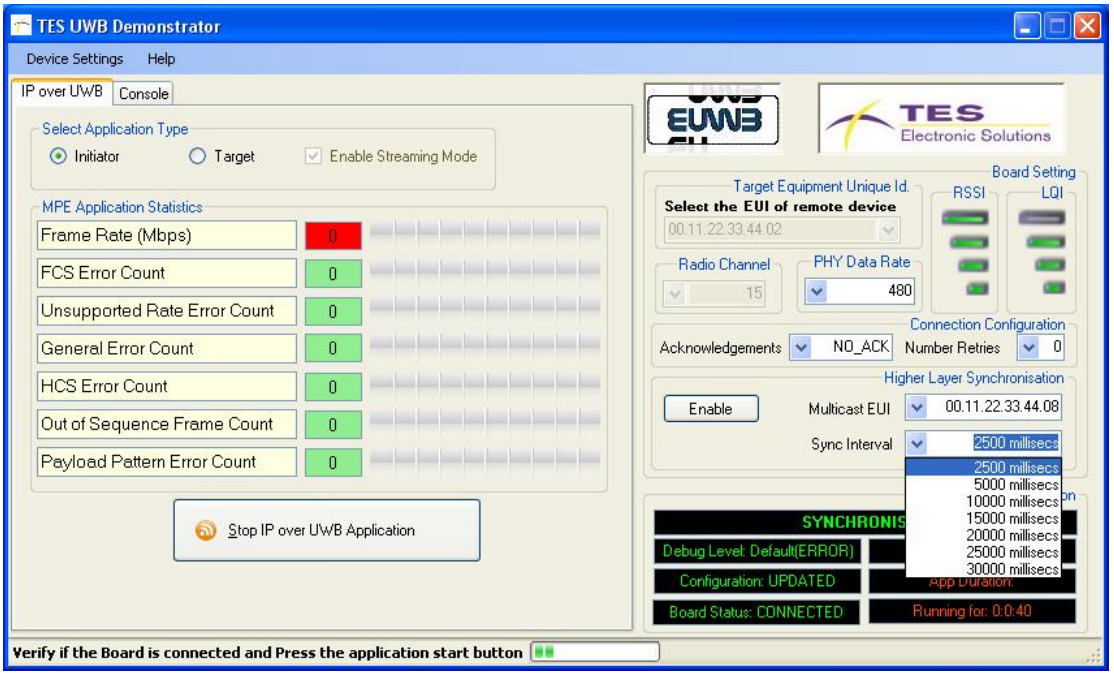

FIGURE 3.14: Extended functionality of host demonstration application.

3.6.2.2 Extending the PAL

In extending the PAL, a new primitive was created and a higher layer clock was configured.

1) *New Primitive:* A new primitive *APP-DeviceHigherLevelSync.request* is generated and passed to the PAL when the higher layer synchronisation mechanism is enabled on the host demonstrator application. This starts the process of higher layer synchronisation and ensures that the multicast EUI address and user-defined synchronisation interval are passed to the MAC layer. The message parameters for this primitive are shown in Table 3.1.

TABLE 3.1: Message parameters for *APP-DeviceHigherLevelSync.request*.

Name	Type	Description
tMcstEUI	tEUI48	Multicast destination address for synchronisation frames
u16HLSyncInterval	u16	User-defined synchronisation interval in milliseconds

2) *Higher Layer Clock:* A higher layer clock was configured at each UWB node, based on the 125 MHz 32-bit XPS Timer/ Counter module which is attached to the processor bus. A full specification of the clock is provided in [66]. The higher layer clock is implemented in two forms: the hardware/ physical clock and the virtual clock. As described in Section 3.3.3 , the virtual clock is simply a linear function comprising of offset and skew parameters which can be changed to transform the value of the physical clock in order to achieve synchronisation with another clock.

3.6.2.3 Modifications in the MAC layer

As described in Section 3.4, it makes sense for the synchronisation algorithm to be implemented in the MAC, so that it can be accessed by any MAC client. On the TES demonstration platform, the implementation is done in the UMAC. Thus the modified UMAC also provides a service to send synchronisation frames to peer MAC entities. The modifications done in the MAC layer include the creation of a new synchronisation stream, low-layer timestamping, and the creation of MLME primitives.

1) *Synchronisation Stream:* In the OPNET network simulation, the timestamps were transmitted in the form of command frames; however for the (V)HDR platform demonstration, data frames were used instead. This was due to the fact that the transmission and reception of command frames, which was outwith the scope of this thesis, was not yet fully implemented on the platform. Since transmission of data frames is achieved by creating links in the UMAC and streams in the LMAC, the transmission and reception of sync data frames required a separate link and stream, with a corresponding set of allocated MASs.

For both streaming and non-streaming modes of the IPoUWB, two MASs in each superframe were used for the transmission of synchronisation data frames, as depicted in Fig. 3.15 and Fig. 3.16.

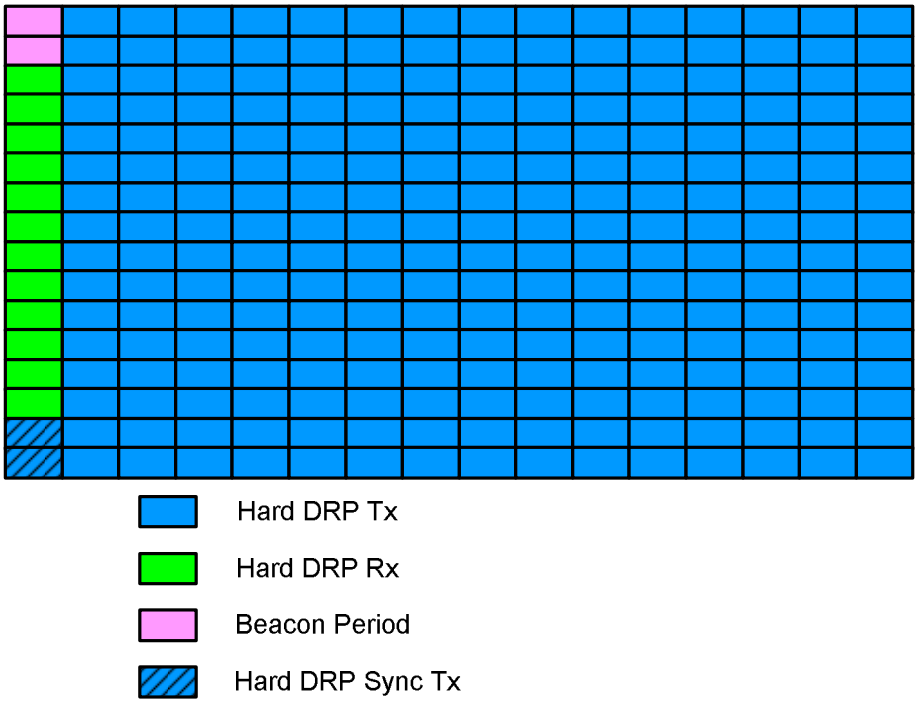

FIGURE 3.15: Modified IPoUWB MAS reservation map at initiator for streaming mode with higher layer synchronisation.

2) *Low-layer Timestamping:* Since synchronisation frames can only be sent on a synchronisation stream which occurs at a specific point in the superframe, the synchronisation interval in terms of superframes is computed using (3.4), where f represents the synchronisation interval in seconds and 0.065536 is the length of a superframe in seconds.

$$SyncInt_{SF} = \frac{f}{0.065536}. \tag{3.4}$$

If a synchronisation frame is sent during superframe i, then the next synchronisation frame will be sent in superframe $(i + SyncInt_{SF})$. The PAL prepares the synchronisation frame containing the current higher layer clock value of the sync master at the start of the superframe. The synchronisation frame is then

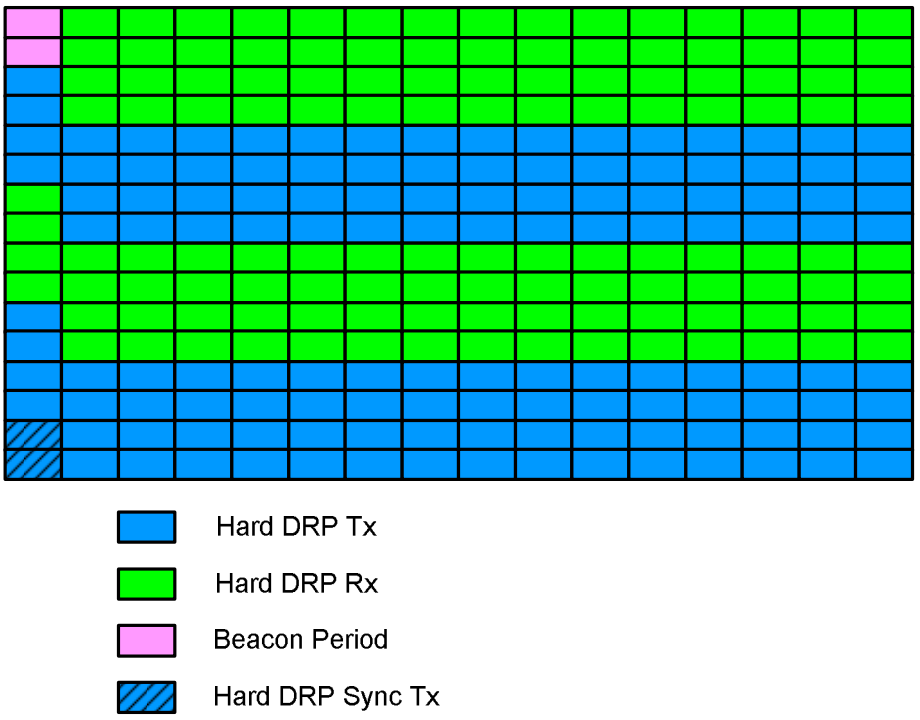

FIGURE 3.16: Modified IPoUWB MAS reservation map at initiator for non-streaming mode with higher layer synchronisation.

transferred to the UMAC and subsequently queued in the LMAC until the synchronisation MASs are reached. This queuing in the LMAC introduces some latency, measured in Fig. 3.17, that can seriously degrade the performance of the synchronisation algorithm. To determine the latency for each synchronisation packet, we obtained the timestamp when the packet was created in the application layer and obtained another timestamp when the LMAC forwarded the packet to the HMAC for transmission. The latency was calculated as the difference between the two timestamps.

From Fig. 3.17, it is clear that the latency consists of two components: a fixed component measured at about 3320μs, and random component that varies between 0 and about 180μs. The fixed component represents the delay that is inherent in the platform, between the UMAC layer and the PHY. The random component is due to the way the scheduler handles the transmission of synchronisation frames. Even though two MASs are reserved for the synchronisation frames, the scheduler does not always begin transmission at the start of the slot. Since the magnitude of the latency is very much larger than the desired

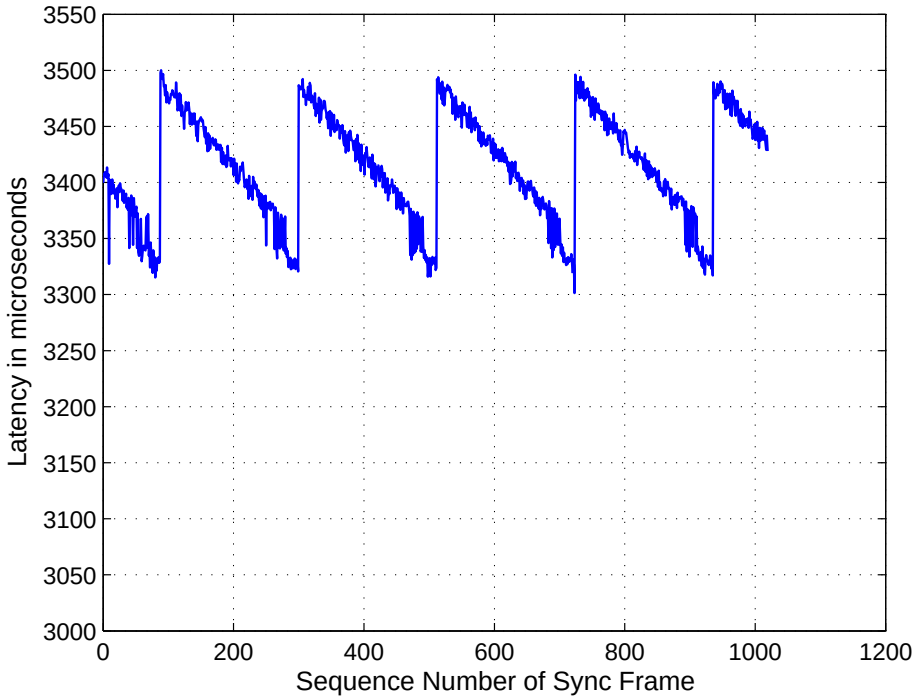

FIGURE 3.17: Sync frame transmission latency measured at Sync Master.

synchronisation accuracy, the latency must be dealt with. Hence, a key step in the synchronisation mechanism is the updating of the master's timestamp within each synchronisation frame, just before transmission of the frame. This is accomplished by the LMAC.

3) *MLME Primitives:* The MLME primitives shown in Table 3.2 to Table 3.5 were added to the (V)HDR platform, in order to support the higher layer synchronisation mechanism. *MLME-HL-SYNC.request* requests the activation of the higher layer synchronisation mechanism, *MLME-HL-SYNC.confirm* confirms the activation or non-activation of the higher layer synchronisation mechanism, *MLME-HL-SYNC.indication* indicates the transmission or reception of a synchronisation frame, while *MLME-HL-CLOCK-UPDATE.indication* indicates the completion of the synchronisation algorithm and passes the calculated clock adjustment back to the higher layer.

TABLE 3.2: Message parameters for *MLME-HL-SYNC.request*.

Name	Type	Description
GroupEUI	tEUI48	Multicast destination address for synchronisation frames

TABLE 3.3: Message parameters for *MLME-HL-SYNC.confirm*.

Name	Type	Description
eResultCode	MlmeResultCode_e	Result of the service request

TABLE 3.4: Message parameters for *MLME-HL-SYNC.indication*.

Name	Type	Description
GroupEUI	tEUI48	Multicast address that was the destination address for the synchronisation frame
SrcEUI	tEUI48	Address of the device that sent the synchronisation frame
SequenceNumber	u32	Sequence number of the synchronisation frame that was transmitted or received

TABLE 3.5: Message parameters for *MLME-HL-CLOCK-UPDATE.indication*.

Name	Type	Description
Offset_secs	u32	Computed clock offset seconds
Offset_nsecs	u32	Computed clock offset nanoseconds
OffsetPositive	bool	Sign of the computed offset
Skew	u32	Computed clock skew

3.6.3 Description of Synchronisation Mechanism on the platform

This section uses sequence diagrams to illustrate the higher layer synchronisation mechanism on the platform for both the sync master or initiator, and the sync slave or target.

3.6.3.1 Synchronisation Mechanism at the sync master

Fig. 3.18 illustrates the higher layer synchronisation mechanism at the sync master. The mechanism can be summarised as follows. The user-defined synchronisation interval in milliseconds that is passed as a parameter of the *APP-DeviceHigherLevelSync.request* service primitive is converted into units of superframe, *SyncInt_SF*, at the PAL. This

allows the PAL to determine the transmission time for the next synchronisation frame, *SyncTxTime*, by adding this value to the current superframe count, *SFn*. Thus at the start of each new superframe, the PAL checks to see if the current superframe count tallies with the transmission time for the next synchronisation frame. If it tallies, then a new synchronisation frame is prepared and sent to the MAC layer.

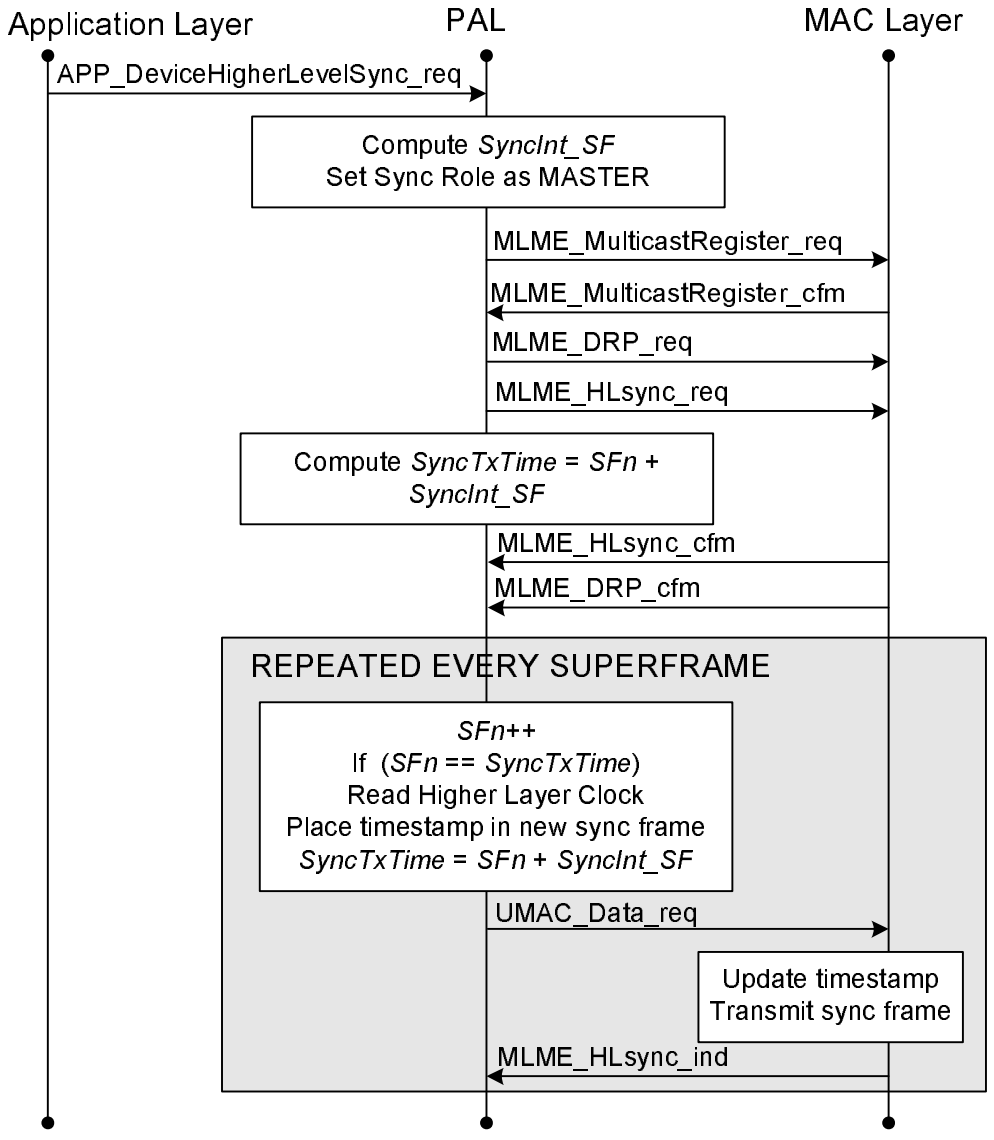

FIGURE 3.18: Sequence diagram for synchronisation mechanism at the Sync Master.

The other primitives in Fig. 3.18 are used as follows. The *MLME-MulticastRegister.request* and *MLME-MulticastRegister.confirm* primitives are for setting up and confirming

the multicast destination address for the synchronisation frames, while the *MLME-DRP.request* and *MLME-DRP.confirm* primitives are for reserving the MASs for the synchronisation frames.

3.6.3.2 Synchronisation Mechanism at the sync slave

Fig. 3.19 illustrates the higher layer synchronisation mechanism at the sync slave. Each time a synchronisation frame is received and the *MLME-HL-SYNC.indication* is sent to the PAL, the higher layer clock value corresponding to the reception time is obtained and paired with the hgiher layer clock value of the master which is contained in the synchronisation frame. After two pairs are obtained, the linear rate algorithm computes the offset and skew and passes these back to the higher layer using an *MLME-HL-CLOCK-UPDATE.indication* primitive. The offset and skew are used to update the parameters of the slave's virtual clock which transforms the hardware clock to mimic the behaviour of the master's clock.

The other primitives in Fig. 3.18 are used as follows. The *MLME-MABIE.indication* primitive notifies the MAC that a multicast address has been set up, while the *MLME-MulticastActivate.request* and *MLME-MulticastActivate.confirm* primitives are used for activating the multicast address at the sync slave.

3.6.4 Implementation Results

The implementation of the linear rate algorithm on the platform was validated by synchronising a target device to the AP initiator. In order to compare the results from the platform with the OPNET simulation results, the same clock parameters detailed in Section 3.5.2.1 were used. The results are shown in Fig. 3.20.

The result obtained from the platform is better than the corresponding simulation result, since the residual clock offset from the platform is about 15 μs less than the simulation result. This can be directly attributed to the fact that the MAC layer and the higher layer reside on the same entity. As a result, the MAC is able to obtain

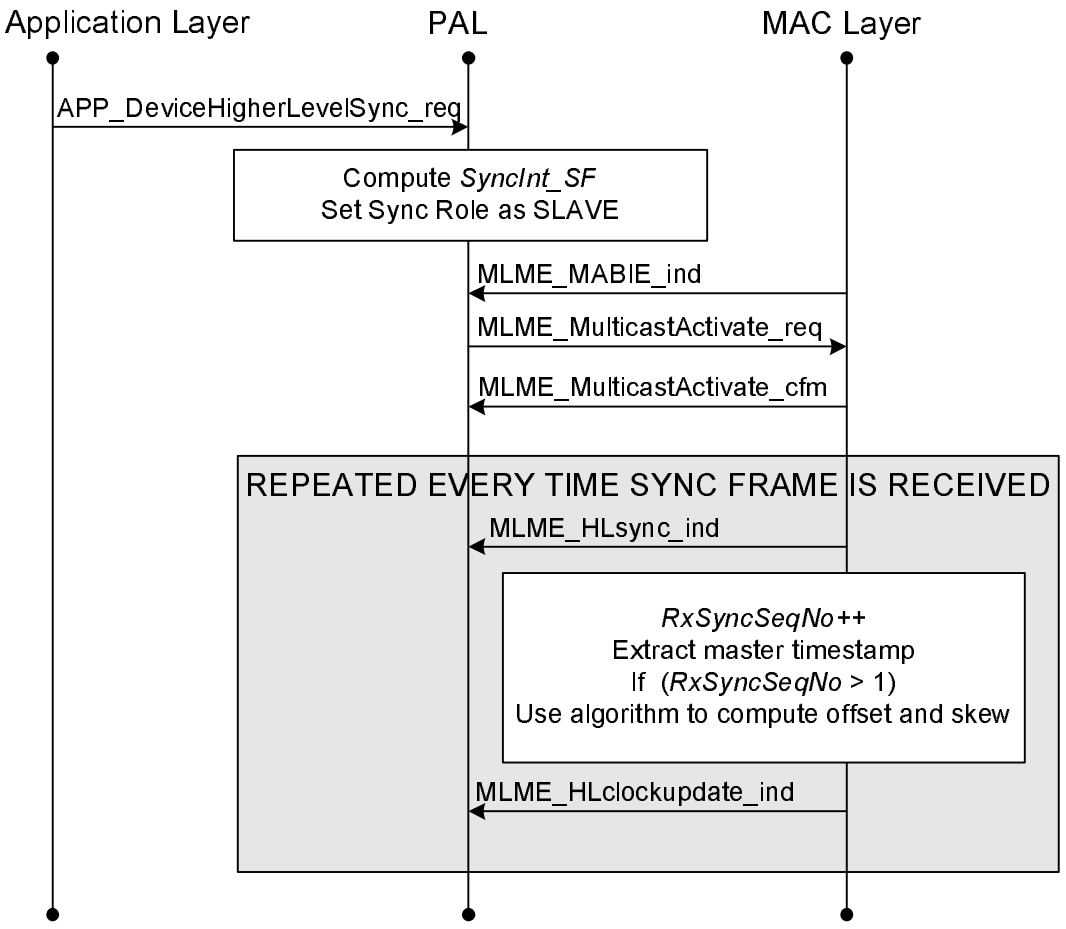

FIGURE 3.19: Sequence diagram for synchronisation mechanism at the Sync Slave.

higher layer timestamps directly and update the timestamps in the LMAC just before the synchronisation frame is transmitted.

3.7 Summary

In this chapter, the application requirements for the synchronisation algorithm have been extracted from the EUWB project documents [53]–[55]. Based on these requirements, we have determined the generic class of algorithms that would be most suitable for the network. We have selected two existing algorithms from this class and also proposed a new algorithm for the class. We have determined that the best place for implementing the algorithm is the MAC layer; hence we have also proposed a method of transferring the higher layer clock to the MAC layer using empty RTP packets when the MAC layer does not have direct access to the higher layer clock. We have further

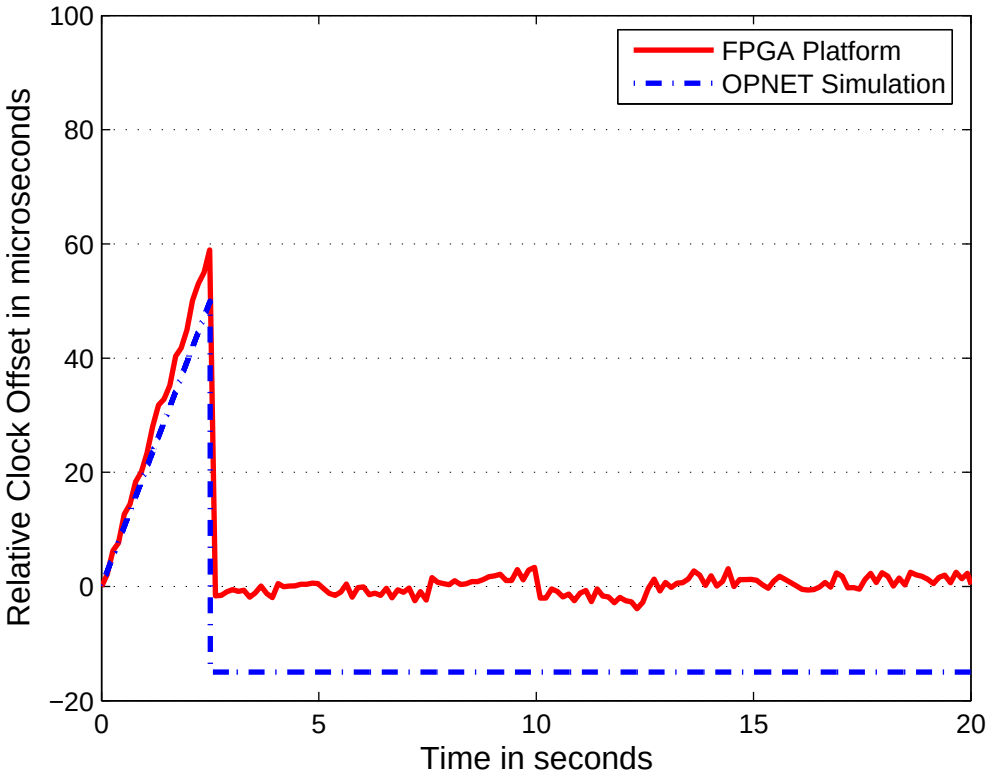

FIGURE 3.20: Comparison of results from OPNET simulation and (V)HDR FPGA Platform.

proposed a new MLME primitive for transferring the computed clock parameters back to the higher layer after synchronisation is complete.

The UWB OPNET models we developed have been described in Section 3.5. The three candidate algorithms have been implemented in the OPNET simulator, and we observed that the Continuous Clock and Linear Rate algorithms perform better than the Delay Time Measurement algorithm since they correct for clock drift and are therefore able to maintain tighter synchronisation in between synchronisation rounds. The Linear Rate algorithm is deemed to be the most suitable for the network, therefore it has been implemented on an FPGA UWB platform developed at TES Electronic Solutions Ltd. The result obtained from the platform has been compared with the corresponding OPNET simulations result and the platform result is markedly better. We attribute this to the fact that the MAC layer is able to obtain the timestamps directly from the higher layer and also update them as close as possible to the PHY, just before the synchronisation frames are transmitted.

Chapter 4

A Sample-Mode PDV Filter for PTP Synchronisation

4.1 Introduction

In Section 2.3.4, we explored the existing techniques for dealing with PDV, noting that a combination of techniques may be required in order to achieve a satisfactory performance. This chapter proposes a new sample-mode PDV filter that combines PDV filtering with priority tagging of synchronisation traffic.

Research has shown that the success of a particular PDV filtering algorithm depends on the packet delay distribution of the network being considered. For instance, in [44], the author showed that the Kalman filtering technique is most useful when the packet delay distribution is Gaussian. Also, the authors of [9] and [10] demonstrated that the best PDV filtering algorithm for a lightly-loaded small cross traffic network was the popular sample-minimum algorithm, since the underlying delay distribution for the network showed that most of the packets experienced the minimum delay. By similarly studying the delay distributions of a heavily-loaded cross traffic network and a heavily-loaded inline traffic network, they showed that the sample-mean and sample-maximum algorithms, respectively, yielded the best synchronisation performance. Hence, we theorise that an algorithm based on the mode delay value should at least match the

performance of the existing algorithms. Furthermore, if the mode delay value does not coincide with the minimum, mean, or maximum delay in the network, then an algorithm based on the mode delay value should outperform the other filters.

Therefore in this chapter, we begin by describing two different network topologies in Section 4.2, before characterising the delay profiles of the networks in Section 4.3. From the observed delay distributions, we suggest the most likely type of existing filter that would perform best. In Section 4.4, we describe the proposed iterative sample-mode PDV filtering technique that selects "good" packets from a mode bin to achieve synchronisation. The sample-mode PDV filter along with the existing sample-minimum, sample-maximum, and sample-mean filters are applied to the two networks using the OPNET network simulator. Simulation results are presented and analysed in Section 4.5, and a chapter summary is provided in Section 4.6.

4.2 System Models

The first system we consider is a 5-hop network with data-centric background traffic based on the ITU-T G.8261 Network Traffic Model 2 [36], as illustrated in Fig. 4.1. Each node generates background traffic that follows the same path as the SYNC packets. The next node extracts the background traffic and injects new (independent) traffic along the synchronisation path. In the literature, this type of traffic pattern is referred to as cross-traffic [10]. QoS was implemented in the model so that the SYNC packets were transmitted with strict priority queuing at the switch output ports.

We also consider the network scenario depicted by Fig. 4.2, where the background traffic follows the same path as the synchronisation traffic. This type of traffic, termed in-line traffic, has practical significance in access aggregation networks such as in mobile backhaul systems where a network controller provides both timing traffic and background traffic (such as voice and data) to base stations. We modelled a 16-hop network in which the size of the packets was uniformly distributed between 64 bytes and 1500 bytes, which are the minimum and maximum packet sizes for Ethernet, respectively.

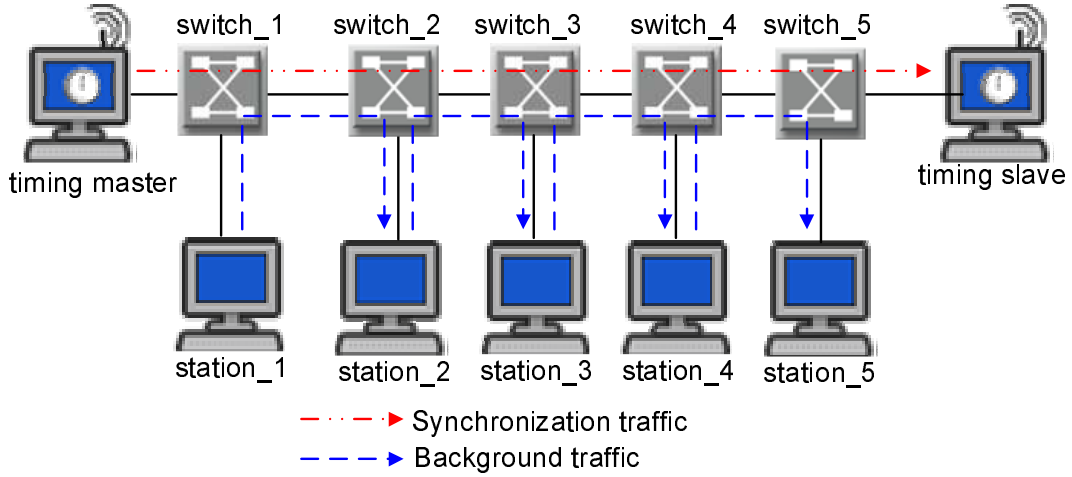

FIGURE 4.1: 5-hop Network Topology for cross-traffic.

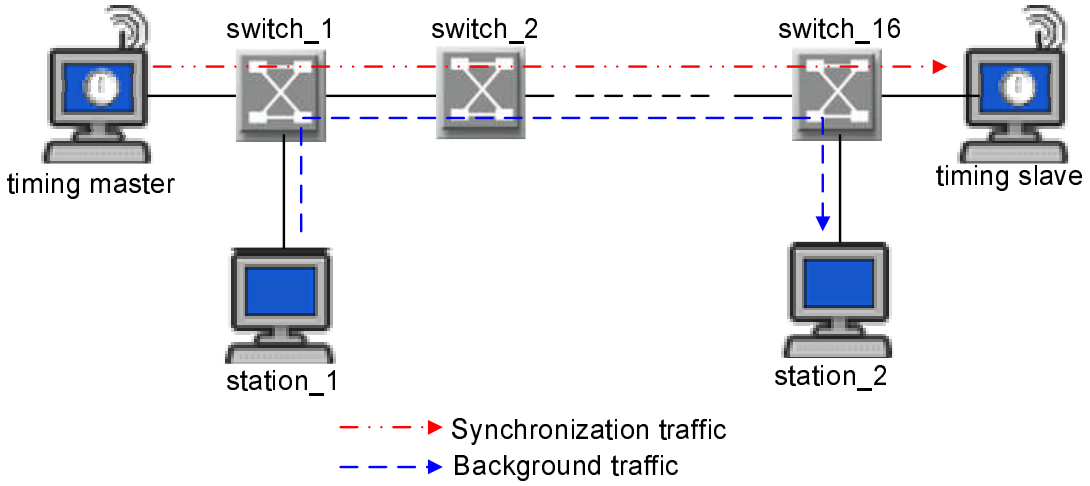

FIGURE 4.2: 16-hop Network Topology for in-line traffic.

Simulation parameters for both networks are shown in Table 4.1.

4.3 Characterisation of Delay Distributions

In order to characterise the delay profile and appreciate the effects of PDV on the synchronisation performance of the network, the 5-hop cross-traffic and 16-hop inline-traffic networks described in Section 4.2 were simulated in OPNET for different levels of background traffic utilisation. For each network, the master node generates a SYNC packet containing the current master time every synchronisation interval and the slave

TABLE 4.1: Simulation parameters for packet delay profiling.

Parameter	5-hop Network	16-hop Network
Distance between nodes	50 metres	50 metres
Line Rate	100 Mbps	100 Mbps
Number of switches	5	16
Type of traffic	Cross	Inline
Background traffic model	ITU-T G.8261 II	64 - 1500 bytes, uniform
Synchronisation Interval	3.90625 ms	3.90625 ms
Slave skew	2 ppm	2 ppm

node takes a timestamp when it receives the packet. Each SYNC packet is priority-tagged such that it is transmitted with strict priority queuing at the switch output ports. For the ith SYNC packet the origin timestamp generated by the master is M_i, the reception timestamp generated by the slave clock is S_i, and the one-way transit delay d is computed as $d = S_i - L_i$, where L_i is the slave timestamp corresponding to the master's origin timestamp. It is important to note that while L_i is easily obtained via network simulation, it cannot be exactly determined in real-life systems unless the slave clock is perfectly synchronised with the master's clock. Thus network simulation allows an in-depth study of the packet delays, as well as providing the opportunity to replicate scenarios accurately.

In this section we explore the frequency of occurence of unqueued packets, the packet delay profiles, and the mean and variance of packet delays, in an attempt to characterise and compare the packet delays in both networks.

4.3.1 Frequency of Occurence of Unqueued Packets

Sample-minimum PDV filtering algorithms make use of the fact that the fastest packets traverse the network without queuing and do so at an approximately constant rate. This observation was made during the initial development of the NTP specification [67]. The frequency of occurence of such packets give an indication of the amount of queuing, and hence the amount of PDV, in the network.

We simulated the 5-hop cross-traffic network using the simulation parameters in Table 4.1 and for different levels of background load. For each load level, we measured the delay of each SYNC packet and calculated the time intervals between the occurrences of fastest packets. Then we obtained the average of all the time intervals. In Fig. 4.3, the average interval between packets that experienced no queuing is shown for different levels of utilisation in the 5-hop cross traffic network.

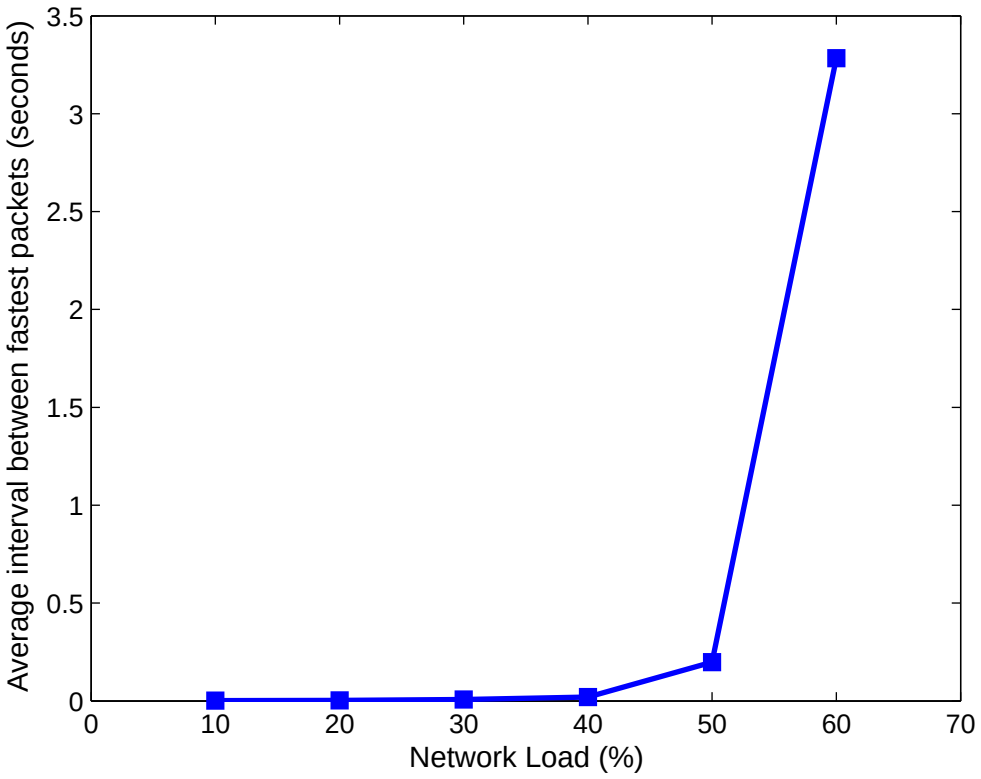

FIGURE 4.3: Average interval between minimum-delayed packets for a 5-hop cross traffic network.

From (2.11), 50% is the utilisation level at which there is an average backlog of 1 packet at each intermediate node so this is the point on the graph where there is a marked increase in the average interval between unqueued packets. At the 70% utilisation level, the mean backlog is 2.33 so all the packets experience some level of queuing; thus the average time interval between unqueued packets approaches infinity. For the 16-hop inline traffic all the packets experience some form of queuing due to the long cascade of queuing elements, even at low utilisation levels. Hence, the average time interval between unqueued packets approaches infinity for all utilisation levels.

4.3.2 Packet Delay Profiles

For both networks simulated, the measured one-way transit delays were used to generate experimental Probability Distribution Functions (PDFs). Fig. 4.4 shows the delay distribution for the 5-hop cross traffic network at different levels of background traffic utilisation. At low loads (typically less than 45%), most of the packets experienced no queuing in the network, as evidenced by the very strong modes at the minimum delay value. As the load increased, the minimum packet delay through the network remained constant but the probability of finding a packet with this minimum delay decreased due to the increased probability of queuing at one or more switches. In fact, the PDFs at higher loads have well-defined shapes and can be fitted to Erlang density distributions.

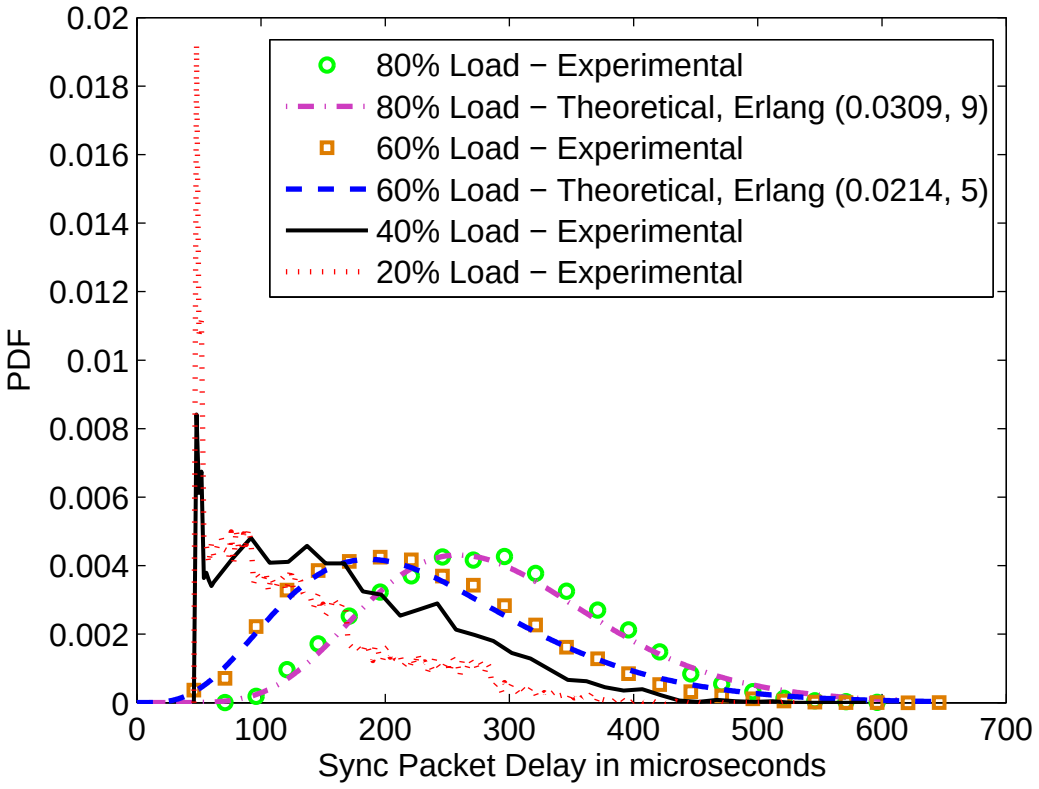

FIGURE 4.4: Packet Delay Distribution for a 5-hop cross traffic network.

For the inline traffic network at 20% load level, the delay PDF in this network can again be fitted to a theoretical Erlang PDF, as depicted in Fig. 4.5; however, none of the packets experience the minimum delay due to the long chain of queuing elements in the network. As the load increases, most of the packets tend to experience

the maximum amount of delay. The resulting PDFs for these increased-congestion scenarios do not fit any popular distributions, but rather resemble mirror-images of the Erlang density distribution with negative values of the shape parameter.

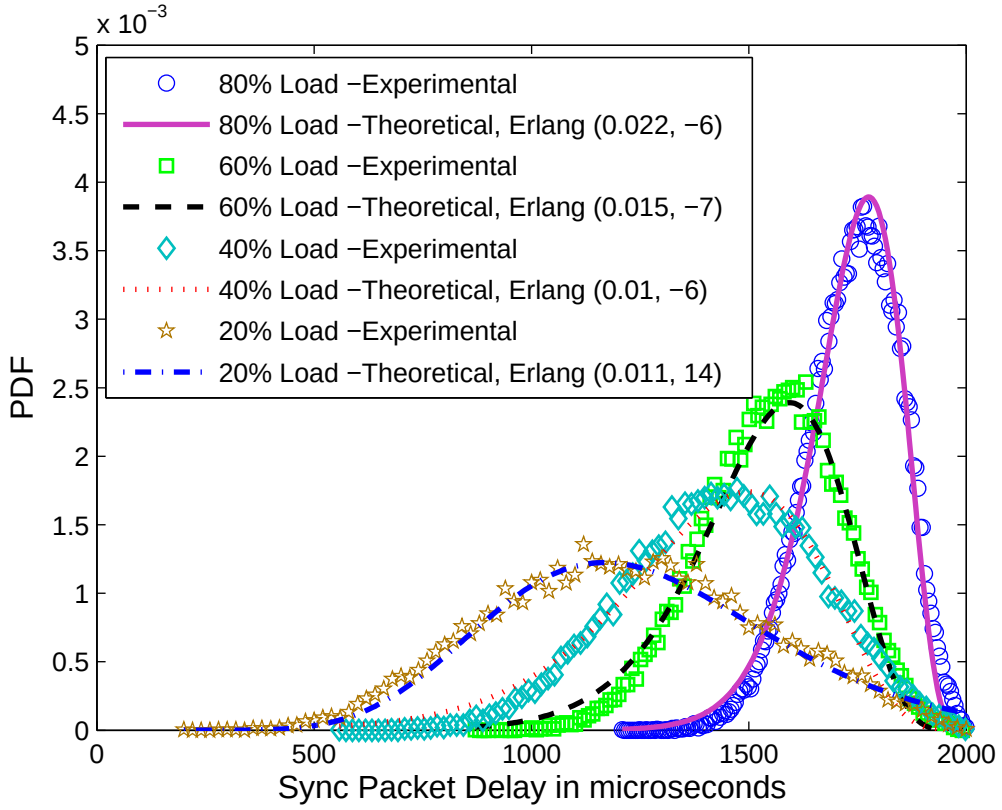

FIGURE 4.5: Packet Delay Distribution for a 16-hop inline traffic network.

Recall that an Erlang density function with rate and shape parameters given by λ and k, respectively, can be expressed by:

$$f(x) = \frac{\lambda^k x^{k-1} \exp(-\lambda x)}{(k-1)!}; x, \lambda \geq 0. \tag{4.1}$$

A mirrored-Erlang density can be obtained from (4.1) by extending the function definition to include negative values of the shape parameter, and shifting the resultant function so that only physically-realistic positive delay values are displayed [10].

Since the delay distributions at higher loads and for higher hop counts tend to follow an Erlang distribution, then in theory, an optimal PDV filter can be designed based on the Erlang distribution parameters. However, the expected computational overhead of such a filter would make it unsuitable for real-time use.

Inspection of the delay profiles in Fig. 4.4 suggests that the low load scenarios are amenable to sample-minimum filtering, while the higher load scenarios might benefit from sample-mean filtering. Inspection of the shapes of the delay profiles in Fig. 4.5 suggests that none of the scenarios would also be amenable to sample-minimum filtering. Sample-maximum filtering might benefit the 80% load scenario, while the other load scenarios might benefit from sample-mean filtering.

4.3.3 Variance and Average Delays

As a further analysis of the impact of the network load on the packet delay, we present the mean and variance of the delays in Fig. 4.6 and Fig. 4.7, respectively. We simulated the 5-hop cross-traffic and 16-hop inline traffic networks using the simulation parameters in Table 4.1 and for different levels of background load. For each load level, we measured the delay of each SYNC packet and calculated the mean and variance of the delays. As expected, the mean packet delay increases with the level of traffic utilisation for both networks; however the cross-traffic network exhibits a more obvious linear relationship.

A more interesting result is observed for the variance. For smaller (low hop count) networks at low loads, the variance is low because most of the packets experience little or no queuing. As the load increases, the variance increases slightly to reflect the increased amount of queuing. The converse is true for larger networks. In these networks the probability of finding a packet that experiences no queuing is statistically small, even at low load levels; hence the variance is high. However, as the load increases most packets tend to experience the maximum delay. Hence, the variance has an inverse relationship with the network load level.

4.4 Proposed Sample-Mode Algorithm

In this section, we describe the rationale behind the idea of the proposed sample-mode filter and postulate as to why it might yield a better performance than existing

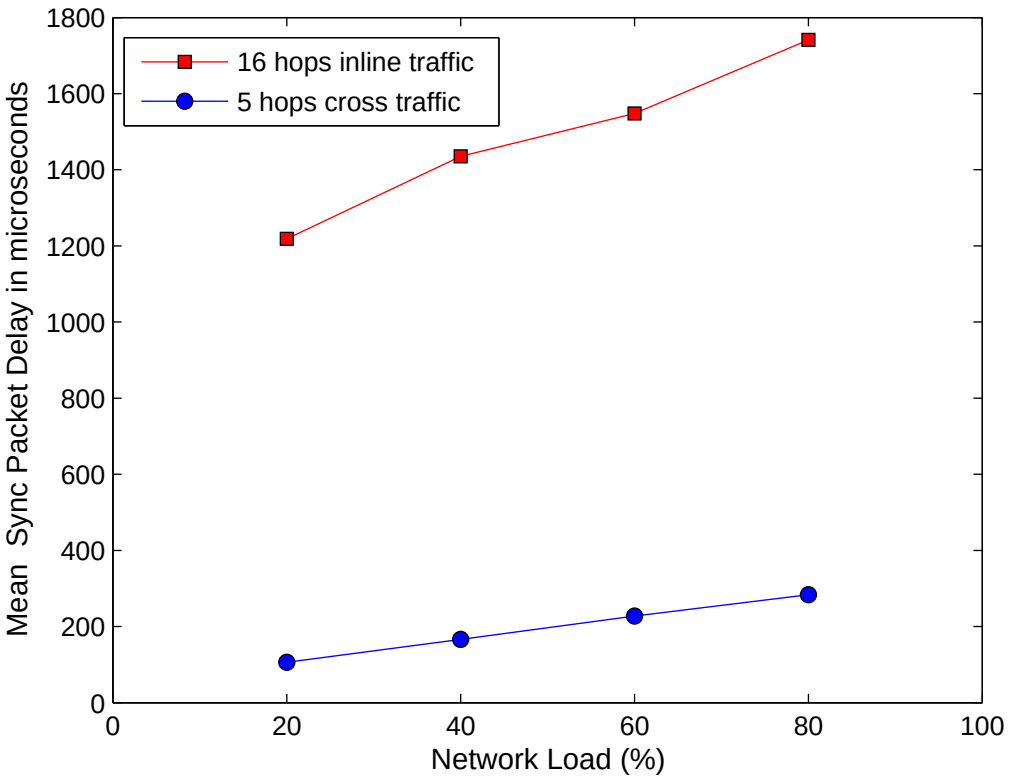

FIGURE 4.6: Mean of packet delays for different network load levels.

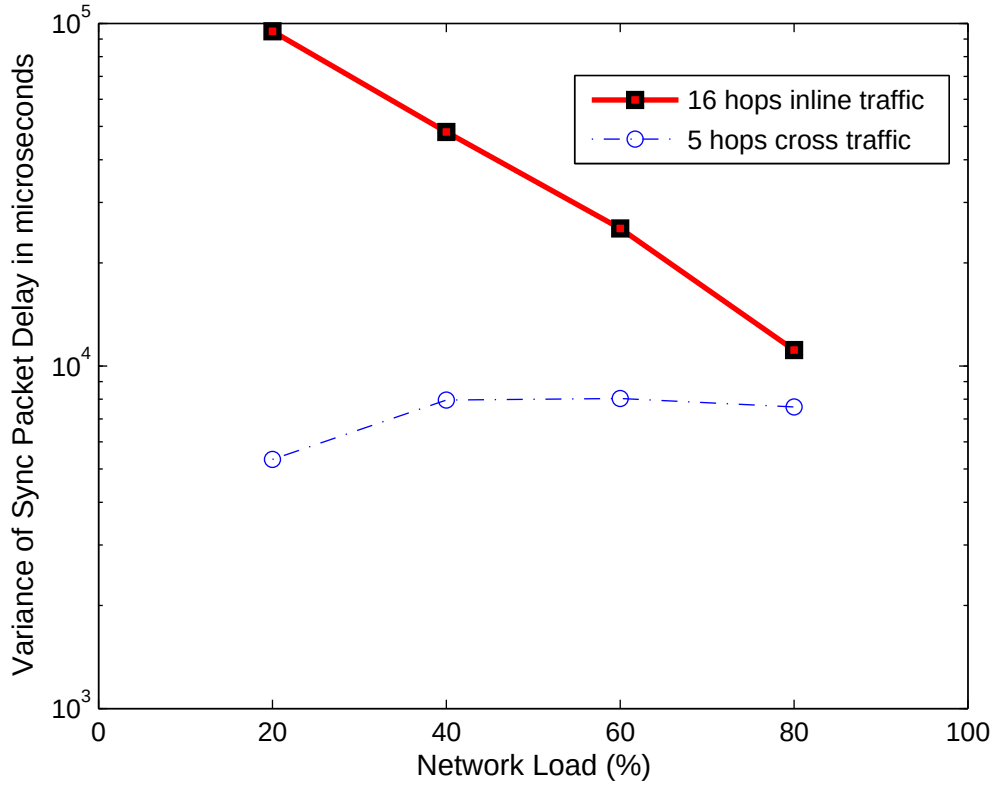

FIGURE 4.7: Variance of packet delays for different network load levels.

algorithms in the packet-filtering category of PDV filters. We then describe the two components of the algorithm; namely, the RCF Estimator and the Offset Corrector.

4.4.1 Rationale

As described in Section 2.3.4, the packet-filtering category of PDV algorithms tend to group the arriving synchronisation traffic into several non-overlapping windows and then select "good" packet(s) from each window. Three main algorithms have been considered in the category, namely sample minimum, sample maximum and sample mean algorithms.

Given a window with W SYNC packets, master origin timestamp M_i, slave reception timestamp S_i, and packet delay delta value $\delta_i = S_i - M_i$ for the ith packet ($0 < i \leq W$), a sample-minimum filter defines a good packet as one which satisfies the following:

$$\delta_i \leq \delta_{min} + \alpha. \tag{4.2}$$

Similarly, a good packet for a sample-maximum filter is one with:

$$\delta_i \geq \delta_{max} - \alpha. \tag{4.3}$$

For a sample-mean filter, a good packet would satisfy:

$$(\delta_{mean} - \alpha/2) \leq \delta_i \leq (\delta_{mean} + \alpha/2) \tag{4.4}$$

where δ_{min}, δ_{max}, and δ_{mean} are the minimum, maximum, and mean, respectively, of all W δ_i samples in the window, and the threshold value α depends on the desired accuracy.

For this category of algorithms, the success of the PDV filtering depends on the probability of finding "good" packets among a sequence of arriving packets within a window. Regardless of the actual magnitude of the delay, all packets selected as "good" packets must have experienced a similar amount of delay. Thus if the distribution of the

delay is known a-priori, then the best filter to use is the one which matches the delay distribution, thus maximising the chances of finding good packets. However, if the delay distribution does not quite match up with any of the filters, then the residual clock offset after synchronisation might be greater than desired.

Since all "good" packets must have experienced a similar amount of delay, it goes without saying that the chances of finding "good" packets can be maximised by selecting packets from around the mode. The rationale behind this approach is that when the delay distribution does not quite match up with any of the existing filters, the sample mode will yield the largest number of good packets. Thus the sample mode filter should give a good fit for all traffic distributions, with a relatively low computational overhead. Therefore, we define a sample-mode filter as one which selects good packets based on

$$(\delta_{mode} - \alpha/2) \leq \delta_i \leq (\delta_{mode} + \alpha/2) \tag{4.5}$$

where δ_{mode} is the centre δ_i value at the mode bin and the threshold value α represents the bin width.

4.4.2 Determining the Mode

Consider the ith SYNC packet received by the slave. If the slave clock is perfectly synchronised to the master, the difference between the reception and origin timestamps for each SYNC packet $\delta_i = S_i - M_i$ will be equal to the end-to-end delay d_i experienced by each packet. However, if the clocks have a non-zero skew σ, then δ_i will also include an accumulated offset, as shown in (4.6).

$$\delta_i = d_i + (M_i + d_i)\sigma. \tag{4.6}$$

This accumulated offset $(M_i + d_i)\sigma$ causes δ_i to gradually increase or decrease over time, depending on whether the slave clock runs faster or slower than the master clock.

Before determining the mode bin, the total number of bins N_{bins} is determined using

$$N_{bins} = \frac{\delta_{max} - \delta_{min}}{\alpha}; \tag{4.7}$$

where α is the width of each bin.

Then for each ith sample, the bin number $b_i : (0 \leq b_i < N_{bins})$ is computed as

$$b_i = \lfloor (\frac{\delta_i - \delta_{min}}{\alpha}) \rfloor. \tag{4.8}$$

Finally, the mode bin is selected as the one with the largest number of samples.

4.4.3 RCF Estimator

The first step in our sample mode PDV filter algorithm is the computation of the RCF. This RCF is used to correct for the relative clock skew at the slave with respect to the master clock. After the first computation of the RCF, subsequent computations are done for every frequency synchronisation interval, rather than for every iteration. This is due to the well-known fact that changes in clock rates are usually caused by aging of the oscillators or temperature changes, and as such they tend to occur extremely slowly. In fact, if the maximum clock drift rate ρ_{max} is known, then the frequency synchronisation interval f can be estimated from the target synchronisation accuracy η as follows:

$$f = \frac{\eta}{2\rho_{max}}. \tag{4.9}$$

In our previous work [68], we showed that the RCF could be calculated using the largest origin timestamp M_{max}, least origin timestamp M_{min}, largest reception timestamp S_{max}, and least reception timestamp S_{min} within the mode bin as follows:

$$RCF = \frac{S_{max} - S_{min}}{M_{max} - M_{min}}. \tag{4.10}$$

For an accurate computation of RCF using (4.10), the packets received by the slave at timestamps S_{max} and S_{min} must have experienced the same delay in the network. In Appendix A, we prove that it is possible for packets that experienced different delays to end up in the same bin. If this happens within the mode bin, the RCF computed using (4.10) will not accurately reflect the actual amount of skew between the master and slave. Conversely, it is also possible for packets that experienced the same delay to end up in different bins, as shown in Appendix B. If similarly-delayed packets are in separate bins, then it might be better to utilise all the samples within a window when computing the RCF, rather than selected samples from the mode bin. Thus, we have explored other algorithms for correcting the skew.

4.4.3.1 Paxson's Algorithm

Paxson's algorithm [69], [70] was designed to remove clock skew from a set of path delay measurements. The W δ_i are partitioned into $\sqrt{W}$ segments, and the minimum delay measurement from each segment is selected. The selected measurements are referred to as the "de-noised" OTTs. The slopes of all possible pairs of the "de-noised" OTTs are computed, and the median slope is selected. If the median slope is negative, the algorithm assumes that the skew is negative. On the other hand, if the median slope is positive, a positive skew is assumed. A cumulative minima test is then performed to see if the number of cumulative minima is large enough to indicate that the sign of the skew is probabilistically likely. If the test is successful, the median slope is output as the skew estimate; otherwise the algorithm outputs a skew of zero.

4.4.3.2 Linear Programming

The method of [15] can be used to formulate a linear programming problem from (4.6). Assuming that $\widetilde{\delta}_i = \delta_i - \delta_1$ and $\widetilde{M}_i = M_i - M_1$, then from (4.6):

$$\widetilde{\delta}_i = (d_i - d_1)(1 + \sigma) + \widetilde{M}_i\sigma. \tag{4.11}$$

Using the relation $\mu = 1 + \sigma$, (4.11) can be re-written as (4.12), where $d_{r_i} = \mu d_i$ represents the end-to-end delay of the ith packet measured at the slave.

$$\widetilde{\delta}_i = (d_{r_i} - d_{r_1}) + \widetilde{M}_i(\mu - 1). \tag{4.12}$$

From (4.12), $\widetilde{\delta}_i$ differs from d_{r_i} by $\widetilde{M}_i(\mu-1)$ minus a constant d_{r_1}. If $\mu > 1$, $\widetilde{M}_i(\mu-1)$ grows linearly with $\widetilde{M}_i$ and $\widetilde{\delta}_i$ gets larger. If $\hat{\mu}$ is the estimate of μ or RCF and $\hat{d}_{r_i}$ and $\hat{d}_{r_1}$ are the estimates of d_{r_i} and d_{r_1}, respectively, then (4.13) can be obtained from (4.12).

$$\hat{d}_{r_i} = \widetilde{\delta}_i - \widetilde{M}_i(\hat{\mu} - 1) + \hat{d}_{r_1}. \tag{4.13}$$

The goal is to estimate μ, given $\widetilde{\delta}_i$ and $\widetilde{M}_i$. Since the delay $\hat{d}_{r_i}$ must always be positive, the linear programming problem can be formulated as:

$$\widetilde{\delta}_i - \widetilde{M}_i(\hat{\mu} - 1) + \hat{d}_{r_1} \geq 0,\ 1 \leq i \leq W. \tag{4.14}$$

The corresponding objective function is stated as:

$$\min \{\sum_{i=1}^{W} (\widetilde{\delta}_i - \widetilde{M}_i(\hat{\mu} - 1) + \hat{d}_{r_1})\}. \tag{4.15}$$

It is important to note that once $\hat{\mu}$ and $\hat{d}_{r_1}$ are obtained, the resulting estimated end-to-end delay of d_{r_i} calculated as $(\widetilde{\delta}_i - \widetilde{M}_i(\hat{\mu}-1) + \hat{d}_{r_1}$ will be greater than zero, instead of being greater than $\min_i d_{r_i}$. Thus, $\hat{d}_{r_1}$ is actually an estimate of $(d_{r_1} + \min_i d_{r_i})$ and $(\widetilde{\delta}_i - \widetilde{M}_i(\hat{\mu} - 1) + \hat{d}_{r_1})$ is actually the variable portion of the end-to-end delay or the PDV. Hence, the linear programming algorithm tries to minimise the sum of the PDV.

4.4.3.3 Linear Regression

The standard linear regression technique can also be used for fitting a line to the set of $\widetilde{\delta}_i$ and $\widetilde{M}_i$ values. For skew estimation, the linear regression algorithm computes

estimates of μ and $\hat{d}_{r_1}$ that minimise the mean square error e in:

$$\sum_{i=1}^{W}\{\widetilde{\delta}_i - \widetilde{M}_i(\hat{\mu}-1) + \hat{d}_{r_1}\}^2. \tag{4.16}$$

4.4.3.4 "De-noised" Linear Programming

We propose a new algorithm that combines the methods of [69] and [15]. We partition the W δ_i samples into Z segments, where $Z = \sqrt{W}$, and the minimum delay measurement from each segment is selected in order to obtain the "de-noised" values δ_{den_i} and M_{den_i}. Following through the steps in Section 4.4.3.2, we formulate the linear programming problem as:

$$\widetilde{\delta}_{den_i} - \widetilde{M}_{den_i}(\hat{\mu}-1) + \hat{d}_{r_1} \geq 0,\ 1 \leq i \leq Z. \tag{4.17}$$

The corresponding objective function is stated as:

$$\min\{\sum_{i=1}^{Z}(\widetilde{\delta}_{den_i} - \widetilde{M}_{den_i}(\hat{\mu}-1) + \hat{d}_{r_1})\}. \tag{4.18}$$

4.4.4 Offset Corrector

Once the RCF has been computed, subsequent iterations attempt to reduce the clock offset between the master and the slave by selecting packets from within the mode bin. The offset corrector also incorporates an optional feedback mechanism for ensuring that an optimum number of packets are available within the mode bin.

A packet selection rate is computed as the quotient of the number of packets in the mode bin and the window size W, and then compared with a packet selection threshold. If the selection rate exceeds the threshold level, the window size can be reduced. If no packet is found within the mode bin after increasing the window size to the maximum, the slave sends a management message to halve the synchronisation interval at the master.

4.5 Simulations and Results

To determine the best skew-estimation algorithm, we used OPNET to simulate the 5-hop cross traffic network depicted in Fig. 4.1, using the simulation parameters in Table 4.2. The three existing skew-estimation algorithms previously described were implemented, as well as our new "de-noised" linear programming algorithm.

TABLE 4.2: Simulation parameters for RCF estimation.

Parameter	Value
Distance between nodes	50 metres
Line Rate	100 Mbps
Number of switches	5
Type of traffic	Cross
Background traffic model	ITU-T G.8261 II
Synchronisation Interval	976.5625 μs
Slave skew	2 ppm
Window Size	10000 samples

Fig. 4.8 shows the residual error after RCF estimation, using the different algorithms. The linear regression algorithm gives unpredictable results because it is not robust in the presence of outliers. Furthermore, it is only optimal if the network delays have a normal distribution. Paxson's algorithm is accurate at low levels of load, where it is possible to find minimum-delayed packets. Since the linear programming objective function aims to minimise the sum of the varible delays, the algorithm works well for low levels of PDV. Combining linear programming with "de-noising" yields the best performance, since "de-noising" gets rid of excess PDV.

The typical network load in real network is 40 - 50%. Both Paxson's algorithm and linear programming yield a low estimation error up to this point. By combining Paxson's de-noising technique with linear programming, we are able to obtain a good skew estimation at 60

We also compared the performance of the proposed sample-mode with those of the existing filters, by simulating the networks depicted in Fig. 4.1 and Fig. 4.2, using the simulation parameters in Table 4.3. In Fig. 4.9, we compare the results obtained from

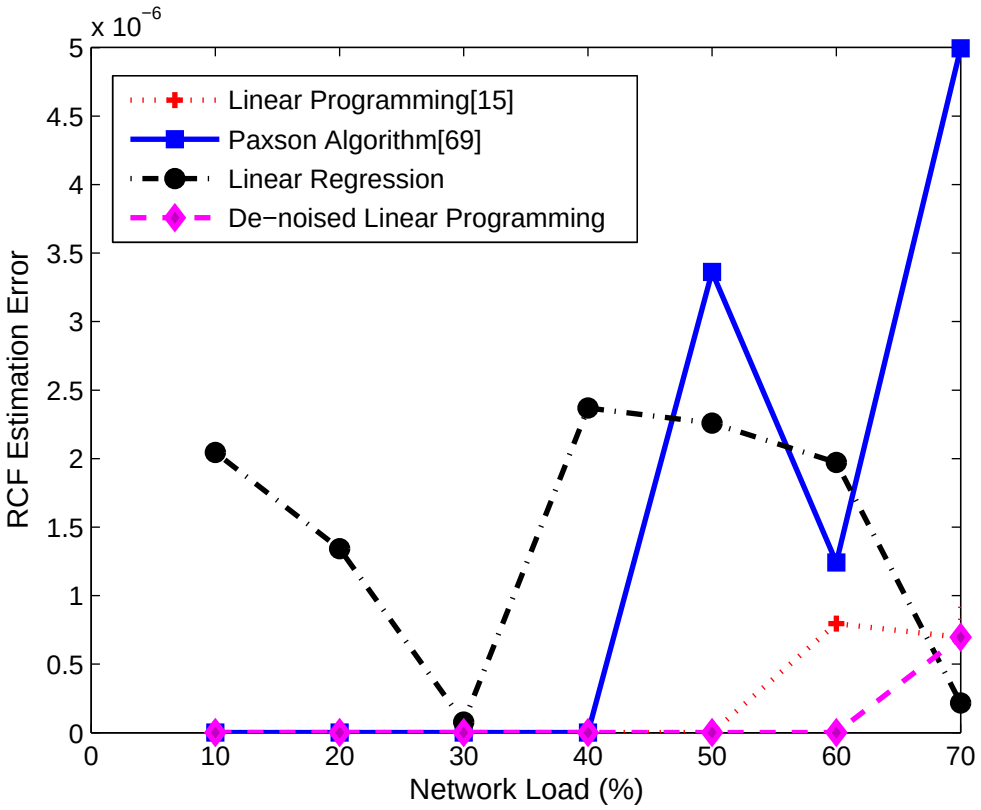

FIGURE 4.8: RCF Estimation Error for 5-hop cross traffic network.

the four different filters after synchronisation in a 40% 5-hop cross-traffic scenario. Most of the packets experience the minimum delay; hence the sample-minimum filter is a good match and performs optimally. Since the mode corresponds to the minimum delay point, the performance of our sample mode filter is also optimal, and identical to that of the sample-minimum. As expected, the sample-mean and sample-maximum filters perform poorly, because they struggle to find "good" packets.

In Fig. 4.10, we compare the results obtained after synchronisation in an 80% 16-hop inline-traffic scenario. None of the packets experience the minimum delay; hence the sample-minimum filter has the worst performance. The delay profile does not match well with the sample-mean or sample-maximum filters either, therefore the sample-mode filter gives the best performance.

As a final analysis, we can observe the performance of a specific filter in both of these scenarios and see how the performance is influenced by the corresponding delay profile. The sample-maximum filter, for example, yields the worst performance in the

TABLE 4.3: Simulation parameters for filter comparison.

Parameter	5-hop Network	16-hop Network
Distance between nodes	50 metres	50 metres
Line Rate	100 Mbps	100 Mbps
Number of switches	5	16
Type of traffic	Cross	Inline
Background traffic model	ITU-T G.8261 II	64 - 1500 bytes, uniform
Synchronisation Interval	976.5625 μs	976.5625 μs
Window Size	500 samples	500 samples
Threshold α	0.2 μs	0.2μs
Residual Offset at the slave after first RCF estimation	0.03 ppm	0.03 ppm

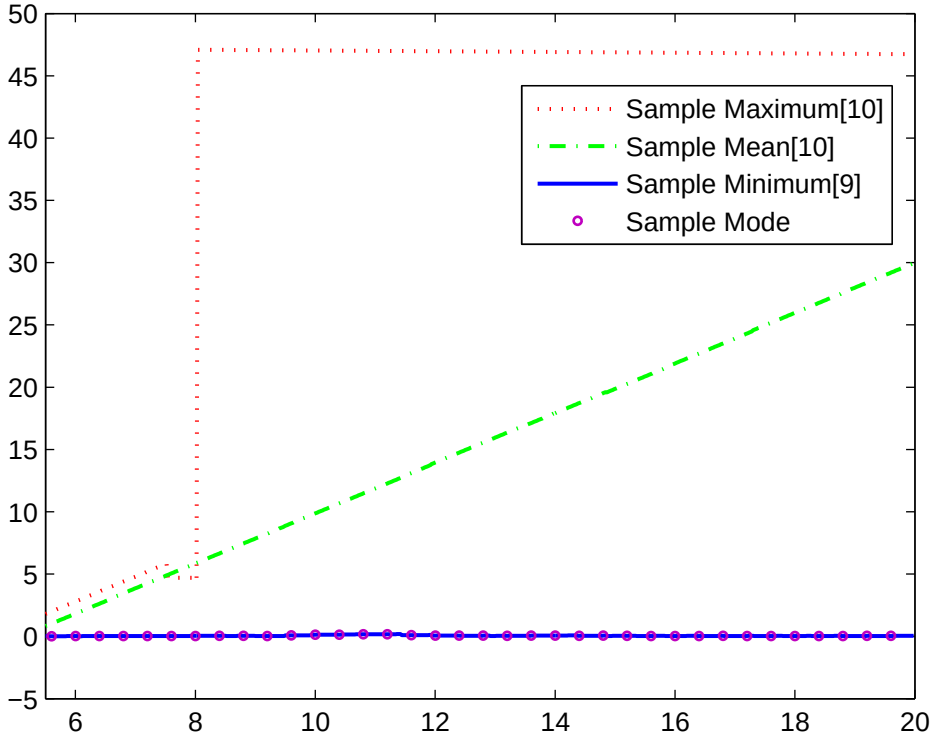

FIGURE 4.9: Relative clock offset for 5-hop cross traffic network at 40% load.

first scenario, as most packets experience the minimum delay. On the other hand, it performs better than both the sample-minimum and sample-mean filters in the larger heavier-loaded network scenario which has higher levels of queuing. The converse is true for the sample-minimum filter.

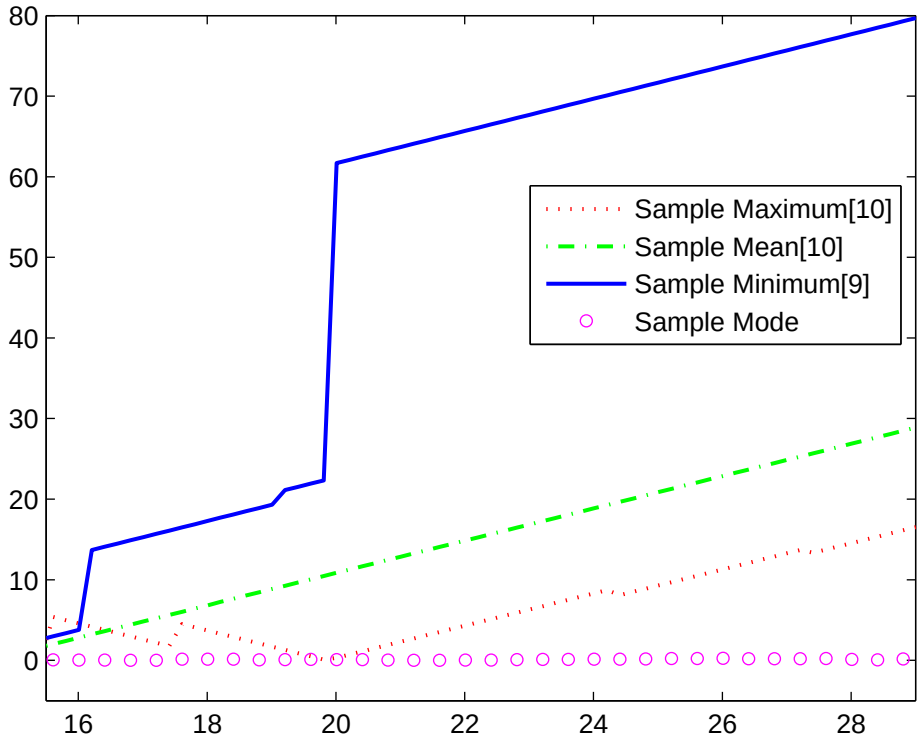

FIGURE 4.10: Relative clock offset for 16-hop inline traffic network at 80% load.

4.6 Summary

In this chapter, we have characterised the IEEE 1588 PTP *SYNC* packet delay profiles for a small cross-traffic network and a large in-line traffic network with different levels of background traffic and observed from the shape of the distributions that the existing sample-minimum, sample-maximum, and sample-mean filters perform sub-optimally for some of the load levels in these scenarios. A new skew-estimation algorithm has been proposed, by utilising some features of two existing algorithms. This skew-estimation algorithm forms the basis of a low-computation sample-mode filtering algorithm which selects packets from the mode bin and uses these "good" packets to achieve synchronisation. Numerical simulations have shown that when the delay profile is a good match for an existing filter, the sample-mode filter performs as well as the existing filter. When the delay profile is not a good match for an existing filter, the sample-mode filter outperforms the existing filters.

Chapter 5

An Alternate Master Technique for Dealing with PTP Master Failures

5.1 Introduction

In Section 2.4.2, we explored the existing techniques for dealing with master failures in PTP, describing the drawback(s) of each technique and noting that the suitability of a particular technique depends on the specific application or scenario. This chapter proposes a new alternate master cluster inspired by the optional alternate master and grandmaster cluster features of the PTP standard, as well as a new alternative BMCA that reduces both the downtime caused by a master failure and the amount of offset in the re-synchronisation phase.

In this chapter, we first of all describe the system model for our application scenario and show why the existing techniques are unsuitable. The alternate master cluster is described in detail, along with the necessary modifications to the basic PTP algorithm. The new alternative BMCA is also described. Results from simulating the alternate master cluster in OPNET are presented and analysed, and conclusions are drawn.

5.2 Problem Statement

This research work was derived from the following problem observed in a customer's project. A group of DECT base stations designed in-house were connected over an Ethernet backbone and PTP was used to achieve synchronization among the base stations, by means of a third-party chip in each base station. Up to 8 microphones were connected to each base station over the DECT air interface and the inter-base station synchronization was necessary in order to facilitate seamless handover. The required synchronisation accuracy was 2μs in order to provide frame and multiframe synchronisation, as specified in the DECT standard [71]–[74]. Fig. 5.1 illustrates the application scenario.

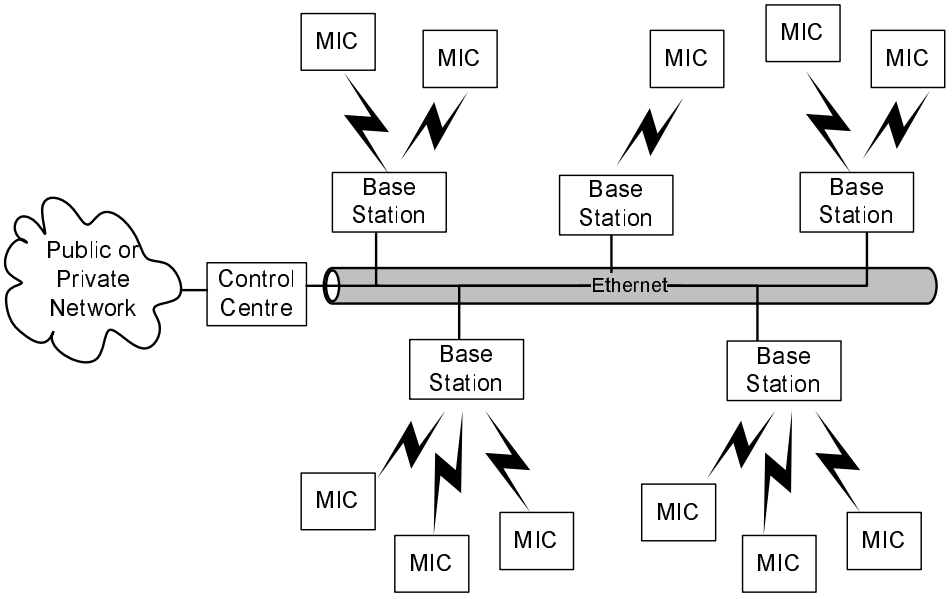

FIGURE 5.1: DECT base station application scenario for PTP master failure.

We derived a system model based on the application scenario. The system model is an Ethernet network consisting of 5 PTP nodes and 2 Ethernet switches, as illustrated in Fig. 5.2. Each PTP node represents a DECT base station and synchronisation must occur across all the nodes on the network; hence the maximum number of grandmasters is 1.

It was observed that during the downtime resulting from a failure of the PTP master, the relative clock offset between the remaining base stations exceeded the specified 2μs, leading to a total loss of synchronization in the system.

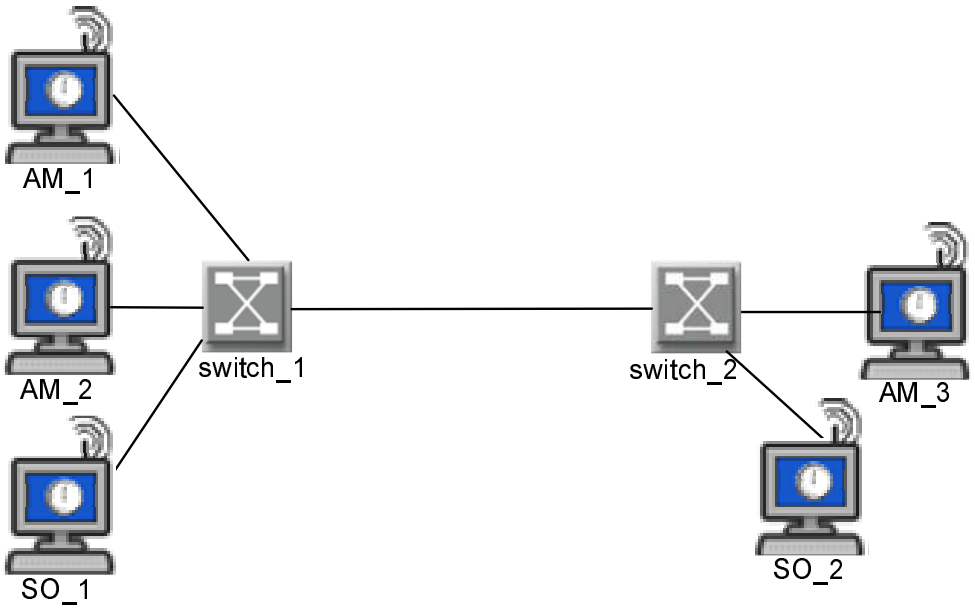

FIGURE 5.2: System model for PTP master redundancy.

5.3 Motivation

The motivation for the proposed alternate master cluster and alternate BMCA is that none of the existing techniques described in Section 2.4.2 are suitable for the application scenario under consideration. In the grandmaster cluster technique, the other grandmaster nodes that are not currently in the *MASTER* state must be in the *PASSIVE* state; hence the nodes in the cluster do not synchronise to each other. The drawback of the democratic master group technique is that it requires an entirely new type of device, the master group speaker, which must also support the democratic algorithm in addition to PTP. Furthermore, the master group speaker becomes a single point of failure in the system. The ITU-T telecoms profile is complex and therefore costly as it utilises multiple clocks at each slave node, and it only provides frequency synchronisation. The technique proposed by [52] is targeted at a system architecture in which it is possible for the grandmaster clocks to use the same oscillator, whilst remaining isolated via separate Virtual Local Area Networks (VLANs). This is markedly different from the system model in Fig. 5.2 where each base station has its own clock and oscillator. Finally, the alternate master technique is promising since it is a good fit for the system model and offers a reduction in the length of the re-synchronisation phase. However, it has no effect on the master failure detection

time and the new master election time. Hence, our proposed alternate master cluster technique borrows the cluster feature from the grandmaster cluster technique which is capable of decreasing the lengths of the detection and election phases and combines it with the alternate master feature, in order to reduce the lengths of the detection, election, and re-synchronisation phases after a master failure. In addition, we also devise an alternative BMCA based on a unique ranking algorithm.

5.4 The Alternative Best Master Clock Algorithm

Fig. 5.3 shows the alternative BMCA developed for the alternate master cluster technique. Just like the default BMCA, the alternative BMCA is run once every *announceInterval* and uses the same state decision algorithm.

The difference between the new BMCA and the default BMCA is that a new attribute, *scaledLogRank*, has been added to the top of the flowchart for the clock comparison algorithm . We define the *scaledLogRank* attribute of a node as an unsigned integer between 1 and 254 that gives an indication of the availability of the node. The lowest value of *scaledLogRank* represents the node with the highest availability, while the highest value represents the node with the lowest availability. If the two nodes under comparison have the same *scaledLogRank* value, then the alternative BMCA reverts to the default BMCA.

5.5 The Alternate Master Cluster Technique

The proposed alternate master cluster consists of 2 to 5 alternate masters that are capable of exchanging unicast *queryAnnounce* messages with each other. Each cluster member is configured with a lower *priority1* value than the non-cluster members so that as long as there is a functional node in the cluster, the best master clock will always be selected from within the cluster. A node that is not operating in the *DISABLED*, *FAULTY* or *INITIALIZING* states is deemed to be functional. Unlike

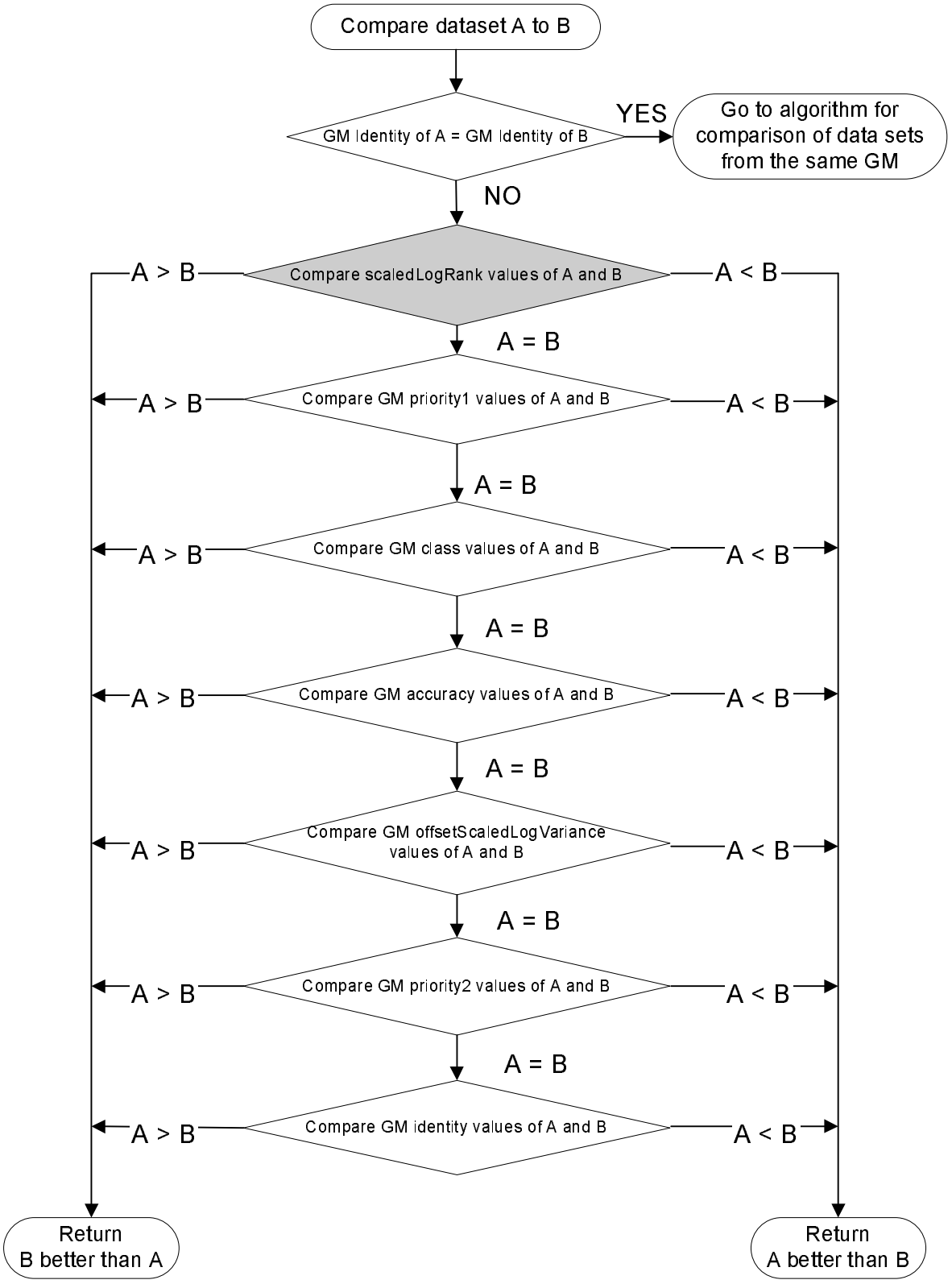

FIGURE 5.3: Alternative BMCA for alternate master cluster.

the grandmaster cluster technique described in the PTP standard, functional alternate masters that are not currently in the *MASTER* state operate in the *SLAVE* state

rather than the *PASSIVE* state, so that synchronisation can also occur within the cluster. For the sake of simplicity, the following types of nodes are defined in this work:

- **Master Node:** A member of the alternate master cluster that is currently operating in the *MASTER* state. This is the best clock in the domain.
- **Alternate Master Node:** A member of the alternate master cluster that is currently operating in the *SLAVE* state.
- **Slave Node:** Any other node in the network that is not part of the alternate master cluster. Slave nodes cannot operate in the *MASTER* state unless all the clocks in the cluster are non-functional.

This section describes the operation of the alternate master cluster as well as the operation of the rest of the domain outside the cluster.

5.5.1 Operation of the Alternate Master Cluster

The master node and alternate master node(s) make up the alternate master cluster. Within the alternate master cluster, nodes exchange unicast *queryAnnounce* messages and transmit *alternateMulticastSync* messages. The *queryAnnounce* messages are used to compute a *scaledRank* for each cluster member, while the *alternateMulticastSync* messages are used to provide origin and reception timestamps so that re-synchronisation to a new master will be quicker if the current master fails.

In this section, we describe the attributes necessary for the functionality of the alternate master cluster, the behaviour of the cluster members at initialisation, as well as the messages transmitted by the cluster members. We also highlight the response of the cluster members to different types of received messages, and show how the cluster members are ranked.

5.5.1.1 Attributes of Cluster Members

Table 5.1 lists the existing attributes required for the operation of the alternate master feature, as specified in the PTP standard. In addition to these, Table 5.2 gives the proposed new attributes required for the operation of the alternate master cluster.

TABLE 5.1: Existing alternate master attributes.

Attribute	Data type	Description
numberOfAlternateMasters	Integer	Number of nodes in the cluster
transmitAlternateMulitcastSync	Boolean	Specifies if alternate masters in *SLAVE* state can transmit *alternateMulticastSync* messages
logAlternateMulticastSyncInterval	Integer	Specifies the frequency of *alternateMulticastSync* messages

TABLE 5.2: Proposed alternate master cluster attributes.

Attribute	Data type	Description
alternateMasterFeature	Boolean	Determines whether the feature is supported by the node
alternateMasterMember	Boolean	Specifies whether a node is a member of the cluster
numberOfQueryAnnounce	Integer	Number of unicast *queryAnnounce* messages to be sent in each announce interval
alternateMasterRecord	List	Stores information about each cluster member

The *alternateMasterRecord* is a list of elements that stores real-time data about each cluster member. The length of the list is equivalent to the number of nodes in the alternate master cluster. The *alternateMasterRecord* is created at initialisation and maintained by each node in the network that supports the alternate master feature. Each element in the list is a compound variable of type *alternateMasterDS*. The definition of this compound variable is given in Table 5.3.

5.5.1.2 Initialisation of Alternate Master Cluster

At initialisation, each node i in the alternate master cluster is given a *scaledLogRank* of $SLR_i = SLR_{INIT} = 254$. Since all the nodes have the same *scaledLogRank* value,

TABLE 5.3: Definition of struct *alternateMasterDS*.

Member	Data type	Description
alternateMasterPortIdentity	PortIdentity	Identity of alternate master cluster member
alternateMasterMacAddress	EUI48	MAC address of alternate master cluster member
u16AnnounceSequenceId	Integer	Sequence ID of most recent announce message
u16NoQueryAnnounceReceived	Integer	Number of unicast *queryAnnounce* messages received in current announce interval
sSyncOriginTimestamp	Timestamp	Origin timestamp of most recently received alternateMulticastSync message
sSyncReceptionTimestamp	Timestamp	Reception timestamp of most recently received alternateMulticastSync message
dfIRankYou	Double	Rank of this cluster member as computed by node
dfYouRankMe	Double	Rank of node as computed by this cluster member
boIsMaster	Boolean	Specifies if this cluster member is the current master node

the alternative BMCA described in Section 5.4 reverts to the default BMCA described in Section 2.4.1.4 and the node with the lowest *priority1* value is elected as the best master.

Once the best master has been elected, all the alternate master nodes achieve synchronisation with it. Subsequently, each alternate master node transmits multicast *ANNOUNCE* messages with the *alternateMasterFlag* set to TRUE. Whenever an alternate master node receives a multicast *ANNOUNCE* message with the *alternateMasterFlag* set to TRUE, it creates a new *alternateMasterDS* data set for the source node (if one does not already exist) and adds this to its *alternateMasterRecord*. Each alternate master node also creates a data set for the master node and adds it to its *alternateMasterRecord*. This is how the entries in the *alternateMasterRecord* list are built.

5.5.1.3 Message Transmission within the Alternate Master Cluster

The master node multicasts *ANNOUNCE* messages and *SYNC* messages as usual, based on the specified announceInterval and syncInterval in the domain. It also sends *DELAY_RESP* messages, as usual, in response to *DELAY_REQ* messages sent by non-master nodes. The only additional transmissions by the master node are the unicast *queryAnnounce* messages it sends to the alternate master nodes. The frequency of the unicast messages is always greater than that of the regular multicast *ANNOUNCE* messages, but they have the same packet structure. All transmissions from the master node have the *alternateMasterFlag* set to FALSE in the *flagField* of the message header, thus indicating that it is in the *MASTER* state.

Alternate master nodes multicast *ANNOUNCE* messages to the entire network and if *transmitAlternateMulitcastSync* is enabled, then they also multicast *SYNC* messages, but with reduced frequency. Additionally, alternate master nodes send unicast *queryAnnounce* messages to the other cluster members including the master node. All transmissions from an alternate master node have the *alternateMasterFlag* set to TRUE, thus indicating that it is not in the *MASTER* state.

5.5.1.4 Message Reception within the Alternate Master Cluster

Within the alternate master cluster, *DELAY_REQ* and *DELAY_RESP* are handled exactly as described in the PTP standard; however the procedures for *SYNC*, *ANNOUNCE*, and *queryAnnounce* messages are handled slightly differently.

- ***SYNC* Messages:** The procedure is described in Fig. 5.4. The message is discarded if the recipient is the master node or if the sender is not a member of the cluster. Otherwise, the recipient uses the message for synchronisation if the sender is the master node or updates the *alternateMasterRecord* if the sender is an alternate master node.

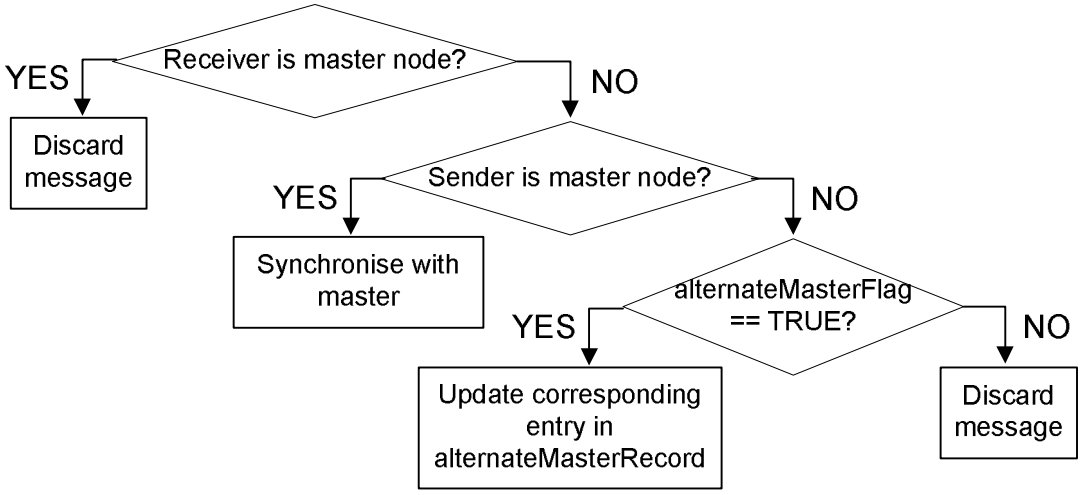

FIGURE 5.4: Flowchart for handling received *SYNC* messages in the alternate master cluster.

- ***ANNOUNCE* Messages:** If the recipient has already received a *queryAnnounce* from the same sender, the *ANNOUNCE* message is discarded. Otherwise if the message is from an alternate master cluster member, a new entry is created in the *alternateMasterRecord*. The procedure is shown in Fig. 5.5.

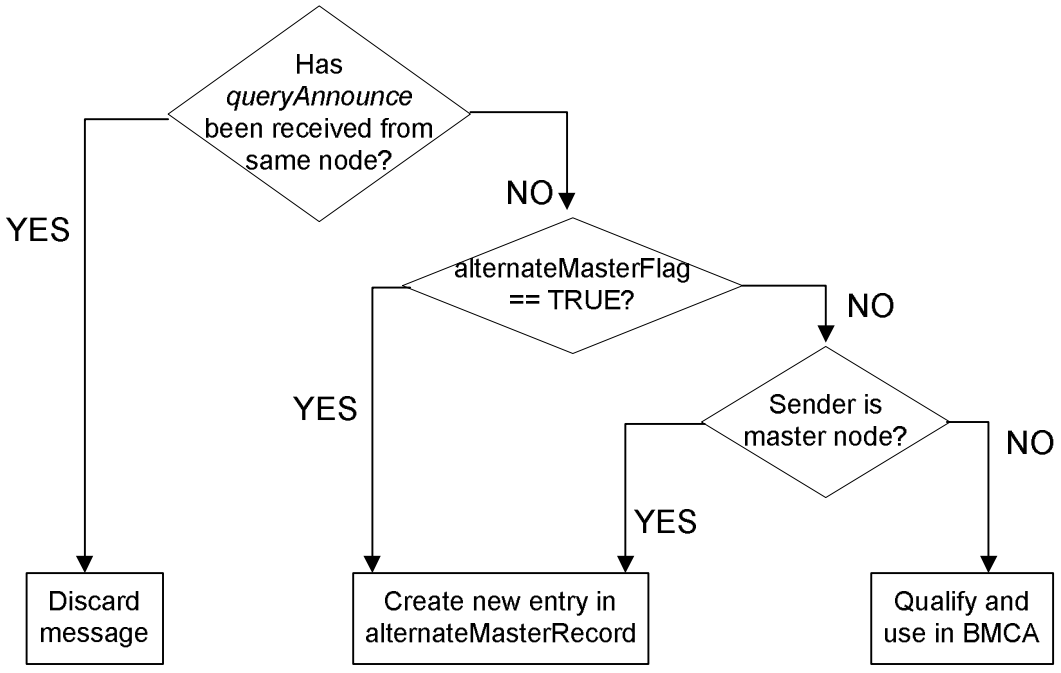

FIGURE 5.5: Flowchart for handling received *ANNOUNCE* messages in the alternate master cluster.

- ***queryAnnounce* Messages:** Upon receipt of a *queryAnnounce* message, an alternate master cluster member computes a rank *iRankYou* for the sender. It also

extracts its own rank, *youRankMe*, as computed by the sender. The *iRankYou* and *youRankMe* values are stored in the *alternateMasterDS* data set for the entry corresponding to the sender in the *alternateMasterRecord*. It transmits the calculated *iRankYou* as part of the next *queryAnnounce* message it sends to the sender. At the end of its *announceInterval*, it uses all the *youRankMe* values it received from the cluster members, to compute its own rank. The ranking procedure is described in Section 5.5.1.5.

5.5.1.5 Ranking within the Alternate Master Cluster

The aim of transmitting unicast *queryAnnounce* messages within the cluster is to allow the cluster members to be ranked, based on their availability or reliability. *numberOfQueryAnnounce* defines the number of *queryAnnounce* messages within an *announceInterval*. Hence, the interval between consecutive unicast messages can be computed as

$$queryAnnounceInterval = \frac{announceInterval}{numberOfQueryAnnounce}. \tag{5.1}$$

Each cluster member maintains a running total of the number of *queryAnnounce* messages it receives within an *announceInterval* from the other nodes within the cluster. Each time a cluster member receives a *queryAnnounce* message, it computes a rank *iRankYou* for the node who sent the message. This rank essentially compares the actual number of received *queryAnnounce* messages at a specific time with the number of messages that **should** have been received at that time. Assuming that the current *announceInterval* expires at time t_{ex} and node i has received n_j *queryAnnounce* messages from node j at the current time t_{cur}, the number of messages that should have been received at t_{cur} is given by

$$N_{exp} = \left\lceil numberOfQueryAnnounce - \left(\frac{(t_{ex} - t_{cur})}{queryAnnounceInterval}\right) \right\rceil. \tag{5.2}$$

The *iRankYou* value for j as computed by i is

$$R_{ij} = \frac{n_j}{N_{exp}}. \tag{5.3}$$

Once every *announceInterval*, node j uses the most recent *youRankMe* values it has received from the other cluster members to calculate a rank *myRank* for itself. It is important to note that the *iRankYou* value for j as computed by i is identical to the *youRankMe* value received by j from i.

If there are N_c nodes in the cluster, *myRank* for node j is given by

$$R_j = \frac{\sum_{\substack{i=0 \\ i \neq j}}^{N_c - 1} R_{ij}}{N_c}. \tag{5.4}$$

The computed ranks R_{ij} and R_j are floating point values. We use a scaled log function to transform these floating point values into 8-bit integers. Given any rank value R, the corresponding *scaledLogRank* value SLR is given by

$$SLR = 1 - (\lceil 2^4 * \log_2 R \rceil). \tag{5.5}$$

SLR_{ij} is transmitted as part of the next unicast *queryAnnounce* message sent to node j from i. The shaded *reserved* field of the message header is used for this purpose, as shown in Fig. 5.6. The computed *myRank* value SLR_j is transmitted in subsequent *queryAnnounce* and *ANNOUNCE* messages transmitted by node j using the *reserved* field of the message body, as shown in Fig. 5.7.

5.5.1.6 Master Failure Behaviour within the Cluster

When the master node fails, it stops transmitting messages. Instead of using the *ANNOUNCE_RECEIPT_TIMEOUT* timer, our master cluster technique shortens the detection phase to a maximum of 1.5 times the *announceInterval*. An alternate master node concludes that the master node has failed if 50% or more of its *queryAnnounce*

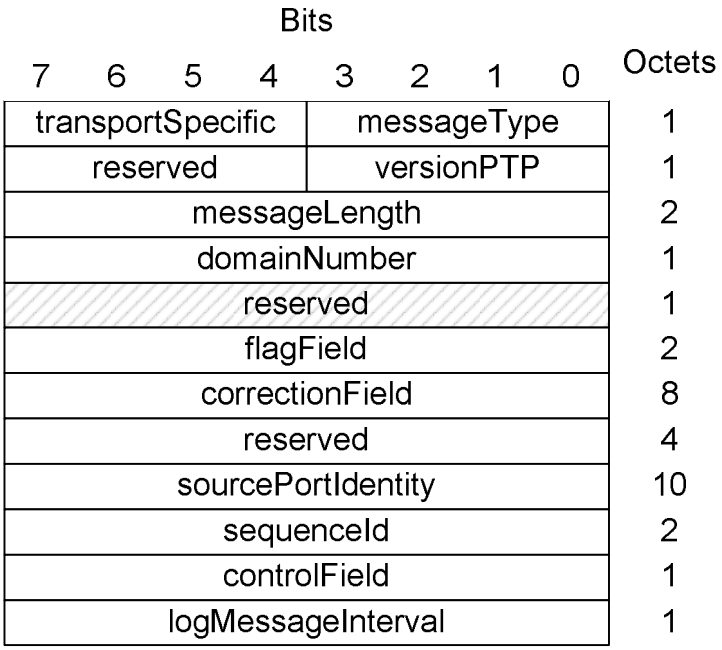

FIGURE 5.6: Message header field for transmitting IRankYou.

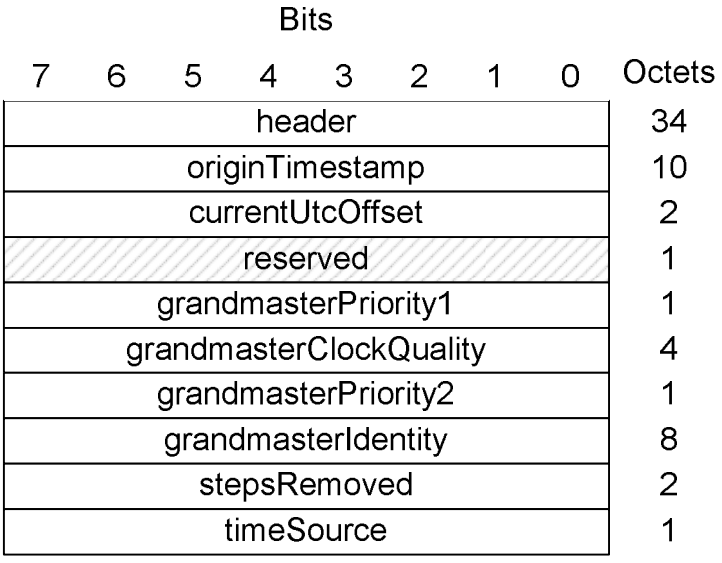

FIGURE 5.7: Message body field for transmitting myRank.

messages **and** its *ANNOUNCE* message were not received **or** if 75% or more of its *queryAnnounce* message were not received in an *announceInterval*.

A new master is elected from the cluster within another *announceInterval*, and re-synchronisation occurs within a further *syncInterval* since the origin and reception timestamps for a *SYNC* message from the new master are already available.

5.5.2 Operation of the Non-Cluster Members

For the best performance of the alternate master cluster technique, the slave nodes outside the cluster **must** be configured with higher *priority1* values than the cluster members. In addition, the scaledLogRank value of each slave node **must** be set to the maximum value of 254, since these nodes do not take part in the ranking process. The same alternate master attributes specified in Table 5.2 apply, although attributes such as *alternateMasterMember* and *numberOfQueryAnnounce* are unused.

5.5.2.1 Message Transmission outside the Alternate Master Cluster

The slave nodes do not necessarily need to transmit any additional messages. However if faster re-synchronisation is required, the slave nodes may also transmit *DELAY_REQ* messages to alternate master nodes.

5.5.2.2 Message Reception outside the Alternate Master Cluster

The sequences for handling received *ANNOUNCE* messages and *SYNC* messages at slave nodes are illustrated in Fig. 5.8 and Fig. 5.9, respectively.

As usual, *SYNC* messages from the master node are used to synchronise the slave nodes. *SYNC* messages from alternate master nodes are used to update the corresponding alternate master entry in the *alternateMasterRecord*; all other *SYNC* messages are discarded.

ANNOUNCE messages from alternate master cluster members are used to update the corresponding alternate master entries in the *alternateMasterRecord*; all other *ANNOUNCE* messages are treated as messages from foreign masters. As usual, whenever an *ANNOUNCE* is received from the master node, the *ANNOUNCE_RECEIPT_TIMEOUT* timer is reset.

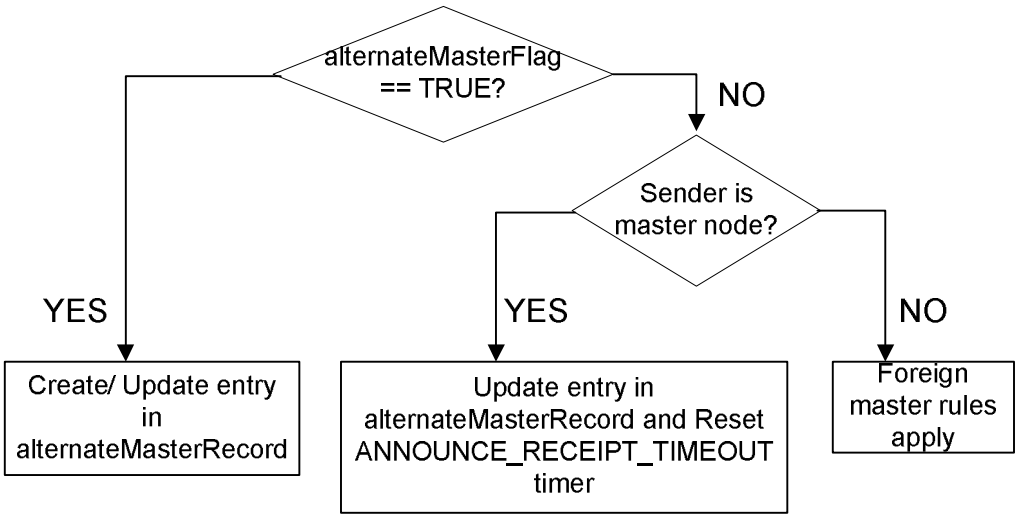

FIGURE 5.8: Flowchart for handling received *ANNOUNCE* messages outside the alternate master cluster.

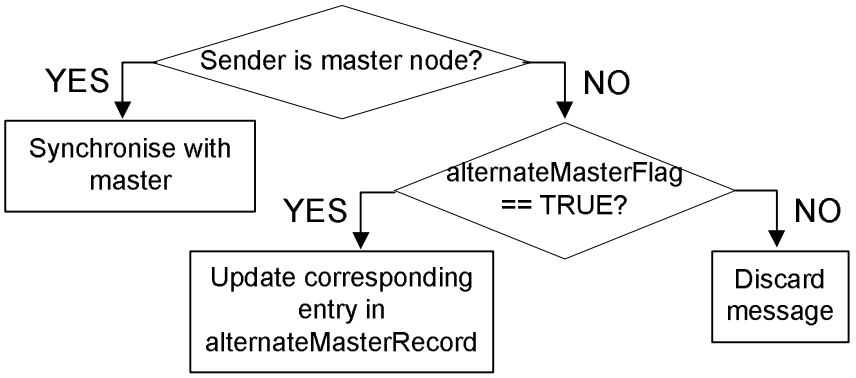

FIGURE 5.9: Flowchart for handling received *SYNC* messages outside the alternate master cluster.

5.5.2.3 Master Failure Behaviour outside the Cluster

In the default PTP implementation when the master node fails, the slave nodes continue including the last received *ANNOUNCE* message from the failed master in the BMCA until the *ANNOUNCE_RECEIPT_TIMEOUT* timer expires. Hence, a new master cannot be elected until this timer expires.

Since our alternate master cluster technique has essentially delegated the role of master selection to the alternate master cluster, some modifications are necessary. The necessary modification is that the slave node shall not include the last received *ANNOUNCE* message from the master node in the BMCA if:

- it did not receive a more recent *ANNOUNCE* message from the master node; **and**
- it received an *ANNOUNCE* message from an alternate master node with *alternateMasterFlag* set to FALSE.

These two clauses indicate that the previous master has failed and a new master has been elected from the cluster. The re-synchronisation time is also shortened since the origin and reception timestamps for a *SYNC* message from the new master are already available at the slave nodes.

5.6 Simulations and Results

To validate our proposed approach, we simulated the network shown in Fig. 5.2. AM_1, AM_2, and AM_3 were configured as the alternate master cluster while nodes SO_1 and SO_2 were the slave nodes.

First of all, we compare the performance of the default BMCA with the proposed alternative BMCA. Then, we show that the alternate master cluster technique is resilient to the addition of new nodes, both inside and outside the cluster. The important simulation parameters are given in Table 5.4.

Table 5.4: Simulation parameters for master failure analysis.

	AM_1	AM_2	AM_3	SO_1	SO_2
announceInterval	2s	2s	2s	2s	2s
syncInterval	1s	1s	1s	1s	1s
numberOfQueryAnnounce	4	4	4	4	4
priority1	1	2	3	10	10
Announce Receipt Timeout value	10	10	10	10	10
Fractional Frequency Offset	0ppm	6ppm	-6ppm	100ppm	-100ppm

5.6.1 Comparing the Default BMCA with the Alternative BMCA

5.6.1.1 The Default BMCA Scenario

In this scenario, the alternate master feature is disabled and the default BMCA is used for master election. After the nodes are initialised, node AM_1 is elected as the master since it has the lowest *priority1* value. A fault was injected into this node at time $t = 5400$s which caused a failure of the master node. After the failure, the clocks of the other nodes run freely until node AM_2 is elected as the master.

Fig. 5.10 shows the clock offset of nodes SO_1, SO_2, AM_2 and AM_3 with respect to the previous master AM_1.

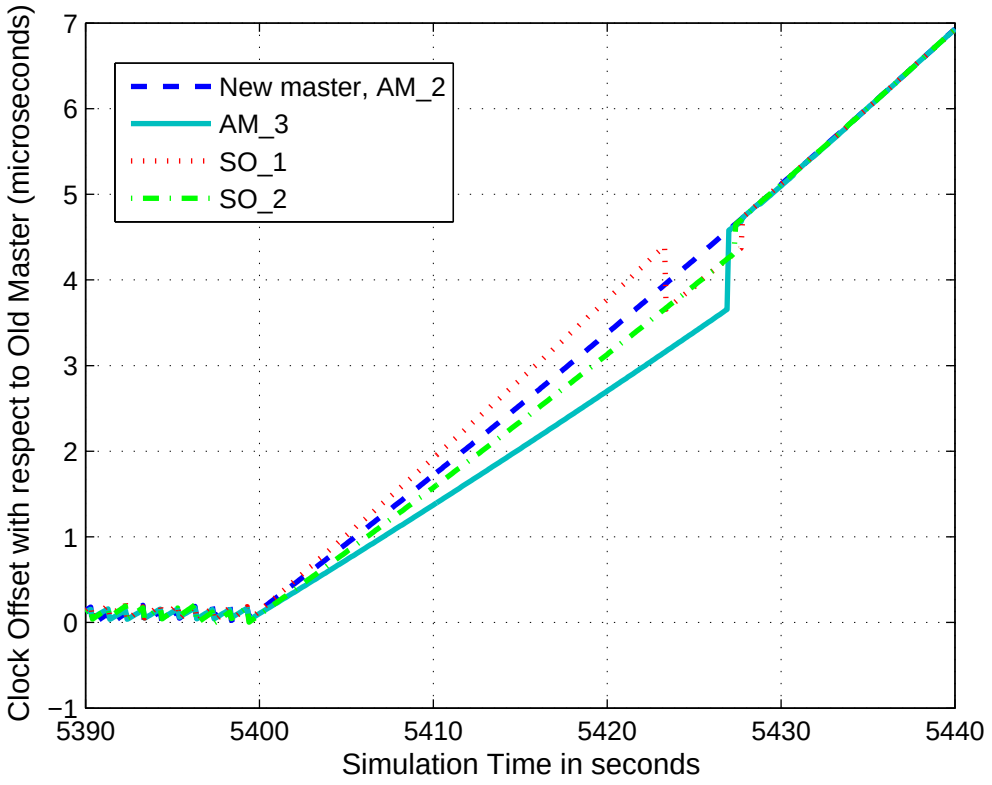

FIGURE 5.10: Evaluation of downtime caused by master failure for the default BMCA scenario.

Before the master failure, the nodes achieve synchronisation and maintain this synchronisation within approximately 0.1μs. After the master failure at $t = 5400$s, the remaining nodes drift apart from the master's clock, and hence each other during the

detection and election phases, until the new master AM_2 transitions to the *MASTER* state.

In the default BMCA scenario, the end of the detection phase coincides with the expiry of the *ANNOUNCE_RECEIPT_TIMEOUT* timer at time $t = 5420$ s. In the election phase which occurs within the next announce interval, slave node SO_1 first tries to synchronise to node SO_2, before finally synchronising to AM_2. The total downtime as a result of master failure is approximately 28s, and the accumulated offset within this period is about 4.5μs across all the nodes.

5.6.1.2 The Alternative BMCA Scenario

In this scenario, the alternate master feature is enabled and the alternative BMCA is used for master election. At power up, all the nodes within the cluster are initialised to the same rank value. Hence, node AM_1 is elected as the master since it has the lowest *priority1* value. A fault was injected into this node at time $t = 5400$s which caused a failure of the master node. After the failure, the clocks of the other nodes run freely until node AM_2 is elected as the master.

Fig. 5.11 shows the clock offset of nodes SO_1, SO_2, AM_2 and AM_3 with respect to the previous master AM_1. Just like the default BMCA scenario, the nodes maintain synchronisation within approximately 0.1μs before the master fails. After the master failure at $t = 5400$s, the remaining nodes drift apart from the master's clock, and hence each other during the detection and election phases, until the new master AM_2 transitions to the *MASTER* state.

Our proposed alternative BMCA uses unicast *queryAnnounce* messages and *alternateMasterSync* to produce shorter detection, election and re-synchronisation phases. The master failure is detected within only 4s, the new master AM_2 is elected within 2s, and the re-synchronisation occurs within a further 2s. In total, the downtime is only 8s, and the accumulated offset within this period is about 2μs.

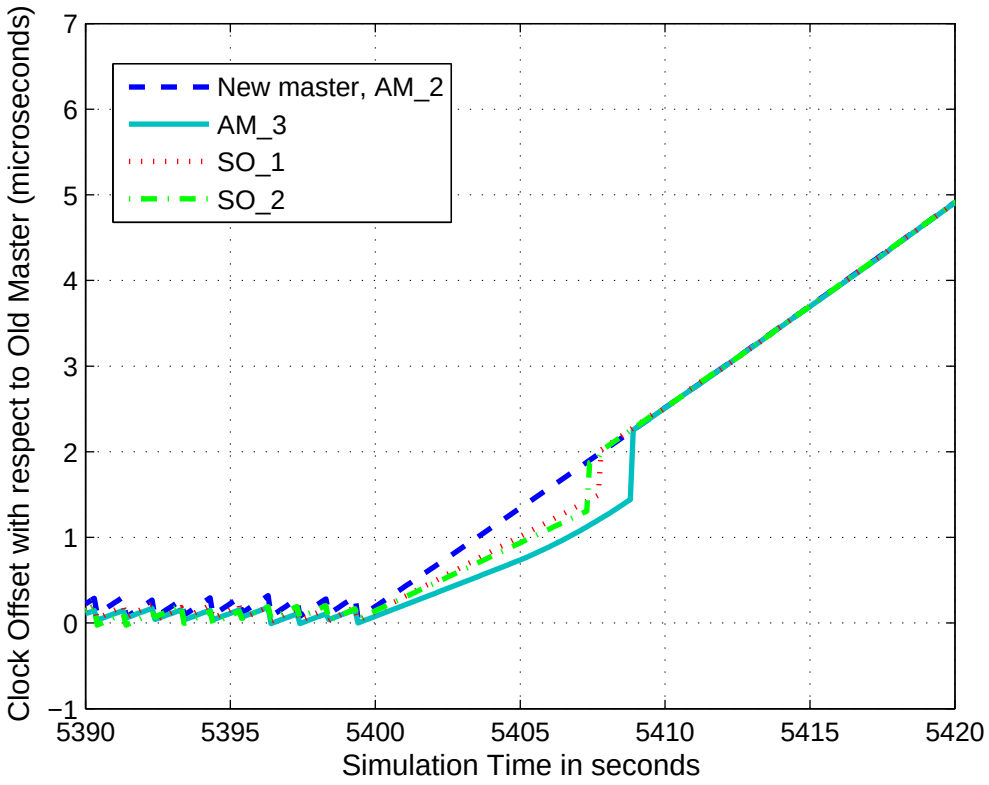

FIGURE 5.11: Evaluation of downtime caused by master failure for the alternative BMCA scenario.

5.6.2 Verifying the Resilience of the Alternate Master Cluster Technique

The alternative BMCA simulation scenario in Section 5.6.1.2 demonstrated the resilience of the alternate master cluster technique to the failure of the master node. In this section, we use simulations to demonstrate that the alternate master cluster technique is also resilient to the addition of both cluster and non-cluster nodes.

5.6.2.1 Introduction of a cluster node

In this scenario we enable the alternate master feature and use the same simulation parameters listed in Table 5.4. However node AM_1 is not powered up until time $t = 5400$s. Hence shortly after initialisation, AM_2 is elected as master and all the nodes achieve synchronisation with it.

Just before AM_1 is powered up, the slave nodes are still synchronised to AM_2 and the relative offset is in the sub-microsecond range as shown in Fig. 5.12. However in terms of the "true" time, there is a significant offset in the order of 10^4 microseconds due to the 6ppm clock drift associated with AM_2.

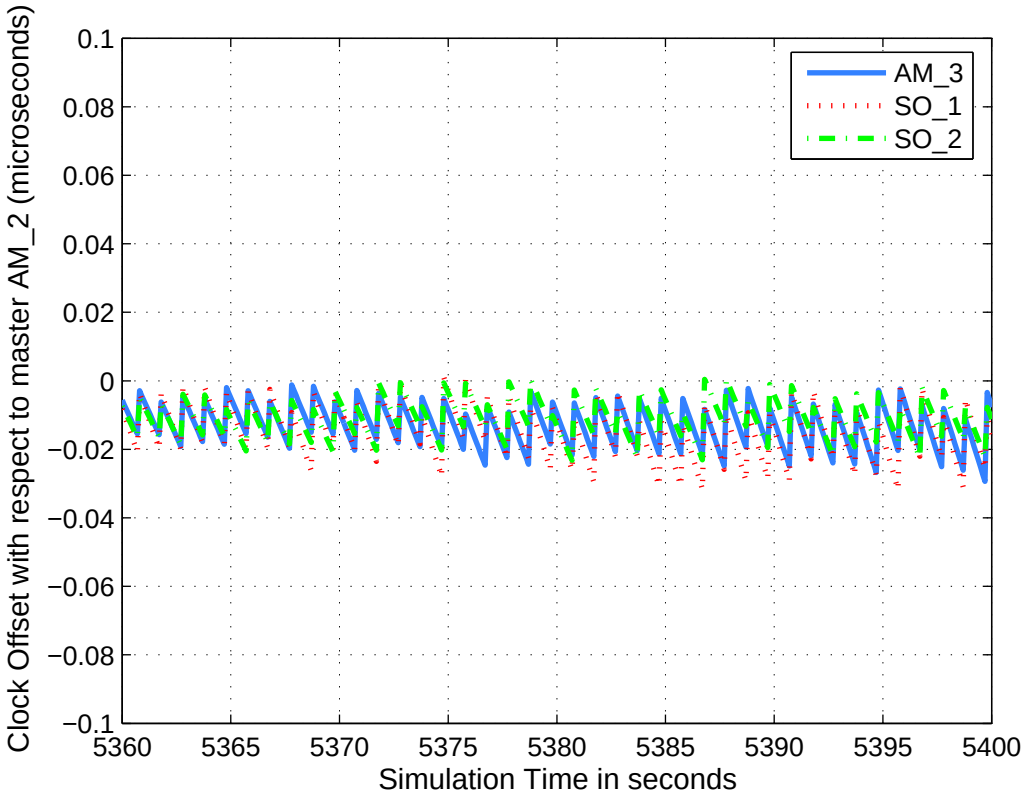

FIGURE 5.12: Clock offset of slave nodes with respect to current master AM_2 before the addition of a cluster node.

When AM_1 is powered up, it discovers the other members of the cluster and exchanges *queryAnnounce* messages with them. It is subsequently elected as master since it has the lowest *priority1* value. When the alternate master nodes and slave nodes synchronise to it, a step change in clock offset occurs. This is illustrated in Fig. 5.13.

Fig. 5.13 verifies the correct operation of the proposed alternate cluster technique, as it proves that the system adapts correctly to the introduction of a master node to the cluster. From an implementation point of view, if the system cannot tolerate the step change in clock offset (e.g. due to the presence of real-time traffic on the network), then the new cluster node should be configured with a higher *priority1* value than

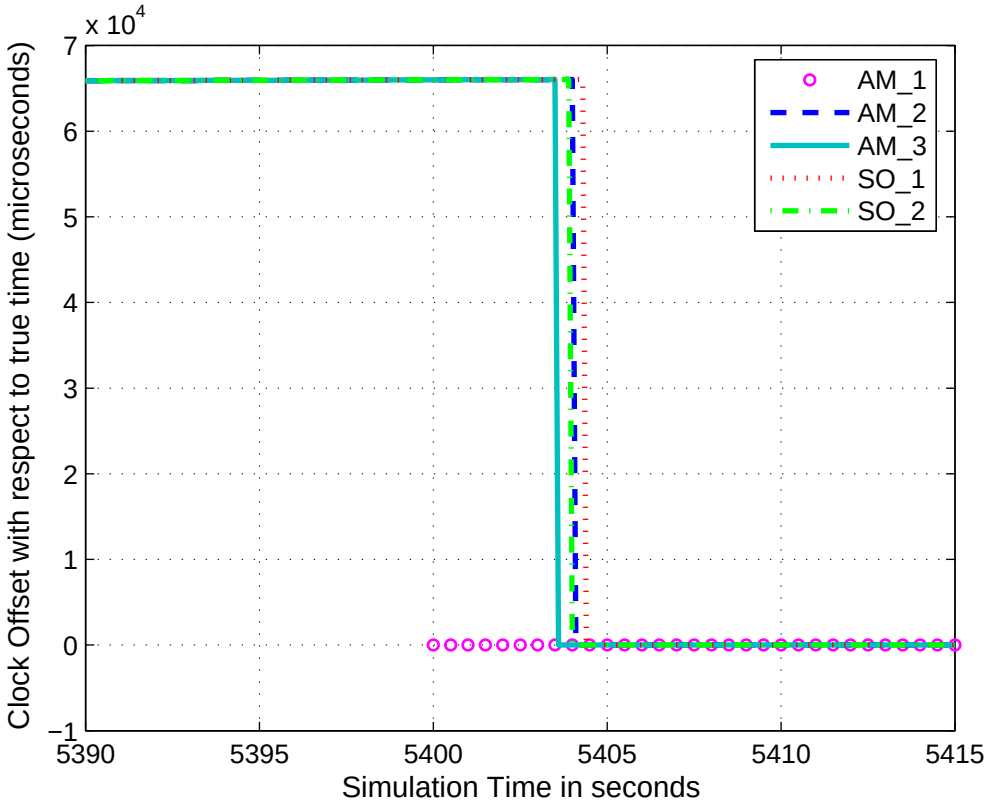

FIGURE 5.13: Clock offset of slave nodes with respect to true time after the addition of a cluster node.

the existing cluster nodes. In this way, it would transition to the *SLAVE* state and adopt the role of an alternate master node.

5.6.2.2 Introduction of a non-cluster node

In this scenario we enable the alternate master feature and use the same simulation parameters listed in Table 5.4. However node SO_2 is not powered up until time $t = 5400$s. Shortly after initialisation, AM_1 is elected as master and all the nodes achieve synchronisation with it. Once SO_2 is powered up, it integrates seamlessly with the network and subsequently synchronises to AM_1, as illustrated in Fig. 5.14.

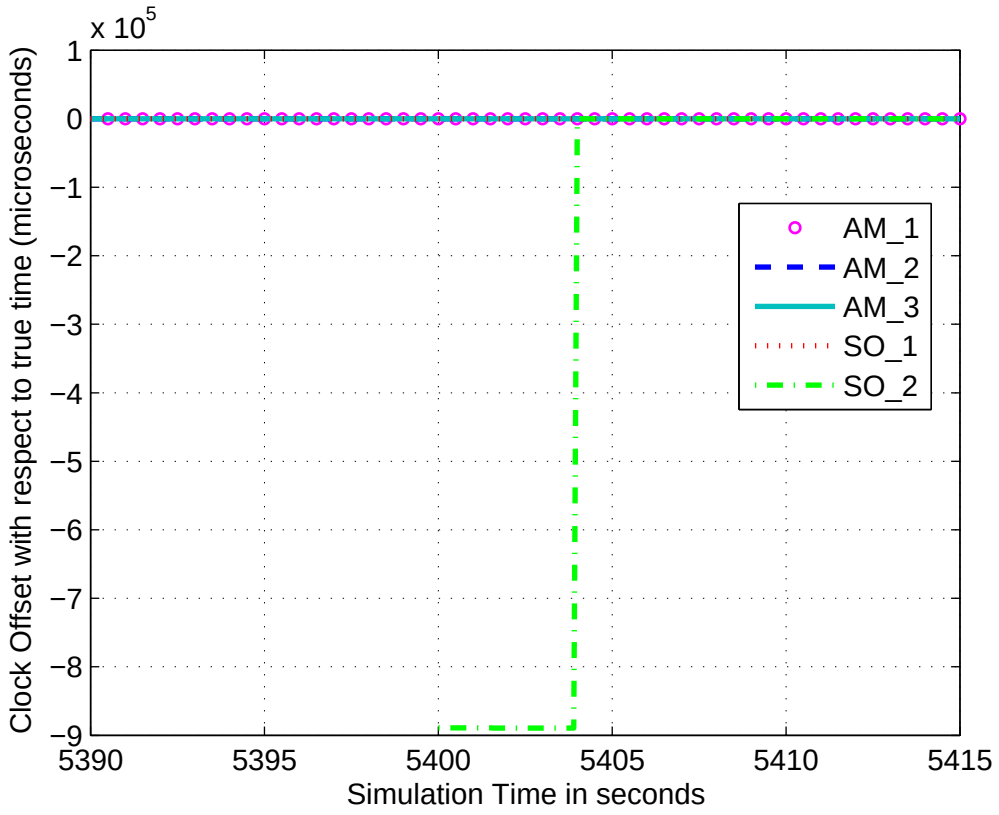

FIGURE 5.14: Clock offset of slave nodes with respect to true time after the addition of a non-cluster node.

5.7 Implementation Considerations

The key implementation requirements for the alternate master cluster members are as follows:

- Support for unicast messaging, so that *queryAnnounce* messages can be transmitted within the cluster.
- Additional memory for storing the details of cluster members in *alternateMasterRecord*.
- Implementation of the ranking algorithm.
- Minor modification to the clock comparison algorithm within the BMCA.
- Utilisation of some reserved fields in the *ANNOUNCE* message for the transmission of *scaledLogrank* values.

All these requirements can be handled in software, with very low effort.

A key advantage of our proposed approach is that the changes in the non-cluster members are trivial. Slave nodes can still utilise the default BMCA, with a reduction in the detection and election phases provided that these two requirements are met:

- Slave nodes have knowledge of the identities of the cluster members, in the form of port identites and/or MAC addresses. This can be configured once at initialisation.
- During an announce interval, if the slave did not receive a more recent *ANNOUNCE* message from the master node but instead received an *ANNOUNCE* message from an alternate master node with *alternateMasterFlag* set to FALSE, this indicates that a master change has occured in the cluster. As such, the previous *ANNOUNCE* message from the master node should be excluded from the BMCA clock comparison algorithm.

5.8 Summary

This chapter has proposed a new alternate master cluster technique for dealing with master failures in PTP. We have described the application scenario which inspired this research work, and then developed a corresponding system model. Careful consideration of the merits and demerits of the existing techniques, revealed that a new technique was required for our application scenario. We have described the alternate master cluster technique in detail; specifying the behaviour of the different types of nodes, describing the alternate BMCA, the ranking algorithms, as well as the attributes required. Network simulations in OPNET have been used to illustrate that our proposed technique can reduce both the downtime resulting from master failure and the accumulated offset. We have also verified the resilience of the alternate master technique to the addition of both cluster and non-cluster nodes. Finally, we have

considered the key requirements for implementing the system and showed that the effort required would be low and most of the changes will be done within the alternate master cluster.

Chapter 6

Conclusions and Future Work

In this thesis, we have explored three different areas in synchronisation, namely: how to achieve higher-layer synchronisation in an UWB network, how to deal with the effects of PDV when PTP is used to synchronise base stations in an Ethernet network, and how to reduce the downtime caused by failure in the master node when PTP is used to synchronise DECT base stations. This chapter concludes the thesis and offers suggestions for future work.

6.1 Conclusions

In Chapter 3, we have developed a higher-layer synchronisation algorithm for an ECMA-368 UWB network. The application requirements for the synchronisation algorithm have been analysed the generic class of algorithms that required for the network has been determined. We have selected two existing algorithms from this class and also proposed a new Linear Rate algorithm for the class. We have determined that the best place for implementing the algorithm is the MAC layer; hence we have also proposed a method for transferring the higher layer clock to the MAC layer using empty RTP packets, when the MAC layer does not have direct access to the higher layer clock. A new MLME primitive has been specified for transferring the computed clock parameters back to the higher layer after synchronisation is complete. The

three candidate algorithms have been implemented in the OPNET simulator and we have observed that the two drift-correcting algorithms perform better. The Linear Rate algorithm has been judged as the most suitable for the network, therefore it has been implemented on an FPGA UWB platform. We have also demonstrated that the performance of the Linear Rate algorithm can be improved if the MAC layer and higher layer applications reside on the same entity; such that the MAC layer is able to obtain the timestamps directly from the higher layer and also update them as close as possible to the PHY, just before the synchronisation frames are transmitted.

Although the higher-layer synchronisation algorithm was designed for a hierarchical UWB network, in theory it can be applied to any other short-range device-device communications network that requires master-slave synchronisation. Whilst it has focused on a multimedia streaming application, it can be used for any other application that requires a similar level of synchronisation accuracy. However if tighter synchronisation is required, then it might be worthwhile to modify the algorithm to use a quadratic or higher-order equation, rather than the linear approach proposed.

Chapter 4 has described a novel sample-mode PDV filtering algorithm. We have characterised the IEEE 1588 PTP *SYNC* packet delay profiles for two types of networks with different levels of background traffic and observed from the shape of the distributions that the existing sample-minimum, sample-maximum, and sample-mean filters perform sub-optimally for some of the load levels in these scenarios. A new skew-estimation algorithm has been proposed, by combining some features of Paxson's "de-noising" algorithm [69], [70] with a linear programming algorithm [15]. This skew-estimation algorithm is used as the RCF estimator in our low-computation sample-mode filtering algorithm. The sample-mode filtering algorithm also incorporates an offset corrector which selects packets from the mode bin and uses these "good" packets to achieve synchronisation. Numerical simulations have shown that when the underlying delay profile of the network is a good match for an existing filter, the sample-mode filter performs as well as the existing filter. However when the mode delay value does not coincide with the minimum, mean, or maximum delay values, the sample-mode filter outperforms the existing sample-minimum, sample-mean, and sample-maximum

filters. Although this research area focussed on the PTP synchronisation protocol, the proposed sample-mode filtering technique can be applied in any other master-slave synchronisation protocol.

Chapter 5 has proposed a new alternate master cluster technique for dealing with master failures in PTP. We have described the application scenario which inspired this research work and by careful consideration of the merits and demerits of the existing techniques, shown that a new technique is required for our application scenario. The alternate master cluster technique has been thoroughly specified. The specification includes the types of nodes, the behaviour of nodes inside and outside the cluster, the alternate BMCA, the ranking algorithm, as well as the required attributes. Network simulations in OPNET have been used to illustrate that our proposed technique can reduce both the downtime resulting from master failure and the accumulated offset. Finally, we have considered the key requirements for implementing the system and shown that the effort required would be low and most of the changes will be done in the alternate master cluster.

6.2 Future Work

Chapter 3 has proposed a novel higher layer synchronisation algorithm for ECMA-368 UWB networks, suitable for multimedia streaming applications. However, the underlying UWB network will be unsuitable for streaming, or indeed any other application, if the MAC layer synchronisation remains unreliable. As mentioned in Section 2.2.2.1, the synchronisation algorithm in the MAC does not actually correct the cloccks. As a result, the accumulation of clock drift can lead to frequent loss of synchronisation and hence temporary loss of connection, if the clock drift remains uncorrected. Future research can consider how to measure the relative clock drift between devices, perhaps by using the transmission time and/or reception time of multiple beacons, so that corrective action can be taken. A possible corrective approach can then incorporate the measured or estimated relative clock drift in the table of relative timing errors.

In Chapter 4, a new sample-mode PDV filtering algorithm was proposed. The offset corrector aspect of the algorithm which uses packets from the mode bin to achieve synchronisation, includes an optional feedback mechanism to manipulate the synchronisation interval and/or window size in order to influence the number of samples in the mode bin. Further work in this area could study the interactions between the synchronisation interval, window size, bin width, and perhaps packer delay variance in order to determine the optimum values for these parameters for any type of network. The de-noising linear programming technique proposed used a segmentation size that was equivalent to the square root of the window size. Future work in the area could explore different values of the segmentation size to see if any benefit can be obtained.

The alternate master cluster technique developed in Chapter 5 uses a ranking attribute to provide quicker detection of a master failure. The ranking attribute is based on how many *queryAnnounce* messages are received within an announce interval by members of the alternate master. Future work in this area could consider how the ranking attribute could be used for detecting congested links within the alternate master cluster so a less-congested link can be selected with corresponding reduction in the probability of packet delays and packet loss in the network. For instance, rather than simply tracking the number of received *queryAnnounce* messages, the time interval between each received message could be monitored in order to detect congestion.

Appendix A

Proof that packets with different delays can end up in the same bin.

Consider the ith and jth SYNC packets received within the same window, where $j - i = n$ and $n > 0$. From (4.6), the corresponding timestamp differences are given by $\delta_i = d_i + (M_i + d_i)\sigma$ and $\delta_j = d_j + (M_j + d_j)\sigma$, respectively. Assuming no packet loss and equal synchronisation interval f, then $M_{i+n} = M_i + nf$ holds. Subtracting δ_i from δ_j with substitution and simplification yields

$$\delta_{i+n} - \delta_i = (d_{i+n} - d_i)(1 + \sigma) + nf\sigma. \tag{A.1}$$

For the two packets to end up in the same bin, the difference in their δ values must be within the bin width α. Hence,

$$\alpha \geq (d_{i+n} - d_i)(1 + \sigma) + nf\sigma. \tag{A.2}$$

Appendix B

Proof that packets with the same delay can end up in different bins.

Again, consider the ith and jth SYNC packets received within the same window, where $j - i = n$ and $n > 0$. In this case, the end-to-end delay is $d_i = d_j = d$. From (4.6), the corresponding timestamp differences are given by $\delta_i = d + (M_i + d)\sigma$ and $\delta_j = d + (M_j + d)\sigma$, respectively. Assuming no packet loss and equal synchronisation interval f, then $M_{i+n} = M_i + nf$ holds. Subtracting δ_i from δ_j with substitution and simplification yields

$$\delta_{i+n} - \delta_i = nf\sigma. \tag{B.1}$$

For the two packets to end up in different bins, the difference in their δ values must be greater than the bin width α. Hence,

$$\alpha < nf\sigma. \tag{B.2}$$

References

[1] G. Heidari, *WiMedia UWB Technology of Choice for Wireless USB and Bluetooth*. West Sussex, UK: John Wiley and Sons, 2008.

[2] A. Sutton, "Building better backhaul," *Engineering and Technology Magazine*, vol. 6, no. 5, pp. 72–75, Jun. 2011.

[3] M. Howard, "Using Carrier Ethernet to Backhaul LTE," White Paper, Infonetics Research, Feb. 2011.

[4] P. Briggs, R. Chundury, and J. Olsson, "Carrier Ethernet for Mobile Backhaul," *IEEE Communications Magazine*, vol. 48, no. 10, pp. 94–100, Oct. 2010.

[5] *IEEE Standard for a Precision Clock Synchronization Protocol for Networked Measurement and Control Systems, 2nd Edition*, IEEE Std. 1588, 2008.

[6] D. Mills, "Network Time Protocol (Version 3) Specification, Implementation and Analysis," RFC 1305, Mar. 1992.

[7] R. Steinmetz, "Human perception of jitter and media synchronization," *IEEE Journal on Selected Areas in Communications*, vol. 14, no. 1, pp. 61–72, Jan 1996.

[8] *High Rate Ultra Wideband PHY and MAC Standard, 3rd Edition*, ECMA Std. 368, 2008.

[9] I. Hadzic and D. R. Morgan, "On Packet Selection Criteria for Clock Recovery," in *Proc. IEEE International Symposium on Precision Clock Synchronization for Measurement, Control and Communication (ISPCS'09)*, Brescia, Italy, Oct. 2009, pp. 35–40.

[10] ——, "Adaptive Packet Selection for Clock Recovery," in *Proc. IEEE International Symposium on Precision Clock Synchronization for Measurement, Control and Communication (ISPCS'10)*, Portsmouth, USA, Sep. 2010, pp. 42–47.

[11] D. T. Bui, A. Dupas, and M. L. Pallec, "Packet Delay Variation Management for a better IEEE 1588v2 Performance," in *Proc. IEEE International Symposium on Precision Clock Synchronization for Measurement, Control and Communication (ISPCS'09)*, Brescia, Italy, Oct. 2009, pp. 75–80.

[12] T. Murakami and Y. Horiuchi, "Improvement of Synchronization Accuracy in IEEE 1588 Using a Queuing Estimation Method," in *Proc. IEEE International Symposium on Precision Clock Synchronization for Measurement, Control and Communication (ISPCS'09)*, Brescia, Italy, Oct. 2009, pp. 12–16.

[13] B. Sundararaman, U. Buy, and A. D. Kshemkalyani, "Clock synchronization for wireless sensor networks: a survey," *Ad Hoc Networks*, vol. 3, no. 3, pp. 281–323, May 2005.

[14] L. Lamport, "Time, clocks and the ordering of events in a distributed system," *Communications of the ACM*, vol. 21, no. 7, pp. 558–565, Jul. 1978.

[15] S. B. Moon, P. Skelly, and D. Towsley, "Estimation and Removal of Clock Skew from Network Delay Measurements," in *Proc. IEEE Eighteenth Annual Joint Conference of the IEEE Computer and Communications Societies (INFOCOM'99)*, vol. 1, New York, USA, Mar. 1999, pp. 227–234.

[16] "BIPM Com. Cons. Df. Seconde, 1980, 9, S15 and Metrologia, 1981, 17, 70," CCDS Recommendation S 2, Bureau International des Poids et Mesures, 1970.

[17] V. Paxson, G. Almes, J. Mahdavi, and M. Mathis, "Framework for IP Performance Metrics," RFC 2330, May 1998.

[18] S. Bregni, *Synchronization of Digital Telecommunications Networks*. West Sussex, England: John Wiley and Sons, 2002.

[19] P. Marsch and G. P. Fettweis, *Coordinated Multi-Point in Mobile Communications: From Theory to Practice*. New York, USA: Cambridge University Press, 2011.

[20] "Synchronization Interface Standards for Digital Networks," ANSI/T1.101-1987, ANSI, Mar. 1987.

[21] H. Kopetz, *Real-Time Systems Design Principles for Distributed Embedded Applications*, 2nd ed., J. A. Stankovic, Ed. New York, USA: Springer, 2011.

[22] M. Ghavami, L. B. Michael, and R. Kohno, *Ultra Wideband Signals and Systems in Communication Engineering (Second Edition)*. West Sussex, UK: John Wiley and Sons, 2007.

[23] C. Wei, P. Ranta, T. A. Brown, and C. Reed, "Wireless Video Streaming over UWB," in *IEEE International Conf. on Ultra-Wideband, ICUWB'07*, Singapore, Sep. 2007, pp. 933–936.

[24] S. Zeisberg and V. Schreiber, "EUWB - Coexisting Short Range Radio by Advanced Ultra-Wideband Radio Technology," in *ICT-Mobile Summit 2008 Conference Proceedings*, P. Cunningham and M. Cunningham, Eds. IIMC International Information Management Corporation, 2008.

[25] E. Dimitrov, T. Kaiser, A. Anttonen, A. Krause, and A. Weir, "The PULSER II view towards very high data rate OFDM based UWB systems," in *Proc. 16th IST Mobile and Wireless Communications Summit*, Budapest, Hungary, Jul. 2007, pp. 1–5.

[26] (2007) EUWB Website. [Online]. Available: http://www.euwb.eu/

[27] M. Balakrishnan and L. Taylor, "Time Synchronization of New Devices in Ad-hoc Multimedia Networks," in *4th IEEE Consumer Communications and Networking Conf., CCNC'07*, Las Vegas, USA, Jan. 2007, pp. 336–341.

[28] R. Aiello and A. Batra, *Ultra Wideband Systems Technologies and Applications*. Oxford, UK: Elsevier Inc., 2006.

[29] S.-P. Liou, C. Toklu, and K. Heckrodt, "VideoTalk: a collaborative environment for video content discussion," in *Proc. IEEE International Conference on Multimedia Computing and Systems*, vol. 2, Florence, Italy, Jun. 1999, pp. 454–459.

[30] "Precision Time Protocol Telecom Profile for Frequency Synchronization," Recommendation G.8265.1/Y.1365.1, ITU-T, Oct. 2010.

[31] "Synchronization for Next Generation Networks - The PTP Telecom Profile," White Paper, Symmetricom, 2011.

[32] "IP-DECT System data sheet," ikon GmbH, Ulm, Germany.

[33] "HiPath Cordless IP data sheet," Siemens Enterprise Communications GmbH, Munich, Germany.

[34] "Deployment of Precision Time Protocol for Synchronization of GSM and UMTS Basestations," Application Brief, Symmetricom, may 2008.

[35] R. Zarick, M. Hagen, and R. Bartos, "The Impact of Network Latency on the Synchronization of Real-World IEEE 1588-2008 Devices," in *Proc. IEEE International Symposium on Precision Clock Synchronization for Measurement, Control and Communication (ISPCS'10)*, Portsmouth, USA, Sep. 2010, pp. 135–140.

[36] "Timing and Synchronization Aspects in Packet Networks," Recommendation G.8261, ITU-T, Apr. 2008.

[37] B. Mochizuki and I. Hadzic, "Improving ieee 1588v2 clock performance through controlled packet departures," *IEEE Communications Letters*, vol. 14, no. 5, pp. 459–461, May 2010.

[38] C. Na, R. Scheiterer, D.Obradovic, and J. Nossek, "A Kalman Filter Approach To Clock Synchronization Of Cascaded Network Elements," in *Proc. First IFAC Workshop on Estimation and Control of Networked Systems*, Venice, Italy, Sep. 2009, pp. 54–59.

[39] H. Abubakari and S. Sastry, "IEEE 1588 style synchronization over wireless link," in *Proc. IEEE International Symposium on Precision Clock Synchronization for Measurement, Control and Communication (ISPCS'08)*, Ann Arbor, USA, Sep. 2008, pp. 127–130.

[40] "Improving Real World Synchronization Accuracy with IEEE-1588 Transparent Clocks," White Paper, Symmetricom, 2009.

[41] W. Stallings, "A practical guide to queuing analysis," *BYTE*, vol. 16, no. 2, pp. 309–316, Feb 1991.

[42] "Cisco Nexus 5548P Switch Architecture," White Paper, Cisco, 2010.

[43] "IXF1110 MAC data sheet," Cortina Systems, California, USA.

[44] A. Bletsas, "Evaluation of kalman filtering for network time keeping," *IEEE Transactions on Ultrasonics, Ferroelectrics, and Frequency Control*, vol. 52, no. 9, pp. 1452–1460, Sep. 2005.

[45] W. E. Leland, M. S. Taqqu, W. Willinger, and D. V. Wilson, "On the self-similar nature of ethernet traffic," *IEEE/ACM Transactions on Networking*, vol. 2, no. 1, pp. 1–15, Feb. 1994.

[46] S. Johannessen, "Time synchronization in a local area network," *IEEE Control Systems Magazine*, vol. 24, no. 2, pp. 61–69, Apr. 2004.

[47] G. Gaderer, R. Holler, T. Sauter, and H. Muhr, "Extending IEEE 1588 to Fault Tolerant Clock Synchronization," in *Proc. IEEEIEEE International Workshop on Factory Communication Systems (WFCS'04)*, Vienna, Austria, Sep. 2004, pp. 353–357.

[48] G. Gaderer, S. Rinaldi, and N. Kero, "Master Failures in the Precision Time Protocol," in *Proc. IEEE International Symposium on Precision Clock Synchronization for Measurement, Control and Communication (ISPCS'08)*, Ann Arbor, USA, Sep. 2008, pp. 59–64.

[49] G. Gaderer, P. Loschmidt, and T. Sauter, "Improving fault tolerance in high-precision in clock synchronization," *IEEE Transactions on Industrial Informatics*, vol. 6, no. 2, pp. 206–215, May 2010.

[50] F. Praus, W. Granzer, G. Gaderer, and T. Sauter, "A Simulation Framework for Fault-Tolerant Clock Synchronization in Industrial Automation Networks," in *Proc. IEEE Conference on Emerging Technologies and Factory Automation(ETFA'07)*, Patras, Greece, Sep. 2007, pp. 1465–1472.

[51] J.-L. Ferrant, M. Gilson, S. Jobert, M. Mayer, L. Montini, M. Ouellette, S. Rodrigues, and S. Ruffini, "Development of the first ieee 1588 telecom profile to address mobile backhaul needs," *IEEE Communications Magazine*, vol. 48, no. 10, pp. 118–126, Oct. 2010.

[52] Y. Kozakai and M. Kanda, "Keeping Clock Accuracy on a Master Clock Failure in Substation Network," in *Proc. IEEE International Symposium on Precision Clock Synchronization for Measurement, Control and Communication (ISPCS'10)*, Portsmouth, USA, Sep. 2010, pp. 25–29.

[53] S. Bovelli and F. Leipold, "Requirements for public transport applications," EUWB Deliverable D8a.2, Dec. 2008.

[54] ——, "Scenario description for public transport applications," EUWB Deliverable D8a.1, Jul. 2008.

[55] P. Hafezi and M. del Rey, "System Parameters and Technical Requirements for Multiband/Multimode UWB Home Environment Applications," EUWB Deliverable D8c.2, Dec. 2008.

[56] M. Mock, R. Frings, E. Nett, and S. Trikaliotis, "Continuous Clock Synchronization in Wireless Real-Time Applications," in *19th IEEE Symp. on Reliable Distributed Systems, SRDS'00*, Nürnberg, Germany, Oct. 2000.

[57] S. Ping, "Delay Measurement Time Synchronization for Wireless Sensor Networks," Intel Research, IRB-TR-03-013, Jun. 2003.

[58] M. Mock, R. Frings, E. Nett, and S. Trikaliotis, "Clock Synchronization for Wireless Local Area Networks," in *Proc. Euromicro-RTS 2000*, Stockholm, Sweden, Jun. 2000.

[59] M. Anyaegbu, A. Weir, and C.-X. Wang, "Higher Layer Synchronization in an ECMA-368 Ultra Wideband Network," in *IEEE International Conf. on Ultra-Wideband, ICUWB'10*, vol. 2, Nanjing, China, Sep. 2010, pp. 1–4.

[60] *OPNET Modeler Documentation Set*, OPNET Technologies, Inc., Bethesda, MD, 2011, release 16.0.

[61] Y. Quan and G. Liu, "Drifting Clock Model for Network Simulation in Time Synchronization," in *Proc. 3rd International Conference on Innovative Computing Information and Control (ICICIC'08)*, Dalian, China, Jun. 2008, pp. 385–388.

[62] B. Ngamwongwattana and R. Thompson, "Measuring One-Way Delay of VoIP Packets Without Clock Synchronization," in *Proc. IEEE International Instrumentation and Measurement Technology Conference (I2MTC'09)*, Singapore, May 2009, pp. 532–535.

[63] *MAC-PHY Interface for ECMA-368, 3rd Edition*, ECMA Std. 369, 2008.

[64] *ML505/ML506/ML507 Evaluation Platform User Guide*, UG347, Xilinx, 2011.

[65] lwIP Documentation (lwIP 1.3.0). [Online]. Available: http://http://www.nongnu.org/lwip/

[66] *Xilinx LogiCORE IP XPS Timer/ Counter (v1.02a)*, DS573, Xilinx, 2010.

[67] D. Mills, "Internet Time Synchronization: The Network Time Protocol," RFC 1129, Oct. 1989.

[68] M. Anyaegbu, C.-X. Wang, and W. Berrie, "A Sample-Mode Packet Delay Variation Filter for IEEE 1588 Synchronization," in *Proc. IEEE International Conference on ITS Telecommunications (ITST'12)*, Taipei, Taiwan, Nov. 2012.

[69] V. Paxson, "Measurements and analysis of end-to-end internet dynamics," Ph.D. dissertation, Univ. of California, Berkeley, Apr. 1997. [Online]. Available: ftp://ftp.ee.lbl.gov/papers/vp-thesis

[70] ——, "On calibrating measurements of packet transit times," in *Proceedings of SIGMETRICS'98)*, Madison, Wisconsin, Jun. 1998.

[71] *Digital Enhanced Cordless Telecommunications (DECT); Common Interface (CI); Part 1: Overview, version 2.4.1*, ETSI Std. ETSI EN 300 175-1, 2012.

[72] *Digital Enhanced Cordless Telecommunications (DECT); Common Interface (CI); Part 2: Physical Layer (PHL), version 2.1.1*, ETSI Std. ETSI EN 300 175-2, 2007.

[73] *Digital Enhanced Cordless Telecommunications (DECT); Common Interface (CI); Part 3: Medium Access Control (MAC) layer, version 2.2.0*, ETSI Std. ETSI EN 300 175-3, 2008.

[74] J. A. Phillips and G. MacNamee, *Personal Wireless Communications with DECT and PWT*. Norwood, USA: Artech House Inc., 1998.